STRATIGRAPHY, STRUCTURE, AND ORIGIN OF THE MENDELEEV RIDGE FROM BATHYMETRY, CONTROLLED SOURCE SEISMIC, AND GRAVITY OBSERVATIONS

By

Dayton W. Dove

RECOMMENDED: _____

_____

_____

_____
Advisory Committee Chair

_____
Chair, Department of Geology and Geophysics

APPROVED: _____
Dean, College of Natural Science and Mathematics

_____
Dean of the Graduate School

_____
Date

STRATIGRAPHY, STRUCTURE, AND ORIGIN OF THE MENDELEEV RIDGE FROM BATHYMETRY, CONTROLLED SOURCE SEISMIC, AND GRAVITY OBSERVATIONS

A

THESIS

Presented to the Faculty

of the University of Alaska Fairbanks

In Partial Fulfillment of the Requirements

for the Degree of

MASTER OF SCIENCE

By

Dayton W. Dove, B.S.

Fairbanks, Alaska

May 2007

Abstract

Multi-channel-seismic (MCS), seismic refraction, and gravity data collected over the Mendeleev Ridge have been processed and interpreted to describe the crustal style of the ridge, as well as the structural and depositional history. These results provide constraints on the origin of the ridge, and the tectonic evolution of the Amerasian Basin. MCS images reveal two primary sediment sequences separated by an unconformity that persists across the entire Mendeleev Ridge. The basement and lower sediment sequence exhibit pervasive normal faulting and the regional unconformity is interpreted to mark the end of extensional deformation. Modeling of the seismic refraction data reveals an upper crustal velocity structure consistent with either a volcanic rifted continental margin, or an oceanic plateau. Gravity anomalies collected along the MCS lines can be reproduced with models containing bathymetry, sediment and basement horizons, and a crust of 2.86 g/cm^3. This result is consistent with homogeneous, mafic crust. Comparing the velocity and density structures of the Mendeleev Ridge to the Alpha Ridge suggests they are contiguous and share a common geologic origin. Three tectonic models are presented for the origin of the Alpha Mendeleev Ridge (AMR) that satisfy constraints set by this and previous studies.

Table of Contents

Page

Signature Page.....i

Title Page......ii

Abstract.....iii

Table of Contents.....iv

List of Figures vi

List of Other Materials.....viii

List of Appendices.....viii

Acknowledgements.....ix

Introduction.....1

Canada Basin and the Opening of the Amerasian Basin 1
Alpha and Mendeleev Ridges.....7
Alpha Ridge.....8
Potential Field Observations 10
Mendeleev Ridge 11
Chukchi Borderland 12
Makarov Basin 13
Circum-Arctic Cretaceous Volcanism.....14
Arctic Large Igneous Province.....14
Canadian Arctic Margin.....15
East Siberian Sea.....16

Cruise Description and Project Objectives.....16

Experiment Overview, Methodology, and Results.....17

Seismic Reflection.....17
Experiment Overview and Methodology.....17
Results.....20
Seismic Refraction.....30
Experiment and Methodology Overview.....30
Results.....37
Gravity 40
Experiment and Methodology Overview.....40

Discussion 50

Constraints on the Geological Nature of the Mendeleev Ridge Crust.....50
Upper Crust.....50

Page

Deeper Crust – Evidence of Homogenous Crust and Contiguity with the Alpha Ridge 56
Synthesis 60
Depositional and Structural Histories 60
Structural History 62
Subsidence 66
Regional Unconformity and Timing of Most Recent Tectonism 67
Applying Lomonosov Ridge Sedimentation Rates 69
Alternative Hypothesis 69
Models for the Origin of the Alpha Mendeleev Ridge (AMR), Implications for the Amerasian Basin, and Potential Global Analogues 70
Rifted Volcanic Continental Margin 71
Potential Global Analogues 73
Oceanic Plateau Formed at a Spreading Center ~Perpendicular to the AMR 74
Oceanic Plateau Formed at a Spreading Center ~Parallel to the AMR 77
Potential Global Analogues 79

Conclusions 80

References 83

Appendices 96

List of Figures

Page

Fig. 1 Regional Bathymetry Map of the Arctic Ocean 2
Fig. 2 Regional Magnetic Anomaly Map.....5
Fig. 3 Regional Gravity Anomaly Map.....6
Fig. 4 Mendeleev Ridge Study Area.....18
Fig. 5 Multi-channel Seismic Reflection (MCS) Line Locations.....19
Fig. 6 MCS Images and Interpreted Images.....21-27
Fig. 7 Sediment Thickness Histograms.....29
Fig. 8 Seismic Refraction Model; Sonobuoy 34.....42
Fig. 9 Seismic Refraction Model; Sonobuoy 35.....43
Fig. 10 Seismic Refraction Model; Sonobuoy 37.....44
Fig. 11 Seismic Refraction Model; Sonobuoy 44.....45
Fig. 12 Seismic Refraction Model; Sonobuoy 58.....46
Fig. 13 Compiled Velocity Structure Stack Plots 48
Fig. 14 Empirical Velocity-Density Relations.....42
Fig. 15 Gravity Profile A-A'; Plot of Potential Moho Boundaries 44
Fig. 16 Gravity Profile B-B'; Plot of Potential Moho Boundaries.....45
Fig. 17 Gravity Profile A-A'; Gravity Modelling Results.....47
Fig. 18 Gravity Profile B-B'; Gravity Modelling Results 49
Fig. 19 Regional Seismic Refraction Results from the Amerasian Basin 52
Fig. 20 Velocity-Depth Functions Compared with Normal Oceanic Crust.....53
Fig. 21 Velocity-Depth Functions Compared with Iceland and the NAVP 55
Fig. 22 Average Crustal Velocity Structure for Six Continental Tectonic Provinces..57
Fig. 23 Velocity and Density Structures of the Mendeleev and Alpha Ridges 59
Fig. 24 Structural Interpretation.....63
Fig. 25 3D-visualization; Regional and Ship Bathymetry with MCS Lines 64
Fig. 26 3D-visualization; View of Large Graben and Associated Scarp.....65

Page

Fig. 27 Simplified Tectonic Models for the Emplacement of the Alpha Mendeelev Ridge 72
Fig. 28 Model for Continental Microplate Formation 75

List of Other Materials

Compact Disc High Resolution Multi-Channel Seismic Reflection Images

List of Appendices

Page

Appendix A Seafloor Depth Comparisons Between Bathymetry and MCS Data.....96

Appendix B Seismic Refraction Full Record Sections.....101

Acknowledgements

The crew of the USCG icebreaker Healy. Their hard work helped make the H0503 trans-Arctic crossing as successful as it was. Paul Henkart, for instruction and continual support with SIOSEIS; Vibeke Bruvol, for useful discussions, her constant energy, and for being an all around good ship-mate; The geophysics group (with which I was proud to be a member) aboard the Healy, which implemented a highly successful marine seismic experiment; Yngve Kristofferson, who designed the seismic experiment with colleagues at the University of Bergen, for his will to make things work despite regular adversity, and for his expectation that you are working hard, and enjoying it.

Christina Williams, for innumerable discussions concerning the Arctic, and for being such splendid office-mate; Paul Layer, for his useful comments on the work; Bill Witte, for his useful comments on the work, and his constant help and good advice; John Hopper, for teaching me a thing or two about the principles of controlled-source seismic data, and for the exceptional amount of time he spent helping process the data; Bernie Coakley, for bringing me along, providing help in general, though especially with the gravity data, and in particular, for giving me the latitude to develop into a mostly self-sufficient student while also providing the necessary resources to help with whatever questions might arise.

Family, for making me a happy man; Friends here in Fairbanks, for your company in town, or in the mountains and streams of our surrounds; Lastly, many thanks to Hannah Clilverd, for the regular sharing of ideas on our respective research and all else, for fresh blueberry pies, and for being a lovely person in more ways than I knew possible.

Introduction

The Arctic Ocean can be divided into two distinct basins: the Eurasian Basin and the Amerasian Basin (Fig. 1). The Eurasian Basin was formed by the propagation of the very slow spreading Gakkel Ridge (6-12.7 mm/yr), concurrent with the opening of the N. Atlantic Ocean at ~56 Mya (Ostenso and Wold, 1973; Coles et al., 1978; Vogt et al., 1979; Kristofferson, 1990; Cochran et al., 2003). The spreading system is of great interest to geodynamicists as it is the slowest and deepest on earth and the crustal thickness ranges from ≤ 4km over the Eurasia basin to "vanishingly thin" at the spreading ridge (Coakley and Cochran, 1998; Cochran et al., 2003). The Amerasian and Eurasian Basins are separated by the Lomonosov Ridge, which is a continental fragment rifted off the Barents shelf by spreading along Gakkel Ridge. This hypothesis, first proposed by Heezen and Ewing (1961) became generally accepted through seismic reflection imaging of the crust, (Jokat et al. 1992; Jokat, 2005), and was confirmed by the recent ACEX drilling of the ridge (Moran et al., 2006).

In contrast to the Eurasian Basin, the geologic history of the Amerasian basin is more complex, and less understood. The basin is subdivided into the following physiographic provinces: Canada Basin, Alpha and Mendeleev Ridge (AMR), Makarov Basin, and the Chukchi Borderland that includes the Northwind Ridge and the Chukchi Pleateau (Fig. 1). The history of the basin is not well understood primarily because its component parts are of uncertain relations and affinities.

Canada Basin and the Opening of the Amerasian Basin

Multiple tectonic reconstructions have been proposed for the Amerasian Basin. The origin of the Canada Basin is the fundamental difference that typically distinguishes these models. All agree that it consists of oceanic or at least derived oceanic crust (Baggeroer and Falconer, 1982; Grantz et al., 1990; Grantz, 2006). Shatskiy (1935) describes the Canada Basin as oceanized lithosphere that was previously a continental

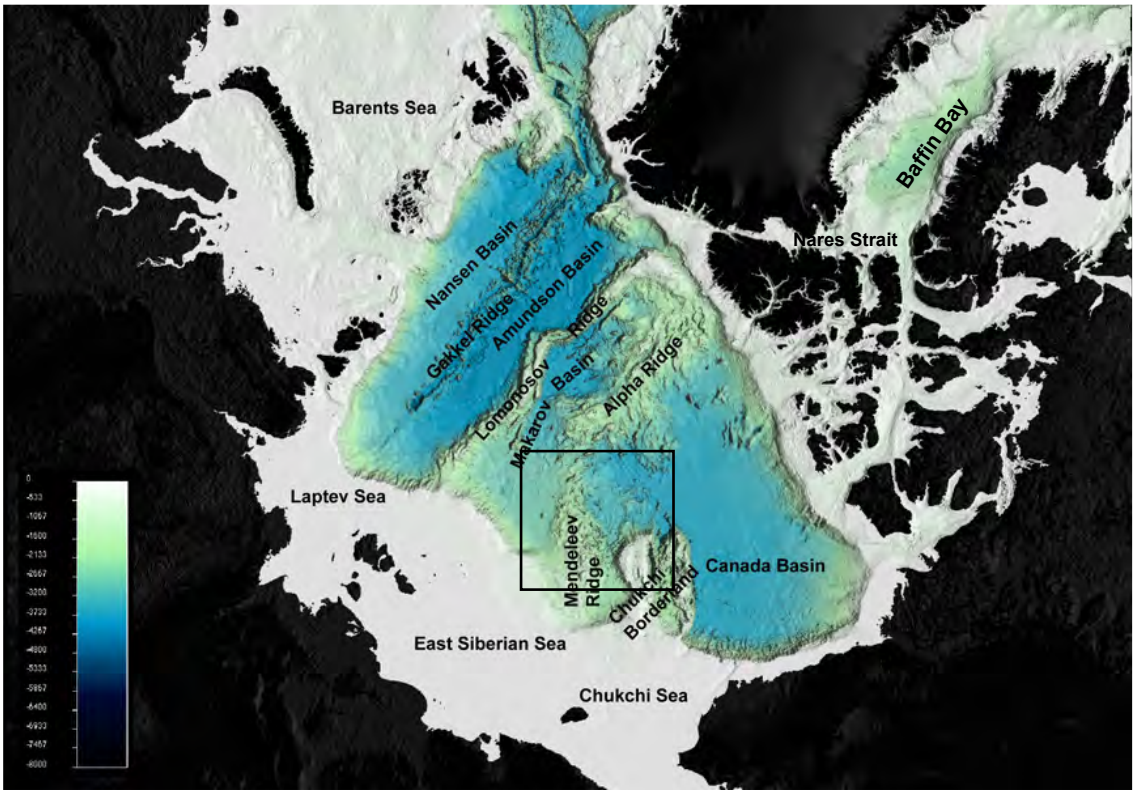

Fig. 1: Regional Bathymetry Map of the Arctic Ocean. Bathymetry data are from the IBCAO grid (Jakobsson et al., 2000). Box delineates study area shown in greater detail in Fig. 4.

cratonic high, which shed sediment to its margins. Through mantle convection, which eroded the root, the basin subsided. Another model refers to a fragment of the Kula Plate becoming isolated in the Arctic during Mesozoic or Paleozoic (Churkin, 1970).

Seafloor spreading is the most accepted origin for the Canada Basin. Lawver and Scotese (1990) review four of these models. One model describes the AMR as a spreading center with the north slope of Alaska as a passive margin, rifted from the Lomonosov Ridge (Hall, 1970; Ostenso and Wold, 1973). Delaurier (1978) argues against this hypothesis by citing the present sediment corrected depth of the AMR as too shallow for a normal Late Cretaceous spreading center. The recovery of non-MORB, alkali basalts from the Alpha Ridge also challenges the spreading center hypothesis (Van Wagoner et al., 1986; Muhe and Jokat, 1999; Jokat, 2003). Another model describes east Siberia as rifting away from Arctic Canada, which requires transform faults along the northern Alaskan margin and at the Lomonosov Ridge (Herron et al., 1974). The third model includes some combination of trapped Paleozoic crust and dextral faulting along the north slope of Alaska, though no such regional scale faulting has been observed (Jones, 1980).

The fourth and most widely accepted model is the rotational model which proposes that the Canada Basin formed as the Arctic-Alaska, Chukotka microplate rotated ~66º counter-clockwise from Arctic Canada about a pole near the Mackenzie Delta (Carey, 1958; Tailleur and Brosge, 1970; Grantz et al., 1979; Vogt et al., 1979; Forsyth et al., 1986; Coles and Taylor, 1990; Laxon and McAdoo, 1994; Lawver et al., 2002; Grantz, 2006).

The first geological evidence to justify this model came from observations of the stratigraphy of the North Slope. The north prograding Torok/Nanushuk interval unconformably overlies the south prograding, normal faulted Kingak shale with the Pebble shale as a transition between the two systems (Tailleur and Brosge, 1970). The directional change of sediment progradation across the Hauterivan unconformity is taken to indicate the moment at which the Arctic Alaska micro-plate was sufficiently transported away from the proto-Canadian Arctic margin such that it was no longer

influenced by the northerly sourced sediments. Grantz and May (1982) further considered the Hauterivan breakup unconformity or "Lower Cretaceous Unconformity" of Alaska. Embry and Dixon (1990) describe several breakup unconformities in Arctic Canada. Their analysis suggested continental rifting initiated just prior to Albian/Cenomanian seafloor spreading predating the Alaskan unconformity. Addressing this ambiguity, the authors suggest that the Alaskan margin was further complicated by tectonic loading in the foreland basin, hence disturbing "normal", thermal subsidence, conditions in which breakup unconformities typically develop (Falvey, 1974; McKenzie, 1978).

The rifted, south dipping paleo-margin under the north slope of Alaska, along with western Seward Peninsula and Chukotka are considered to be a part of the Arctic Alaska microplate, which may have rotationally rifted away from Canadian North America at the opening of the Canada Basin (Moore et. al., 1994; Lawver and Scotese, 1990). Miller et al. (2006) compiles the results from multiple geological studies that describe the Arctic Alaska micro-plate as a cohesive continental body and Grantz et al. (1994), and Moore et al. (1994) give thorough summaries of north Alaskan geology.

Unfortunately, due in part to the great thickness of sediments of the Canada Basin (≤ 12 km), the magnetic anomalies of the Canada Basin are rather diffuse, and low relief (~200 nT), making interpretations difficult (Grantz et al., 1990; Coles and Taylor, 1990). Still, a fan shaped pattern of anomalies is observed in the Southern Canada basin which Taylor et al, (1981) and Coles and Taylor, (1990) correlate with magnetic anomalies (M25-M12) to indicate orthogonal, then rotational seafloor spreading at 153-127 Ma (Fig. 2). Gurevich et al. (2005) present a slightly varied model, where the Canada Basin opens in two stages. During the first stage between ~148 Ma and 141 Ma, spreading was fast and also coincident with two other spreading centers, one being the Alpha Ridge and the other being in the northern Canada Basin that was separated from the southern Canada Basin by the continental Chukchi Plateau. During the second stage, 141 Ma – 127.5 Ma, spreading became slow and then ceased.

These magnetic anomalies are coincident with a north-south lineated gravity low which has been interpreted as a fossil spreading center, similar to the Aegir rift (Fig. 3)

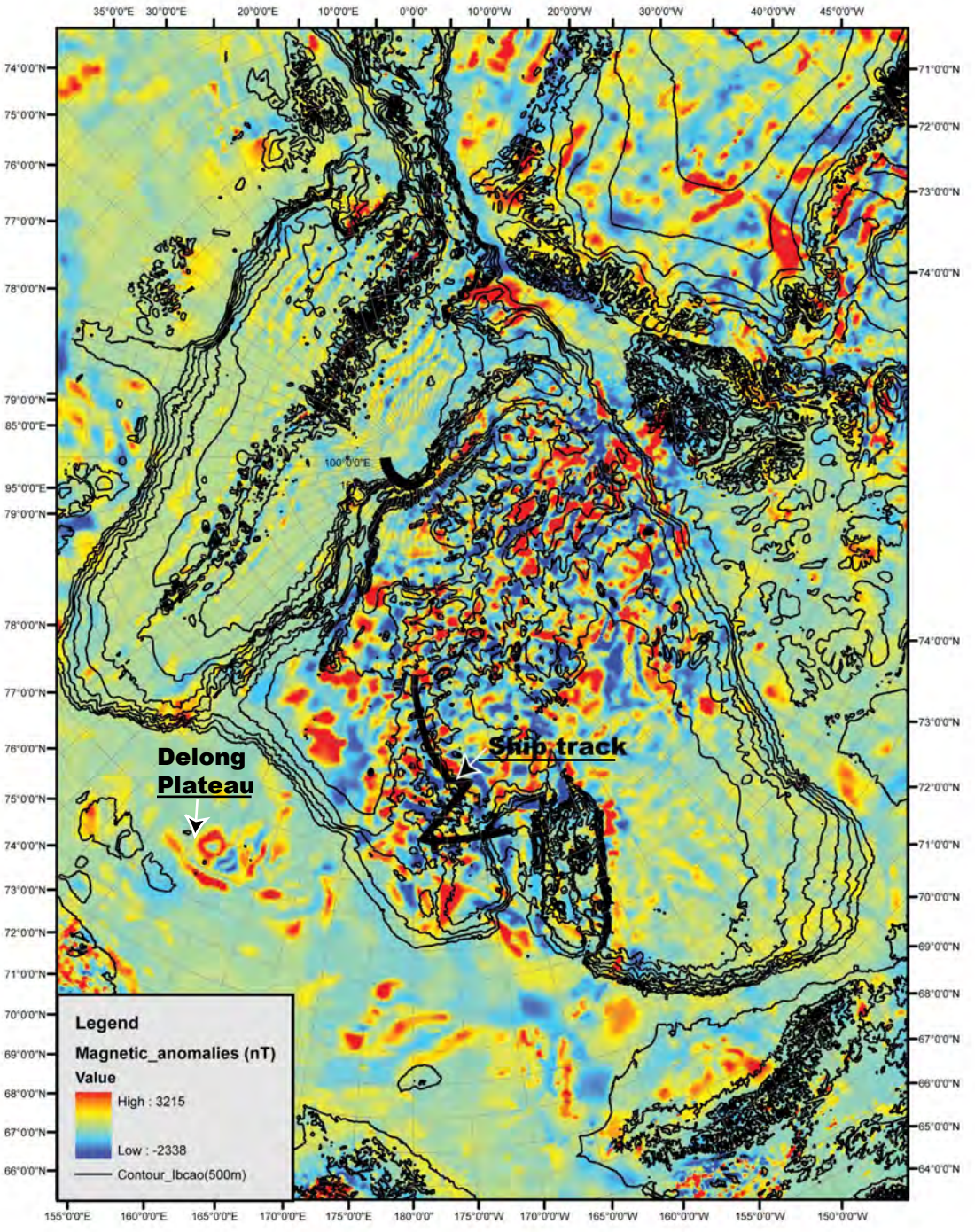

Fig. 2: Regional Magnetic Anomaly Map. IBCAO bathymetry contours (500m) overlay the magnetic data (Verhoef et al., 1996).

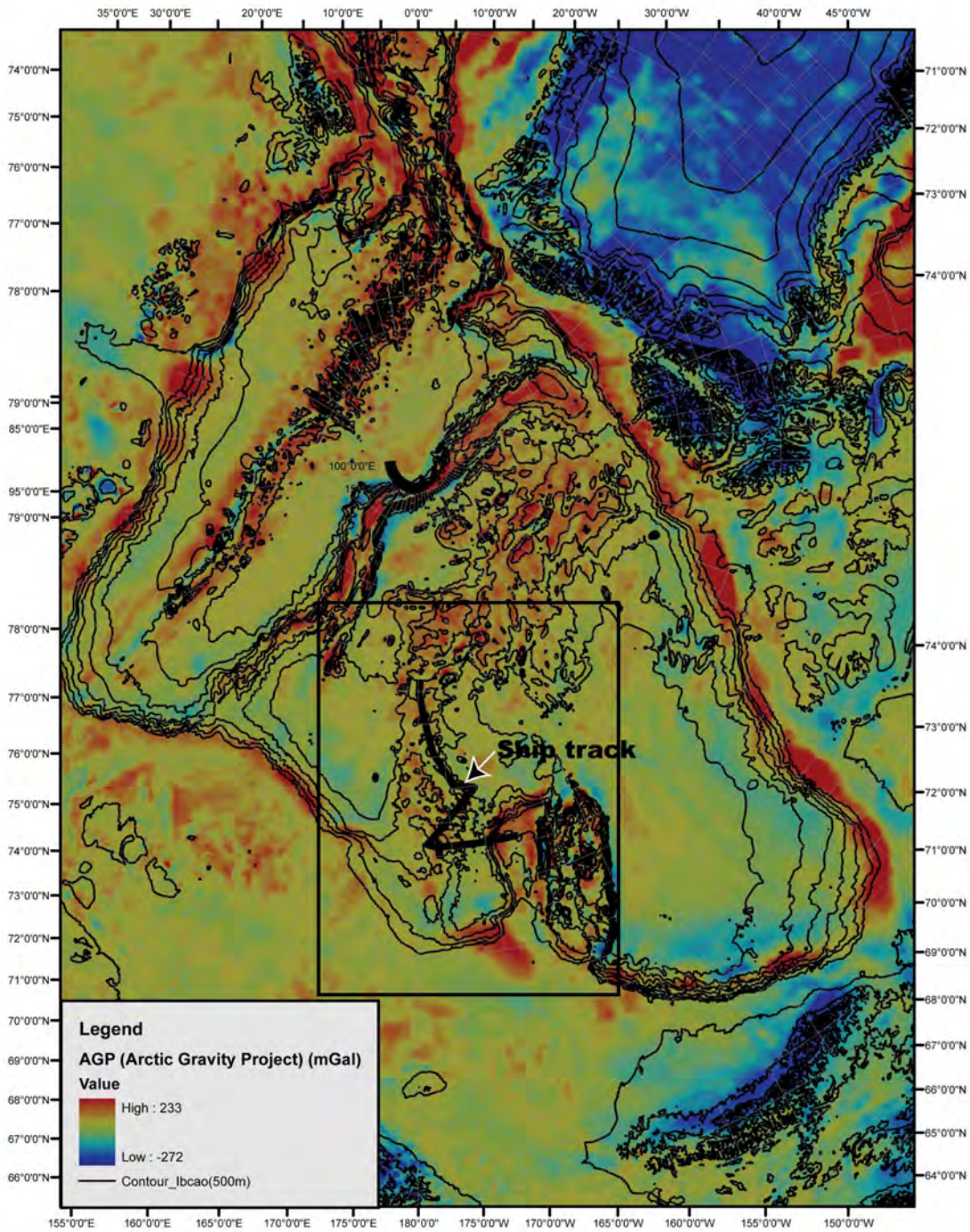

Fig. 3: Regional Gravity Anomaly Map. Data used are from the Arctic Gravity Project (AGP) grid (Kenyon and Forsberg, 2001), with IBCAO bathymetry contours (500m) overlain. Free-air anomalies are shown for marine areas and Bouguer anomalies over terrestrial areas. Box delineates inset shown in Fig. 24.

(Laxon and McAdoo, 1994). Seismic refraction/reflection experiments over the Canada Basin reveal horst and graben basement structures coincident with the potential field anomalies (Grantz et al., 1990; Grantz et al., 1998). Grantz (2006) presents a refined model for the Canada Basin that like, Gurevich et al. (2005), suggests the basin opened in two phases. Continental extension leads to rifting between ~195 Ma and ~131 Ma, resulting in transitional crust. Phase 2 seafloor spreading takes over, creating MORB and the fan shaped, lineated magnetic anomalies between ~131 Ma and ~127.5 Ma.

The rotational model has been accepted due to a variety of supporting geologic and geophysical observations but also due to the absence of substantial direct evidence supporting other models. Lane (1997), and Miller et al. (2006) present alternatives to the rotational model. Miller et al. (2006) dated zircon suites from several terrigenous sandstones surrounding the Amerasian basin to test for common geographic sources. The results suggest that Chukotka is not part of the Arctic-Alaska microplate, but rather originated from the east, near Taimyr and Verkhoyansk. These results do not preclude the rotational model for the southern Canada Basin, but do argue against this model for the whole of the Amerasian basin. The authors go on to infer that the Chukchi Borderland, like the AMR, is thinned continental crust that was transported to its present position from the direction of the Barents Shelf, not from the Sverdrup Basin as predicted by the rotational model.

This illuminates the unique way in which the geologic evolution of the Amerasian Basin has been researched and described. Unlike most oceanic basins, where relatively simple models of seafloor spreading or subduction provide a framework in which we understand the complex geology of continents, the paucity of data, and apparent complexity of geologic events in the Amerasian Basin has required to a greater extent that the geologic history of the circum-Arctic provide a framework for how we understand the oceanic basin.

Alpha and Mendeleev Ridges

Due to the absence of strong magnetic lineations in the Canada Basin the rotational model is speculative, but perhaps most inhibiting to a complete tectonic model

of the Amerasian Basin is the AMR. The Alpha and Mendeleev Ridges are bathymetrically contiguous, roughly symmetrical about their axes and together encompass an area 708,000 km^2 (Fig. 1) (Jakobsson et al., 2003). The AMR stretches across the Amerasian Basin, connecting Siberia with N. Canada and separating the Canada Basin and Makarov Basin.

Typically the Alpha Ridge and Mendeleev Ridge are regarded as a contiguous feature, though many questions are outstanding in regards to the formation of the ridge. It has yet to be shown conclusively whether or not they share a geologic origin or if the ridges are composed of oceanic or continental crust. The working hypothesis, based on work primarily conducted at the Alpha Ridge, suggests that the ridges are a single oceanic plateau, created by hotspot volcanism during the Late Cretaceous (Forsyth et al., 1986; Weber, 1986; Asudeh et al., 1988; Lawver and Muller, 1994; Lawver et al., 2002; Jokat, 2003). Although, several of these authors note that they cannot rule out a continental origin for the ridges. Miller et al. (2006) and Ivanova et al. (2006) prefer an interpretation of attenuated continental crust at least for the Mendeleev Ridge. In order to understand the geologic history of the Amerasian Basin, how the Alpha and Mendeleev Ridges relate to one another, and to surrounding features is of utmost importance.

Alpha Ridge

Until recently, the Alpha Ridge has been more thoroughly studied than the Mendeleev Ridge. Early studies of the Alpha Ridge were conducted from US ice stations: ALPHA (1957-1958) T-3 (1953-1957, 1962-1963, 1966-1974), ARLIS II (1962-1964) where depth soundings, gravity, magnetic and single-channel seismic data were collected. Weber and Sweeney (1990) summarize these results.

Hunkins (1961) first interpreted seismic reflection and refraction data from the T-3 ice island and favored a fault block origin for the AMR. The author reports the velocity structure: 0.29 km of 2.0 km/s sediment, 2.8 km of 4.7 km/s upper basement, and 6.44 km/s crust. Jokat (2003) modeled sediment and upper basement velocities equivalent to the T-3 results presented by Hunkins (1961). The author notes large scale normal

faulting over the Alpha ridge flanks and identifies a regional unconformity possibly related to the opening of the Eurasian Basin.

The Canadian expedition to study Alpha Ridge (CESAR) was the first dedicated attempt to discern the geologic history of the Alpha Ridge. Seismic refraction experiments revealed a very thick crust of 38 km below the ridge axis (Forsyth et al., 1986). Together with the refraction results, higher densities, determined from gravity modeling, over the Alpha Ridge than the Lomonosov Ridge, and the homogenous nature of the magnetic anomalies over the ridge, they hypothesize that the Alpha Ridge "may be composed of a large pile of mafic rock, possible unique to this planet (Weber, 1986). Going further, Forsyth et al. (1986), Asudeh et al. (1988), and Weber (1990) cite the thickened crust, the absence of any significant reflector between the top of the basement and the Moho, and the similarities in the velocity gradients of the Alpha Ridge and Iceland, as evidence that the Alpha Ridge is an Oceanic Plateau, possibly a hot spot track similar to Iceland. This is currently the most accepted hypothesis for the Alpha Ridge and is buoyed by multiple lines of support. Jokat (2003) observed upper basement velocities from the Alpha Ridge that are consistent with an oceanic plateau origin. Based on plate reconstructions and estimated ages, Lawver and Muller (1994) argue that the Alpha and Mendeleev Ridges were likely produced by the drift of the Amerasian basin over the Iceland plume.

Dredged samples of basement rock and sediment from the Alpha Ridge provide the only geologic evidence of the origin and formation age of the Alpha ridge. Alkali basalts from Alpha Ridge graben flanks were recovered during two separate expeditions: CESAR: Van Wagoner et al. (1986), and from Polarstern: Jokat (2003). Basalts recovered during the CESAR project, are altered vesicular alkali basalts indicative of intra-plate volcanism (Van Wagoner et al., 1986). Jokat (2003) report a whole rock $^{40}Ar/^{39}Ar$ plateau age of 82 ±1 Ma for the alkali basalts dredged from the flanks of a graben, suggesting a Late Cretaceous age of formation for this feature (Muhe and Jokat, 1999). Mudie and Blasco (1985) describe certain fossil assemblages within the CESAR

cores taken from the Alpha ridge to date to the Campanian and Maastrichtian age, providing an upper limit on the age of formation of the ridge.

Potential Field Observations

These ages are consistent with interpretations derived from regional magnetic anomalies over both the Alpha and Mendeleev Ridges. Potential field measurements (magnetic and gravity) provide the most extensive databases over the AMR. The ridge formed during a period of normal polarity, leading Weber and Sweeney (1990) to suggest the Alpha Ridge formed almost entirely during the Cretaceous quiet period (120-84 Ma).

Regional gravity (Glebovsky et al., 2000; Kenyon and Forsberg, 2001) and magnetic (Verhoef et al., 1996) maps both suggest either by the lateral consistency of amplitudes, or anomaly pattern, or both, that the Alpha and Mendeleev Ridges are a singular geological province (Figs. 2 & 3). It is also apparent from gravity and magnetic anomaly maps that the crustal material of the AMR extends into the Makarov and Canada Basins, beyond its bathymetric expression.

Weber (1986) showed that magnetic anomalies over the Alpha Ridge correlate predominantly with bathymetry and basement topography, hence suggesting a homogenous basement structure, characteristic of oceanic plateaus. Regional gravity models show that the gravity field also correlates with bathymetry, with no observed lateral variation in the crust (Sobzak and Hearty et al., 1990). Weber (1986) also modeled the gravity data recovered from the CESAR project. Derived crustal densities (Sediments: ~2.0 g/cm^3; Upper Crust: ~2.88 g/cm^3; Lower crust $\geq$ 26 km: 3.04 g/cm^3) revealed great lateral continuity, not displaying the variation expected from continental crust but rather suggesting an underlying oceanic crust.

Coles and Taylor (1990) also find that magnetic anomalies correlate with bathymetry, but note that the Alpha Ridge has one of highest observed fields (1500-2500 nT) on earth. They suggest that all other bodies that exhibit such strong magnetic anomalies are either continental or pseudo-continental in nature. Jackson et al. (1986) however, suggests that the magnetic anomalies of the Alpha Ridge are correlated with the thickened crust of the ridge, and that an oceanic origin is viable.

ERS-1 satellite derived gravity data over the AMR is tentatively interpreted by Laxon and McAdoo (1994) to support the now typically rejected hypothesis that the Alpha and Mendeleev Ridge is a normal fossil spreading center, however no supporting evidence is given.

Vogt et al. (2006) synthesize multiple geophysical data sets collected from both aero-geophysical and icebreaker surveys over the whole of the AMR. They find that magnetic anomalies are generally correlated with bathymetry and ± 20 mGal free air gravity anomalies. An estimated magmatic volume of 10,000 km^3 for the AMR is surpassed only by the Ontong Java Plateau for oceanic plateaus. They hypothesize that the magamatism of the AMR is related to volcanics of the Sverdrup Basin but also note that they cannot rule out a continental component in the ridge crust.

Mendeleev Ridge

There have been few geological and geophysical projects dedicated to discerning the geologic history of the Mendeleev Ridge. The Russian Ice station NP-26 crossed the Mendeleev Ridge several times between 1983 and 1986, though seismic reflection data was not published until recently, along with refraction results from the Russian Arctic 2000 seismic refraction profile over the Mendeleev Ridge (Ivanova et al., 2006). These seismic images reveal a rugged basement with sediment thicknesses ranging from 0.1 km to ~2.3 km on the western slopes off the ridge, bordering the Makarov Basin.

Hall (1970), for his Ph.D thesis reexamined the seismic, gravity, and magnetic data taken from T-3 with the assistance of newer bathymetry data (Beal, 1968). Sediment thicknesses were found to vary between several hundred and 1,000 meters. Gravity modeling revealed that the crust was ~32 km thick with the upper 5 km as East Pacific Rise style crust and the lower 27 km representing anomalous crust with a bulk density of 3.15 g/cm^3. Hall (1970) preferred a spreading center hypothesis for the AMR, mapping multiple fracture zones along an axial rift valley on both the Alpha and Mendeleev Ridges. Several spreading events were invoked: Paleozoic, Late Mesozoic, and Early Tertiary. As pointed out earlier, the refutation of the normal spreading center hypothesis was published soon after Hall's work and shows the sediment-corrected depth of the

AMR is too shallow to have formed at a normal Cretaceous spreading center (Delaurier, 1978).

The Arctic 2000 profile crossed the northern Mendeleev Ridge, trending E-W at 82° N was 500 km in length (Ivanova et al., 2006). They collected seismic refraction, shallow reflection, and gravity data. The refraction Moho was imaged at 32 km beneath the ridge and 13 km at the ridge margins. These depths were used to constrain gravity models. The authors presented a velocity-depth structure and gravity anomalies, from which they prefer the interpretation that the Mendeleev Ridge is "highly attenuated continental crust". The results of the Arctic 2000 profile are discussed in greater detail in the discussion and are compared to the results from this study.

The acquisition of wide-angle refraction data over the Mendeleev Ridge presented by Ivanova et al. (2006), along with the MCS reflection, refraction, co-registered gravity and multi-beam bathymetry data presented in this study, provide new insights into the structure of the Mendeleev Ridge and how it relates to the Alpha Ridge and neighboring features.

Chukchi Borderland

The Chukchi Borderland has long been considered a continental fragment (Fig. 1) (Hunkins, 1966; Hall, 1990; Klemperer et al., 2002; Wolf et al., 2002). Consistent with the rotational model for the Canada Basin, Grantz et al. (1998) suggest the Chukchi Borderland rifted away from the Canadian Arctic shelf, together with Arctic Alaska. Piston cores collected perpendicular to the slope of the Northwind Ridge, progressively sampled stratigraphic units from much of the Paleozoic through Late Jurassic. Contemporaneous sections from the Sverdrup Basin were interpreted to support the cross-basin transport of the Chukchi Borderland.

The earliest syn-rift sediments were deposited in the Dinkum Graben by the early Jurassic. Riftogenic lutites recovered from the Northwind Ridge suggest the Chukchi Borderland was isolated from the Sverdrup Basin and Arctic Alaska by this time, and that seafloor spreading initiated by late Jurassic ended no later than Aptian time, the beginning of the magnetic Cretaceous normal period. To account for the present location

of the Chukchi Borderland, which is not oriented such that would result purely from counter-clockwise rotation from North America, Grantz and May (1982) and Grantz (2006) suggest later, clockwise rotation of the Chukchi microplate away from the E. Siberian shelf, possibly contemporaneous with spreading in the Canada Basin and prior to the emplacement of the Alpha and Mendeleev Ridges. Satellite derived gravity anomalies also reveal the Chukchi Borderland as extended continental crust, where extension was oriented E-W (Laxon and McAdoo, 1994). The relationship between the Chukchi Borderland and the Mendeleev Ridge has not been studied directly and is not well understood.

Makarov Basin

The Makarov Basin lies between the AMR and the Lomonosov ridge (Fig. 1). The Basin itself is sub-divided by a basement ridge paradoxically called the Arlis Gap. The basement ridge as revealed by gravity (+10/-15 mGal) and magnetic (800 nT) anomalies, acts as a dam to sediments; thus sediments are ~ 3.5 km thick south of the ridge and ~1.5 km thick north of the ridge (Kutschale, 1966; Sorokin et al., 1999). The region south of the Arlis Gap is the Wrangell Abysall Plain or Podnikov Basin and the area north of the ridge has been called the Fletcher Abyssal Plain though is now simply referred to as the Makarov Basin.

The origin of the Makarov Basin is enigmatic. Taylor et al. (1981) tentatively identify lineated magnetic anomalies 21-34 (49 Ma – 84 Ma) and propose a seafloor spreading origin. Gravity modeling found the Makarov Basin crust to be 23 km thick (Ostenso, 1964). Jackson et al. (1986) hypothesize that similar seismic velocity gradients indicate that the crust underlying the Makarov Basin is structurally contiguous with the Alpha and Mendeleev Ridges. A more recent Russian seismic expedition visited the Makarov Basin where velocity gradients (upper basement = 5.0-5.2 km/s; lower crust = 6.7 km/s) revealed both oceanic layer 2 and 3 respectively. Also finding a total crustal thickness of 23 km, the authors prefer the interpretation of thickened oceanic crust but do not rule out a continental origin (Sorokin et al., 1999)

Circum-Arctic Cretaceous Volcanism

Cretaceous volcanics have been observed in many parts of the circum-Arctic and may constrain the timing of extensional events in the Amerasian Basin, and formation and evolution of the AMR. Volcanics are found in the Canadian Arctic Islands, northern Greenland, Franz Joseph Land, Svalbard, and the East Siberian Shelf. As pointed out by Drachev et al. (1999), the hypothesis regarding the AMR as a hotspot track emplaced onto oceanic crust did not consider the context of extensive continental flood volcanism of the circum-Arctic. As more Cretaceous volcanic events have been described and dated, it appears likely that these events are related, temporally, spatially, and compositionally. Models describing the development of the AMR, and the tectonic history of the Arctic basin, must explain the likely relationship with these volcanic provinces.

Arctic Large Igneous Province

Tarduno et al. (1998) describe Cretaceous basalts from the high Canadian Arctic and suggest they may be part of a large Arctic Large Igneous Province (LIP). Drachev and Saunders (2006) describe tholeites from Franz Joseph Land and the De Long Archipelago in the E. Siberian Sea. They suggest that these basalts are the result plume-related volcanism, and that they are part of a regional set of volcanic occurrences in the circum-Arctic that constitute a LIP that was consequently broken up by the opening of the Amerasian and Eurasian basins. K-Ar dates point to formation between 130 and 100 Ma. They tentatively separate the Cretaceous basalts into two chemically distinct groups: one plotting on a K_2O-TiO_2-P_2O_5 diagram at the divide between continental and oceanic tholeites, and the other more rich in incompatible elements, indicating intra-plate volcanism.

Maher (2001) presents the Alpha Ridge as part of an Arctic Cretaceous LIP along with coeval basalts recovered from Svalbard, Franz Joseph Land, Axel Heiberg Island, and Ellesmere Island; hypothesizing that the ridge is not a relic track of a hotspot, but rather the initial eruption center of a large plume head. Magmatism is suggested to have

occurred in two primary phases between 135 Ma and 90 Ma according to both sample ages and the correlation of regional breakup unconformities.

Canadian Arctic Margin

The presence of Cretaceous volcanics along the Canadian Arctic Margin has been recognized for some time (Embry and Osadetz, 1988; Embry and Dixon, 1990).

Volcanic rocks from Axel Heiberg and Ellesmere Island are divided into two suites by Estrada and Kunst (2004): early Cretaceous tholeitic olivine basalts and Late Cretaceous to Paleocene alkaline volcanics. The tholeitic basalts exhibit chemical and temporal affinities to rocks from Svalbard and Franz Joseph Land with some rocks dated (biostratigraphically and with Sr and Nd isotopes) to 115 Ma and others to 95 Ma. These rocks are interpreted to represent erosional relics from LIP sourced continental volcanism.

The alkaline suite of rocks from northern Ellesmere Island correlate with rocks from northern Greenland and date roughly to 80 Ma. These rocks likely represent branches of rift volcanism over a large region of diffuse extrusion preceding the opening of the Eurasian basin. A genetic link is proposed between these rocks and the younger (61-58 Ma) alkali volcanics of the Nares Straight region. Estrada and Kunst (2004) also recognize the compositional and temporal similarities to the Alpha Ridge alkali basalts (~82 Ma) but stop short of relating the volcanic events due to the small sample population of Alpha Ridge basalts.

Further studies on rocks from the Strand Fiord Formation from Axel Heiberg and Ellesmere Islands by Weaver et al. (2006) also find compositions similar to volcanics of east Greenland and an $^{40}Ar/^{39}Ar$ age of 95 ±.9 Ma. The authors find the predictions of ~130 Ma aged volcanism in the region, derived from plate tectonic models (Lawver and Muller, 1994), are incongruent with their results.

Villeneuve and Williamson (2006) present $^{40}Ar/^{39}Ar$ dates for volcanic rocks and intrusives from Axel Heiberg and northern Ellesmere Island. They find that volcanism in the Sverdrup Basin is defined by two main pulses of magmatism. Intrusive magmatism peaked at 129-127 Ma and flood basalts peaking at 98-92 Ma.

East Siberian Sea

Cretaceous basalts have also been collected from Bennet Island of the Delong Plateau (Fujita and Cook, 1990). Flows are divided into two groups. The lower unit consists of Mg-rich melanocratic picritic basalts of ~119 Ma, and the upper unit resembles evolved continental tholeites of ~112 Ma (Drachev et al., 1999; Drachev and Saunders, 2006). Drachev et al. (1999) introduces the prospect of a genetic relationship between volcanism of the Delong Plateau and the AMR (Fig. 2).

Cruise Description and Project Objectives

In the summer of 2005, USCG Icebreaker Healy (Cruise I.D.: H0503) crossed the Arctic Basin from Dutch Harbor, Alaska to Tromso, Norway to collect geophysical data and take shallow cores to gain greater insight into the paleo-oceanographic, depositional, and tectonic histories of the Arctic Basin. The coring project, analyzing sediments collected from a jumbo piston core, was aimed at reconstructing sedimentation histories and hence, paleo-environments of Arctic sub-basins. Gaining clarity into the mechanisms that drive paleo-environmental cycles in the Arctic lends greater ability to interpret present changes occurring throughout the Arctic.

Data collected from the geophysical project leads to a greater understanding of: 1) The depositional histories of the Arctic sub-basins, 2) The structure and geologic origin of specific submarine features in Amerasian Basin, 3) The tectonic framework of the Amerasian Basin, the results of which extend beyond the Arctic and will aid in completion of the global tectonic circuit, in which the Arctic is typically ignored.

Geophysical data sets collected included: co-registered multi-beam bathymetry (Sea Beam 2112) and marine gravity, chirp sub-bottom profiling, seismic refraction and multi-channel seismic reflection. This was a unique opportunity to image a cross-section across much of the Arctic Basin and to collect data over submarine ridges, plateaus, and basins where little to no research has been focused before. During the course of the cruise, geophysical data were collected over the Chukchi Shelf, the Northwind ridge and Chukchi Plateau, the Mendeleev and Alpha ridges, the Makarov Basin, the Lomonsov Ridge, the Eurasian Basin, and the Yermak Plateau. At times progress was hindered by

the presence of multi-year ice, especially in the Eurasian Basin where little to no seismic data was collected for ~1 ½ weeks due to severe ice conditions obstructing the mobility of the ship. On the whole though, the cruise was a great success with ~2200 km of seismic reflection data collected.

The specific objectives of this project are to process, integrate, and interpret the geophysical data collected over the Mendeleev Ridge during the H0503 deployment (Fig. 4). The scientific aims are to describe: 1) the crustal style of the ridge, 2) the depositional and structural histories, 3) what these results suggest about the origin of the Mendeleev Ridge, and tectonic evolution of the Amerasian Basin.

Experiment Overview, Methodology, and Results

Seismic Reflection

Experiment Overview and Methodology

The seismic experiment was designed and primarily implemented by a group from the University of Bergen. Approximately 730 km of multi-channel seismic reflection (MCS) data was recovered over the Mendeleev ridge during the H0503 deployment, along with co-registered gravity data and seismic refraction data (Fig. 5). The seismic source was two 250 cu in G-guns. The streamer length was limited by ice conditions to ≤ 300 meters. Wear and tear from towing the analog streamer through ice degraded the hydrophones and the number of active channels ranged from 24 to as few as 11. The signal was digitized on board using two Geometrics Geode seismographs. Shot spacing was 20 seconds or ~40 m with a 2 millisecond sampling rate. Shot depth was approximately 5 m although it varied with ship speed and ice conditions. Hydrophone spacing was 12.5 m and stacked data are grouped into 6.25 m CDP (common depth point) bins with an average fold of 4. Straight-line geometry is assumed.

The MCS data required significant manual trace editing and automated noise attenuation to eliminate random electrical noise. Frequency-wave number (FK) filtering was used to eliminate low velocity noise caused by the streamer traveling through heavy ice. After the trace editing and filtering, individual traces were bandpass filtered at 6-100

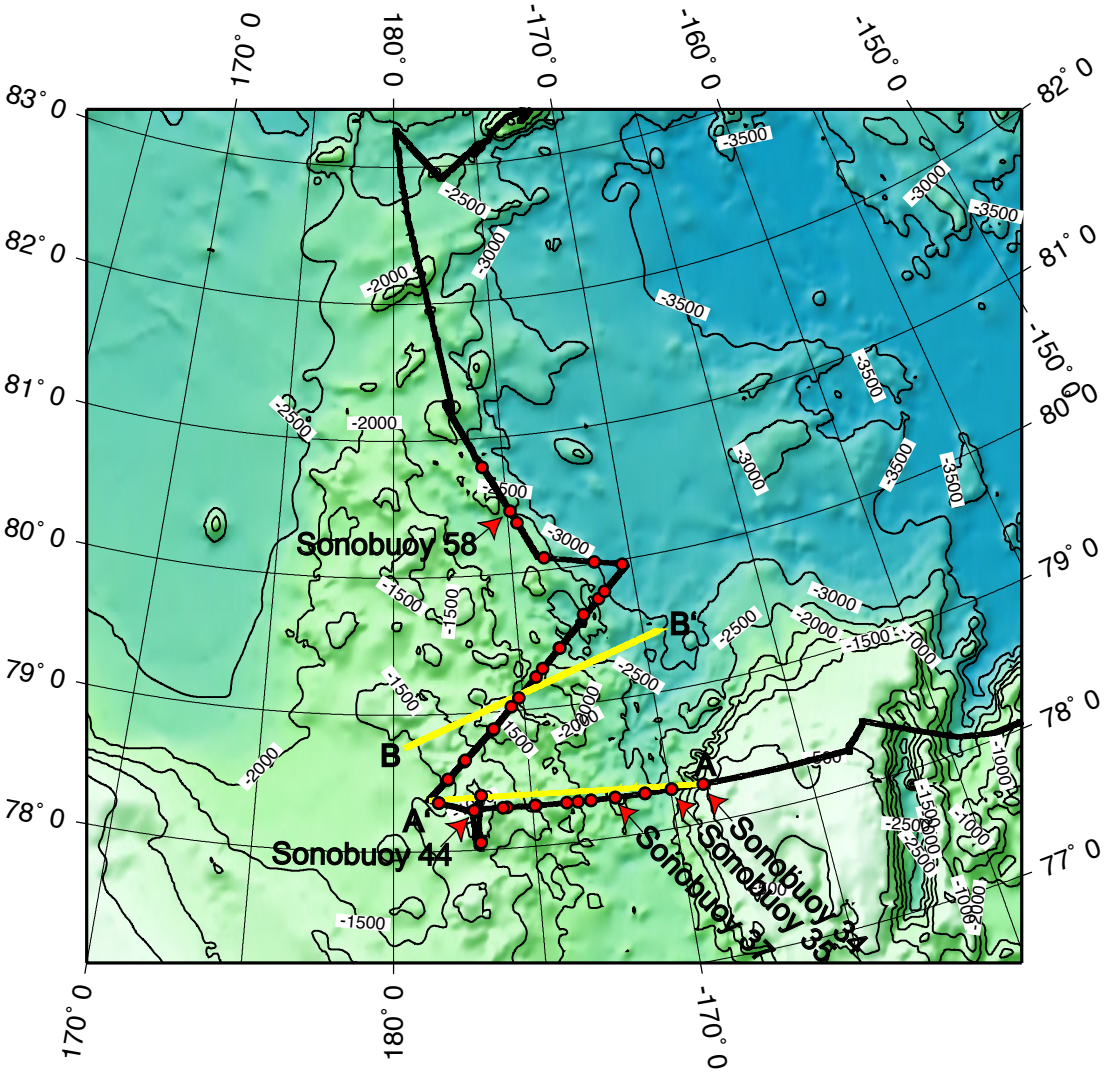

Fig. 4: Mendeleev Ridge Study Area. H0503 shiptrack over the MR is plotted on regional bathymetry map. Red dots indicate sonobuoy drop locations, and modelled sonobuoys (34, 35, 37, 44, 58) are identified. Yellow lines A-A' and B-B' represent projected gravity lines. Gravity models for these profiles are shown in Figs. 17 and 18. Gravity data projection and map generation utilized Generic Mapping Tools (GMT) (Wessel and Smith, 1998).

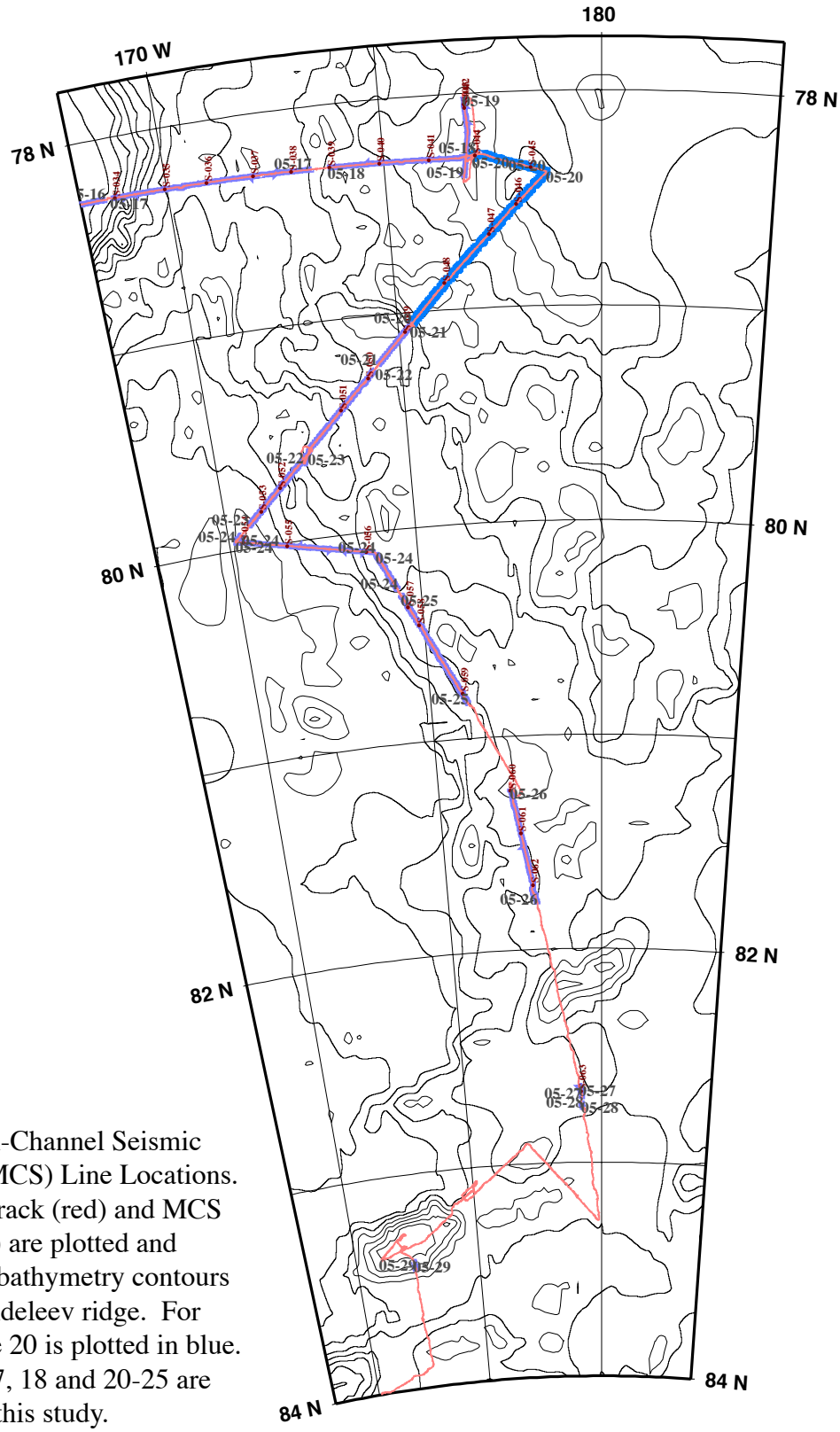

Fig. 5: Multi-Channel Seismic Reflection (MCS) Line Locations. H0503 ship track (red) and MCS lines (purple) are plotted and labeled with bathymetry contours over the Mendeleev ridge. For example, line 20 is plotted in blue. MCS lines 17, 18 and 20-25 are presented in this study.

Hz. Traces were gathered into CDP bins. The normal moveout correction was made assuming constant velocity layers for the water column, sediments, and basement. While imprecise, these velocities are largely consistent with results from the seismic refraction modeling. Initial attempts to derive more accurate layer velocities, through velocity analysis, was not successful as the data were not adequately dense to provide sufficient signal coherency. The data were then stacked and migrated with Stolts' FK, constant velocity (1490 km/s) algorithm (Yilmaz, 2001). Water velocity migration is appropriate here as the CDP data are not sufficiently robust to gather conclusive layer velocity information, and the intended interpretation of this data does not require significant refinement of the velocity structure.

NSF supported SIOSEIS software was used during initial data processing (Henkart, 1981). Final processing utilized Landmark's Promax software as well as SIOSEIS in order to utilize the most effective functions from both programs.

Sediment unconformity and basement horizons were identified and picked digitally for use in both the seismic refraction, and gravity modeling. Layer boundaries were determined according to the following criteria: 1) reflection character i.e. reflector spacing, amplitude, and internal geometry, 2) lateral continuity, 3) (For sediments) stratigraphic relationships e.g. onlap, pinch outs, etc…, 4) results from gravity and refraction modeling provide information whether or not horizons picked sufficiently reproduce the velocity structure or mass distribution across the ridge.

Stratigraphic and depositional interpretations are made considering the following: 1) The criteria listed above, 2) Relative thickness, 3) Relative age, 4) Application of regional sedimentation rates in order to calculate approximate depositional ages.

Results

The MCS survey over the Mendeleev Ridge was broken into seismic lines 17, 18, 20-25 (Fig. 5). The survey can be more coarsely separated into two lines, A-A' (17, 18, 20a), and B-B' (20b-23). These two lines correspond to the two gravity profiles presented here and provide a natural division in which to interpret the structures of the ridge (Fig. 4). The MCS images are shown in Figs. 6a-g.

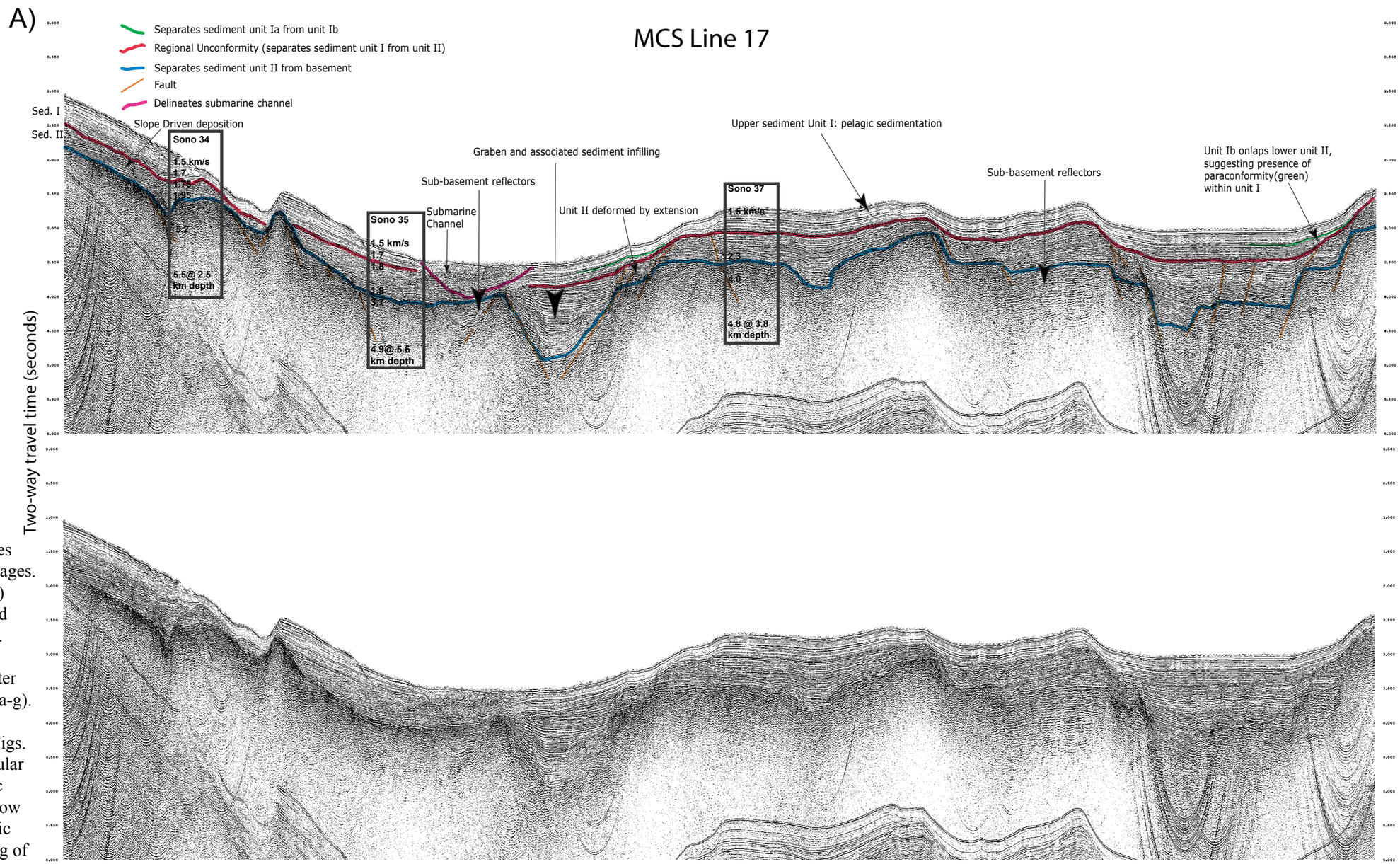

Fig. 6: MCS Images and Interpreted Images. Interpreted (above) and non-interpreted MCS lines(below). MCS line number labeleld at top center of each plot (Fig 6a-g). Location of MCS lines is shown in Figs. 5 and 25. Rectangular boxes with seismic velocities listed show results from seismic refraction modeling of respective sonobuoys.

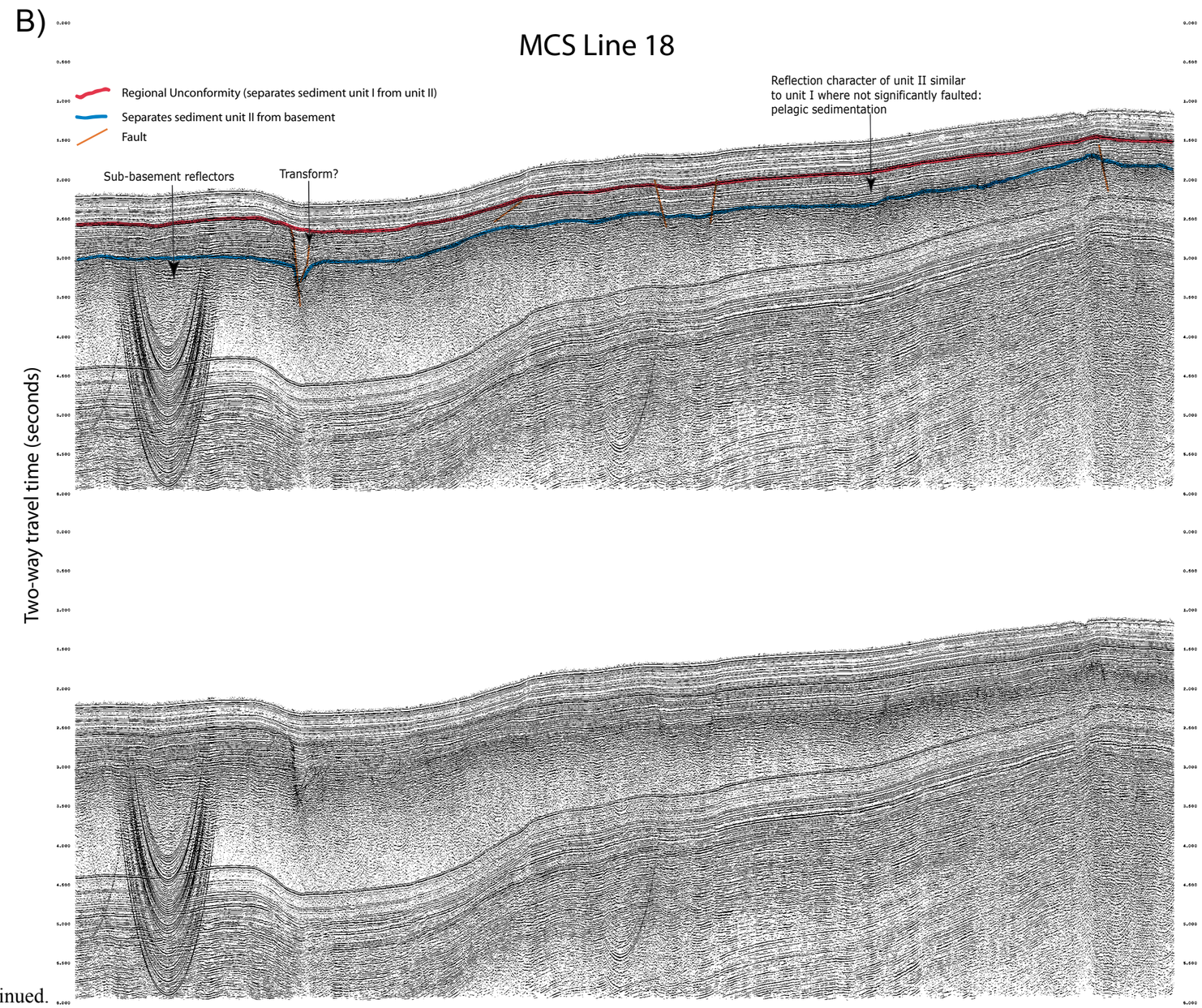

Fig. 6 continued.

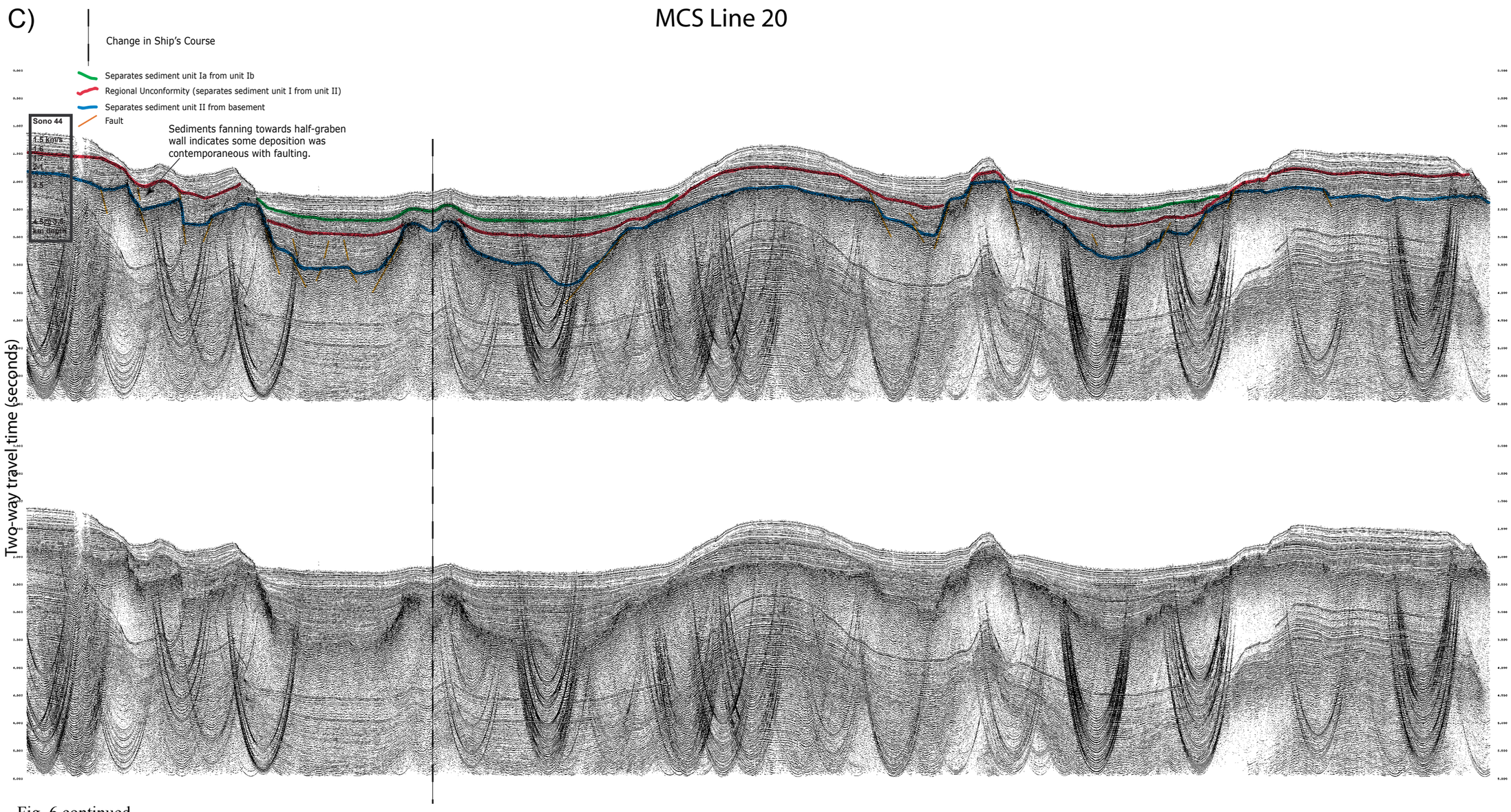

Fig. 6 continued.

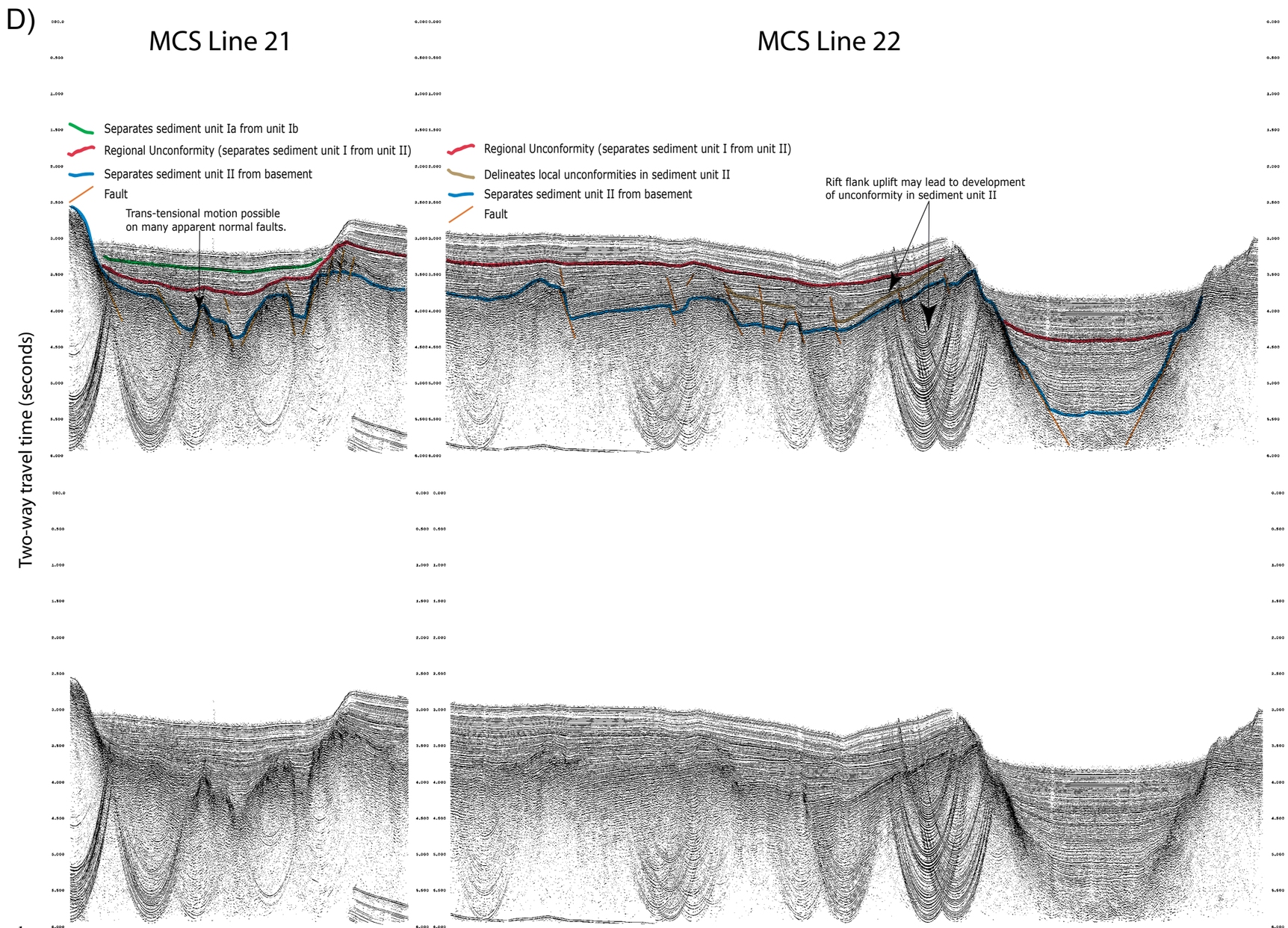

Fig. 6 continued.

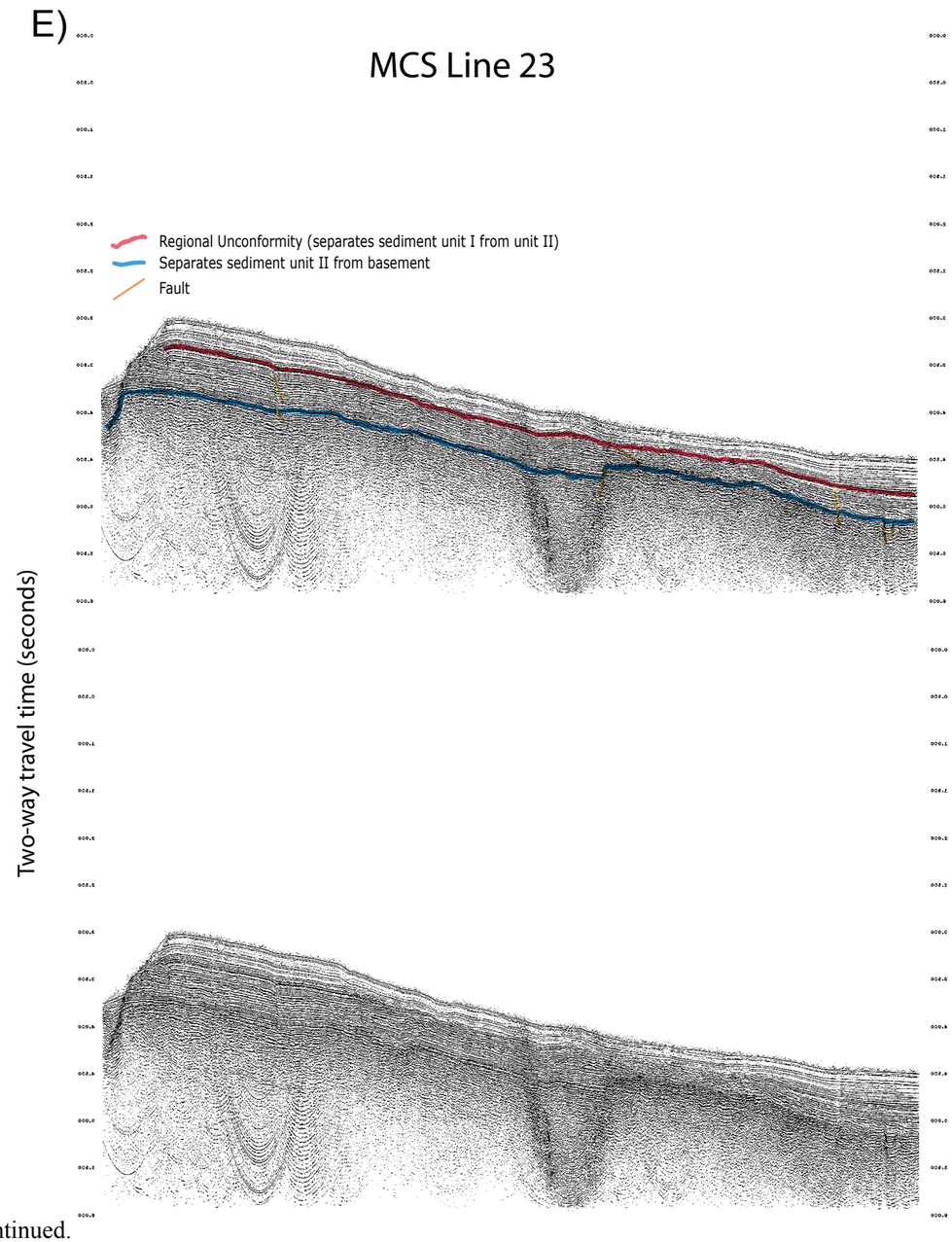

Fig. 6 continued.

F)

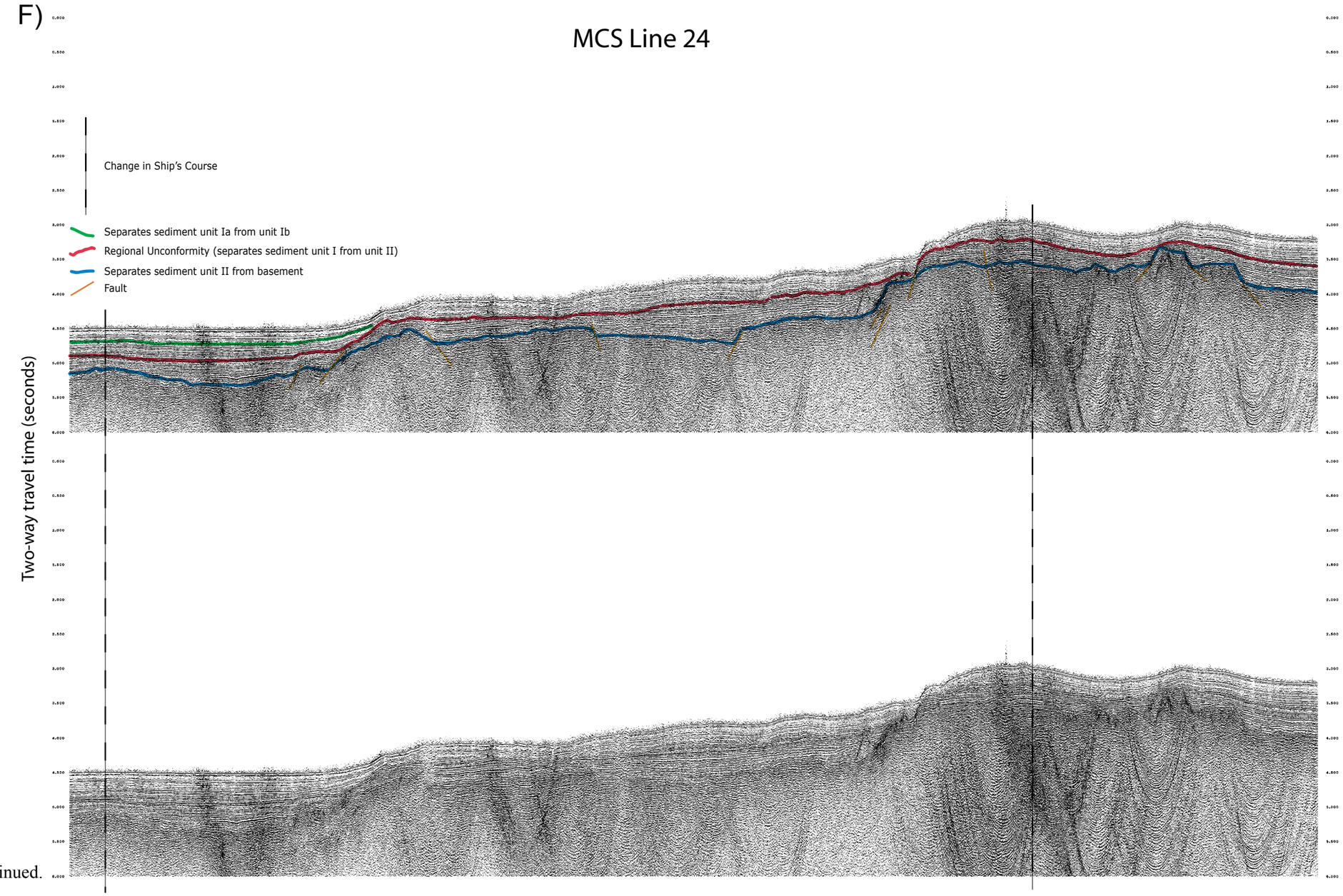

Fig. 6 continued.

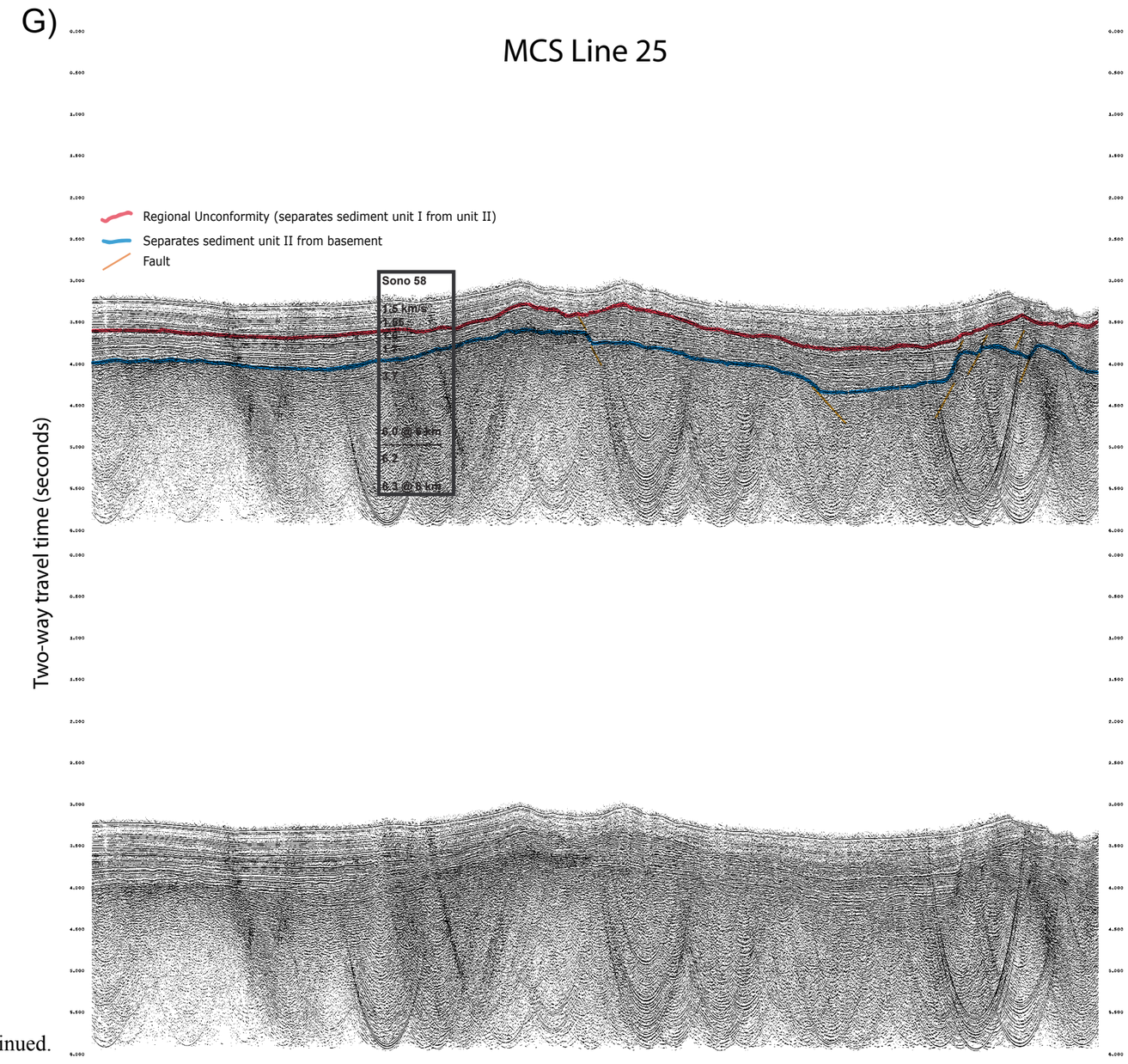

Fig. 6 continued.

Reflection images reveal two distinct sedimentary units. The upper sediment "unit I" (thickness: 0.0-0.7 secs TWT, or approximately 0-560 m) is laterally continuous and appears to derive entirely from pelagic sedimentation (Fig. 6a). This conformable drape layer is present across most of the Mendeleev Ridge with average thickness of ~0.3 secs TWT (~250 m) (Fig. 7). It thins or disappears completely over some steep slopes. In places, small vertical offsets of reflectors in Unit I are likely due to differential sediment compaction. There are likely at least two distinct sediment horizons within Unit I, due to the multiple pinchouts of the lower layer of unit 1 (Ib). On Fig. 6a, unit Ib pinches out against a graben wall. This unconformity may represent a hiatus between two successive passive pelagic units. As there is no significant deformation of Ib, all of Unit I was deposited subsequent to the most recent tectonism. At the base of the Chukchi Plateau, Unit I was entirely scoured and then refilled leaving a channel approximately 6 km wide and 500 m deep (Fig. 6a).

Separating Unit I from lower sediments is an easily identifiable unconformity that is traceable across all of the Mendeleev Ridge (Fig. 6a-6g).

The lower, higher reflectivity Unit II (0.0-1.0 secs TWT or approximately 0 – 900 m) is highly deformed in places. The thickness of Unit II is significantly greater in grabens, and is more variable across all lines than that of Unit I (Fig. 7). In places, it contains more closely spaced reflectors and exhibits more complex reflection patterns. This reflection character may be a consequence of greater compaction. The greatest deformation occurs where the basement is significantly normal faulted. The more complicated sedimentary patterns may also be caused by the geographic migration of sediment delivery mechanisms. In Fig. 6c sediments appear to fan towards half-graben walls, suggesting that deposition and deformation occurred simultaneously. Unit II was likely deposited prior to and contemporaneous with tectonic deformation.

Unit II is mostly conformable over areas not affected by faulting, and has a reflection character similar to Unit I. This observation indicates that Unit II is also predominantly derived from passive sedimentation, though along steep slopes,

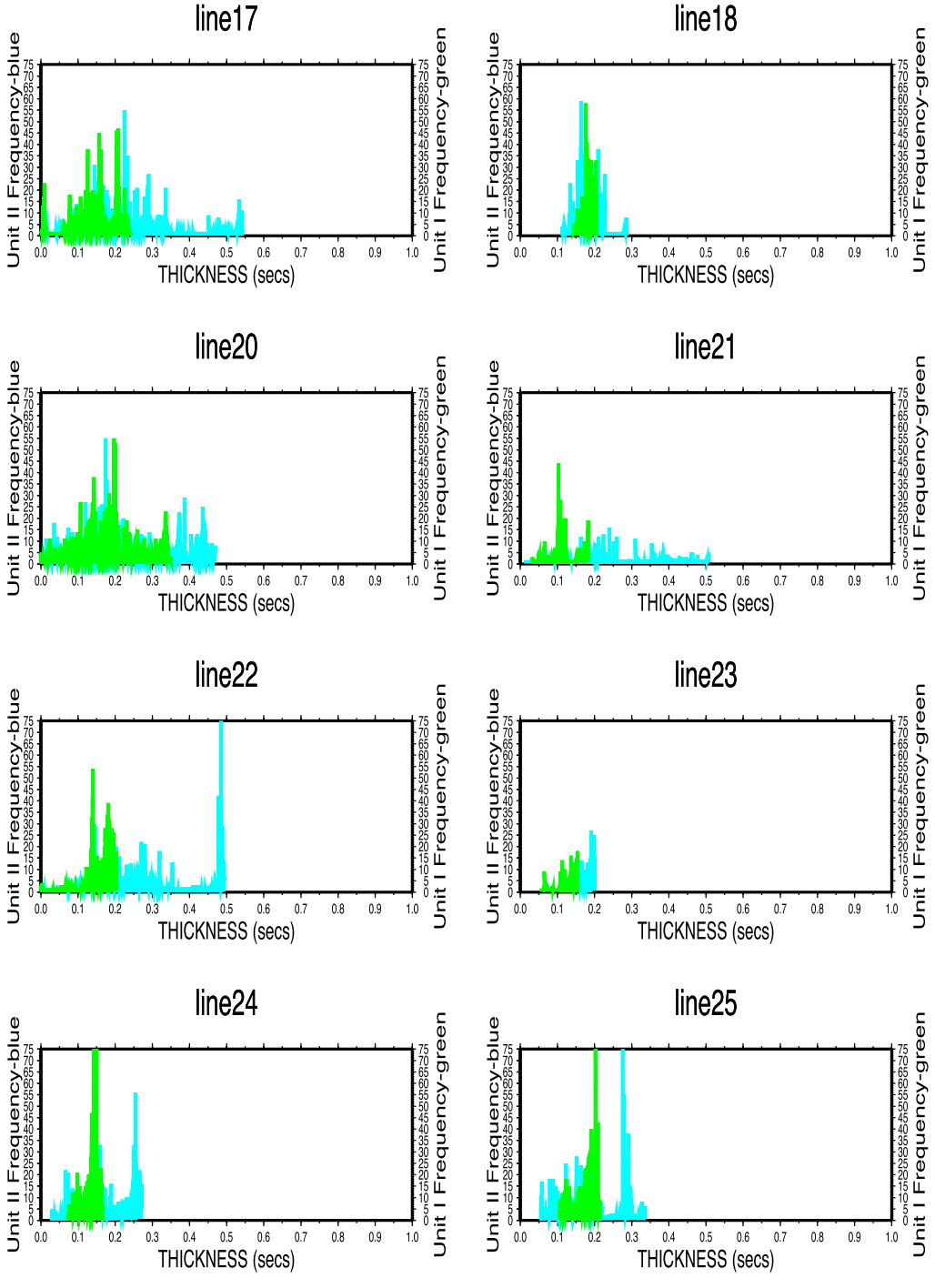

Fig. 7: Sediment Thickness Histograms in seconds (one way travel-time) for both sediment units I and II sampled from each MCS line. The vertical axis records the number of CDP nodes that record a specific thickness. Note the greater variation in thickness for the lower sediment unit II.

specifically on the flanks of the Chukchi Plateau, much of the unit appears to be a product of mass wasting (Fig. 6a).

Unit II is also effected by the large channel scour of Unit I. In Fig. 6b there is a low relief fault that could be strike-slip. It incises both the basement and Unit II exhibiting a small flower structure. Small, high slope features within some grabens also indicate some strike slip motion. In one location, younger sediments within Unit II onlap the basement or older sediments conformably overlying the basement (Fig. 6d). This unconformity may potentially indicate rift flank uplift. See Fig. 7 for measured sediment layer thicknesses.

The basement of the Mendeleev Ridge and between the Chukchi Plateau and the Mendeleev ridge exhibits very high relief due to normal faulting. Mostly the basement appears homogenous, though in some areas we see discrete horizontal to sub-horizontal coherent reflections. Specifically, along the flank of the Chukchi Plateau, there is a visible graben-like structure within the basement (Fig. 6a). This may represent volcanic infilling of the preexisting structure. Sub-basement reflectors observed farther down the line in Figure 6a and in Figure 6b cannot be conclusively interpreted as they may represent lithified stratigraphy or volcanic flows.

The reflection multiple of the basement reveals many deeper reflecting layers but these reflectors cannot be confidently interpreted. The reflectors are likely multiples of multiples or peg leg multiples, but may represent litihified stratigraphy or volcanic flows.

Seismic Refraction

Experiment and Methodology Overview

Seismic refraction was collected along MCS profiles using the same gun source and one-component marine sonobuoys as receivers (Fig. 4). When the seismic reflection experiment was active, and where ice conditions permitted, one active sonobuoy was deployed in the water. For Seismic experiment parameters, see ‘ Experiment and Methodology Overview” from the Seismic Reflection section. In total, 24 sonobuoys were deployed over the Mendeleev Ridge, with 6 containing traceable refractions. Total

sonobuoy offset was limited by line of sight and FM carrier loss. The average total offset achieved was ~25 km. Most refractions however, are visible to only ~15 secs with one sonobuoy showing refractions traceable to > 20 secs. This limitation was the result of utilizing lower volume guns optimized for the MCS experiment. As a result, observed refracted waves likely sampled ≤ 8 km of crust (Figs. 8-12).

Refraction data were bandpass filtered to 6-60 Hz. Predictive deconvolution was applied to refraction plots to aid in identifying phase arrivals, though no picks were made on deconvolved plots, as deconvolution is a transformation of the wave field and we have no knowledge of the source signature

The objective in refraction modeling is to produce a velocity-depth model that accurately predicts the observed travel-times as picked from the refraction data. A 2-D ray-tracing algorithm was used to calculate layer velocities with RAYGUI (Zelt and Smith, 1992; Song and ten Brink, 2004). Results presented here are based only on forward runs through velocity-depth models. Model shot-offset was calculated from the direct arrival assuming a water velocity of 1450 m/s. This was done because the exact location of the sonobuoys was not known and so straight-line geometry was assumed. Acceptable models reproduced the arrival picks to within 0.1 seconds. As an assessment of model fit, whole model root mean square (RMS) differences between observed and calculated arrivals were calculated.

Initial velocity-depth models include bathymetry, unconformity, and basement horizons all picked from the co-registered MCS data (Figs. 4 & 5). Picks for both the refracted arrivals and MCS observed horizons were made in Promax.

Early on, only one sedimentary layer was invoked. However, travel time misfits in the refraction models and the clear presence of a regional unconformity in the MCS data, led to the addition of the unconformity to the velocity-depth models. Including as much reliable a priori information e.g. MCS horizons as well as amplitude, geologic, and tectonic information, yields more accurate modeling results (Zelt, 1999). Models presented here were forced to honor the initial geometries of the subsurface as picked from MCS data.

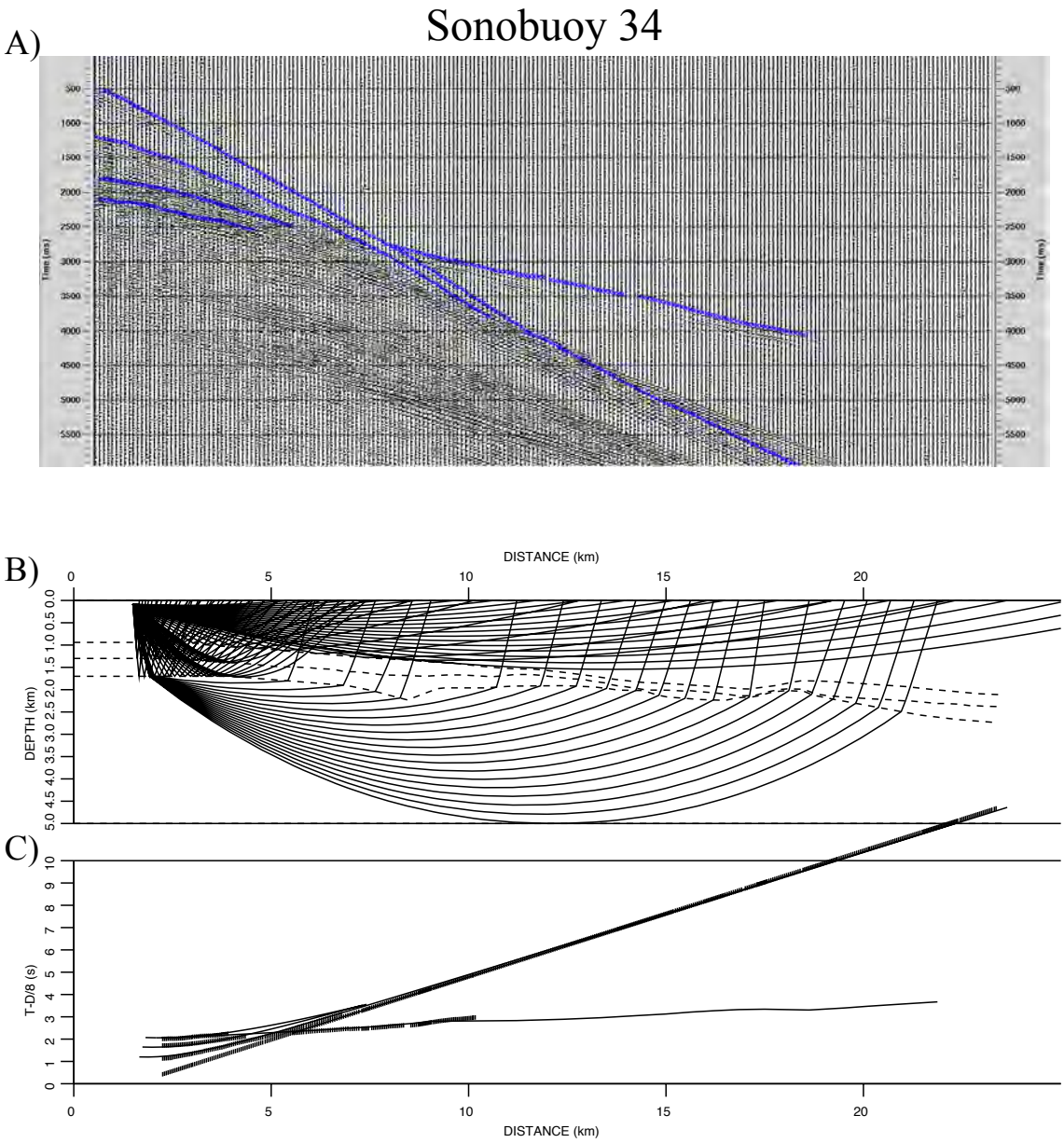

Fig. 8: Seismic Refraction Model; Sonobuoy 34. Complete record sections are shown in Appendix B. A) Record section of sonobuoy data. Arrival picks used for ray tracing are shown in (blue). B) Velocity model. (Solid lines) are ray paths and (dashed lines) are layer boundaries. Synthetic waves are reflected off the seafloor, regional unconformity, and basement. Synthetic refracted waves are modeled through the water column for direct arrivals and through the basement to resolve upper basement velocities. C) Calculated travel-time curves (solid lines) are plotted with observed picks (hachures) to determine model fitness.

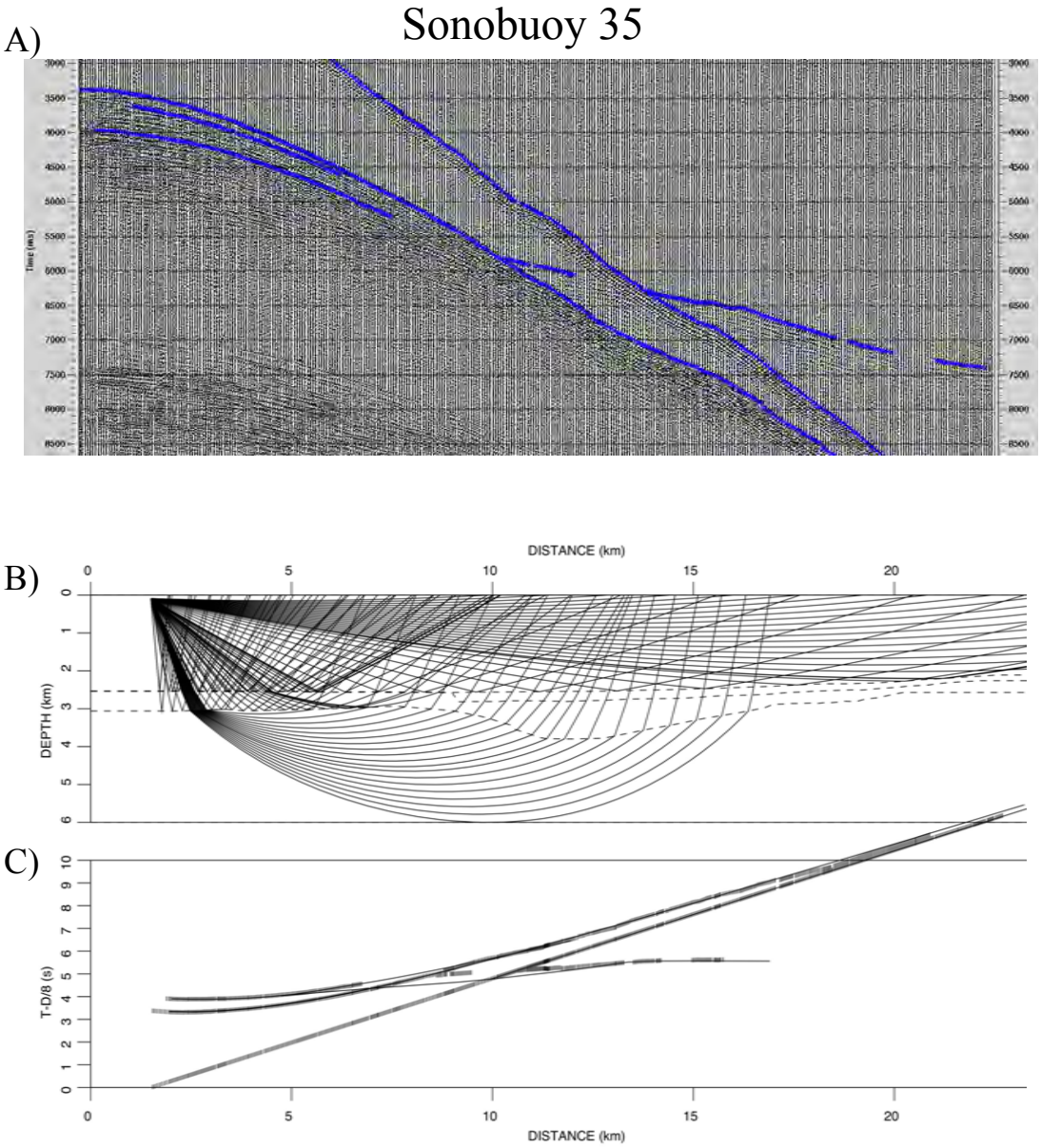

Fig. 9: Seismic Refraction model; Sonobuoy 35.

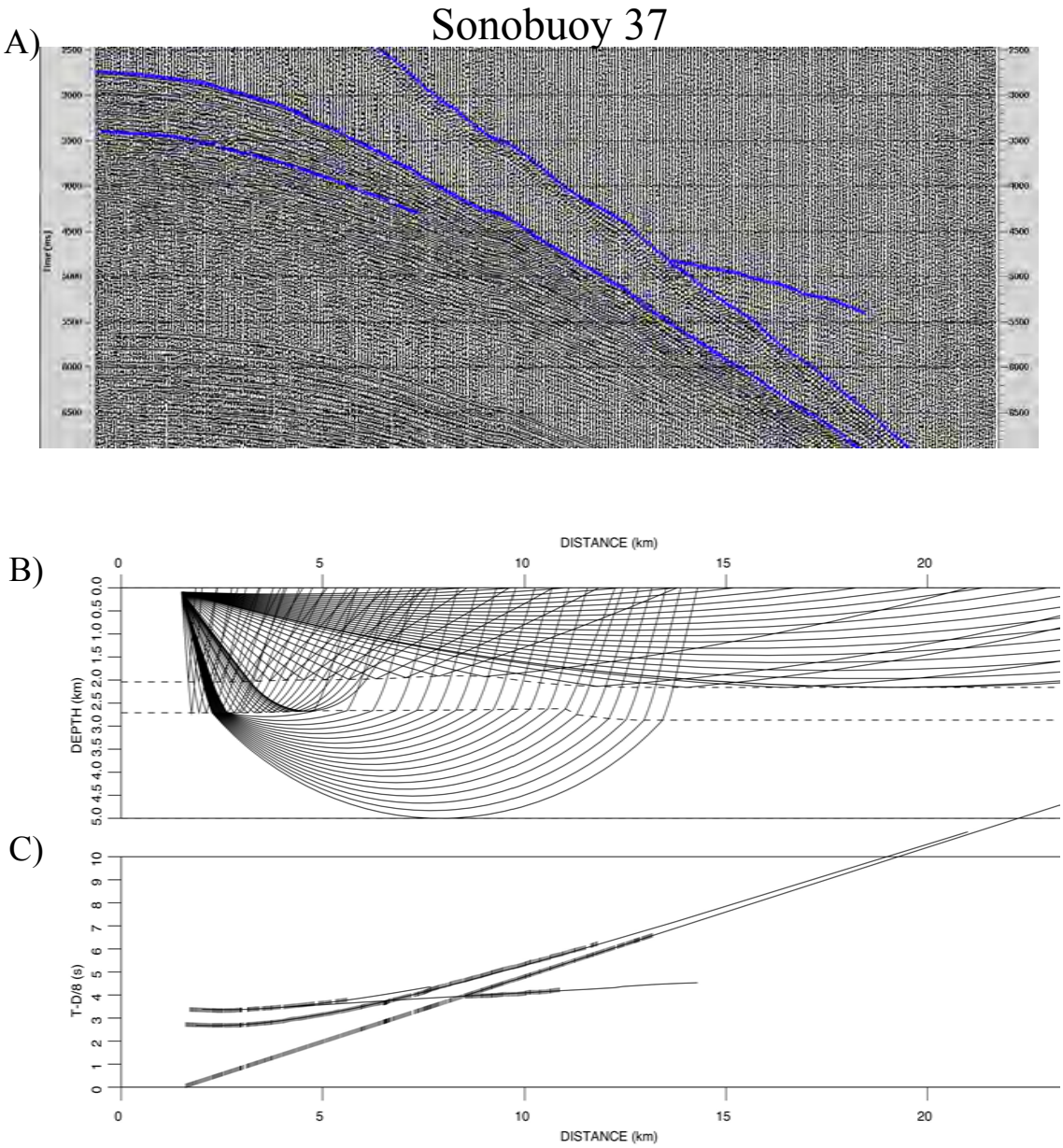

Fig. 10: Seismic Refraction Model; Sonobuoy 37. Note that only one sediment horizon is included in the velocity model here.

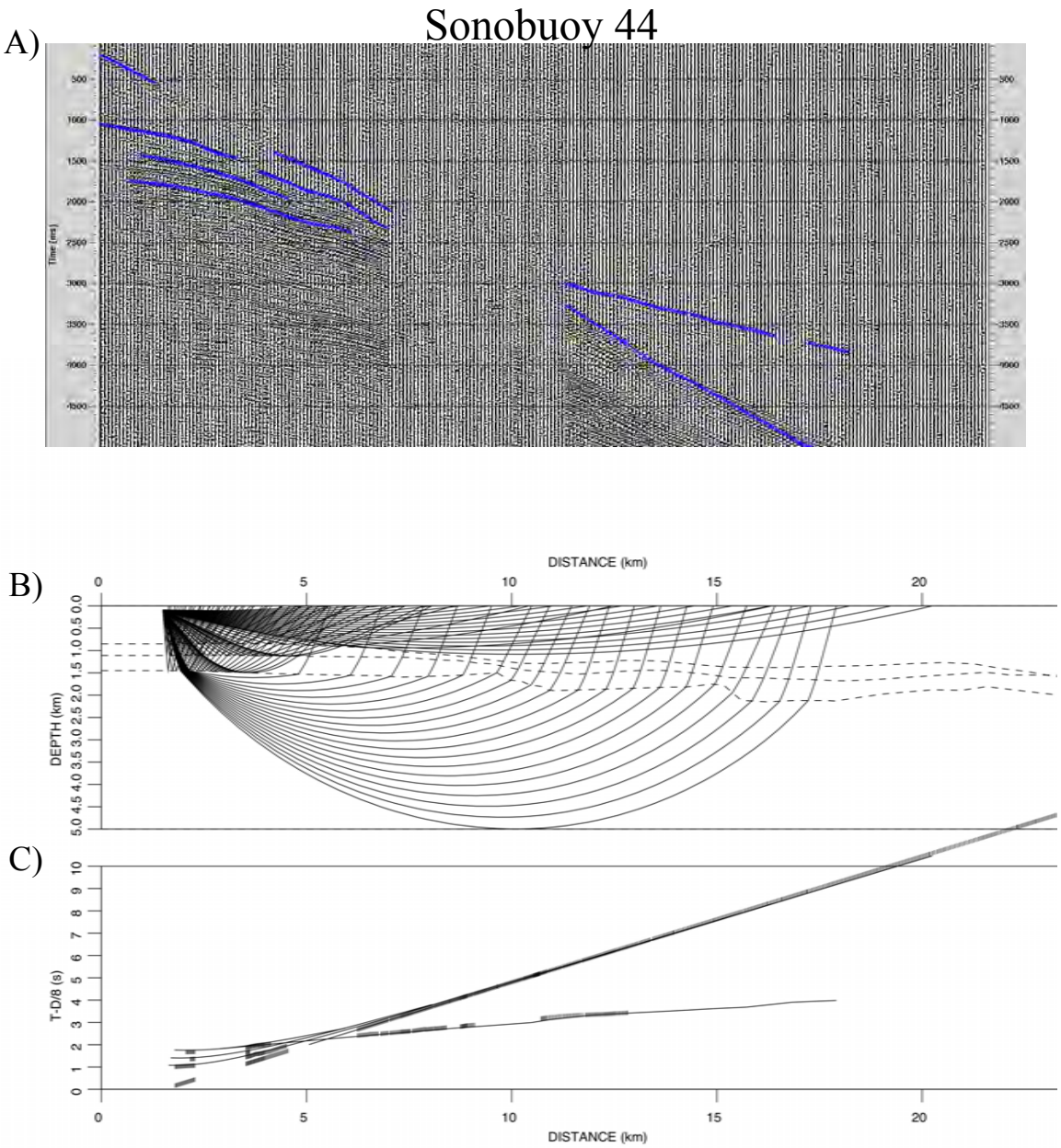

Fig. 11: Seismic Refraction Model; Sonobuoy 44.

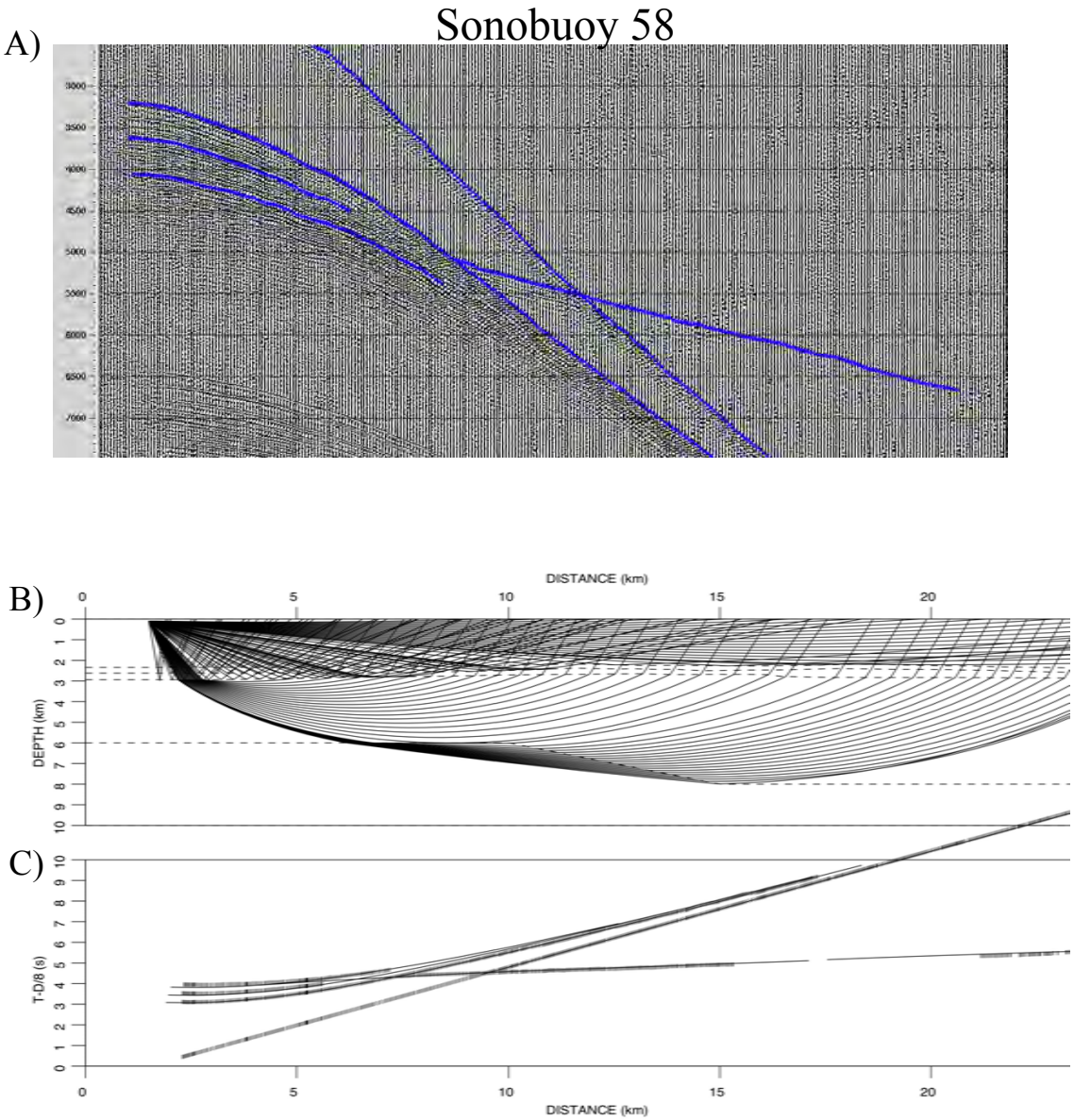

Fig. 12: Seismic Refraction Model; Sonobuoy 58. A) Note that offsets > 15 km are not shown in this record section. Later arrivals can be seen in Appenix B. B) Unlike the previous velocity models, an extra velocity boundary in the basement was required to reconcile later arrivals as seen in panel (C).

Within each velocity-depth model, depths for each velocity boundary were converted from travel-time, and velocities were applied to both the top and bottom of each horizon, increasing linearly with depth (Figs. 8a-e). To achieve better fit, layer velocities were adjusted with each forward run in an attempt to satisfy both reflection and refraction arrivals. A successful model requires that assigned velocities must produce travel-time curves that match the observed zero-offset arrivals within the 0.1 second margin of error, as well as reproduce the gradient of the observed phase arrivals. Interface depths were not adjusted during the modeling process. This trial and error method is repeated until the RMS error ≤ 0.1 seconds to minimize the observed error.

As a further independent check, a comparison is made between the seafloor depths calculated from the MCS data, and the center-beam of the bathymetry data. The results from this analysis reveal that any minor seafloor misfits in the refraction modeling (observed vs. calculated seafloor) are far more likely to occur from variations in regional bathymetry due to the drift of the sonobuoy, or errors in arrival picking. Results from this analysis are presented in Appendix A.

Results

Results are based on the modeling of five sonobuoys over the flank of the Chukchi Plateau and along the Mendeleev Ridge, and results are summarized in Fig. 17. For sonobuoy locations, see Fig. 4. Full record sections are shown in Appendix B. Direct arrivals were typically picked to ~20 km offset and refractions picked with offsets between 10 km and 20 km. Observed refracted waves traveled between 2 km and 8 km beneath the seafloor.

The goal of the seismic refraction work was to provide physical constraints on the sediment and crustal material of the Mendeleev Ridge, as well as constrain the gravity models. Understanding that during this experiment, we would not be imaging depths approaching the crust mantle boundary, the primary objective of the modeling was to test the consistency of the velocity structure from the upper basement as a proxy for lithology. If highly consistent velocities result, it suggests an oceanic origin due to the

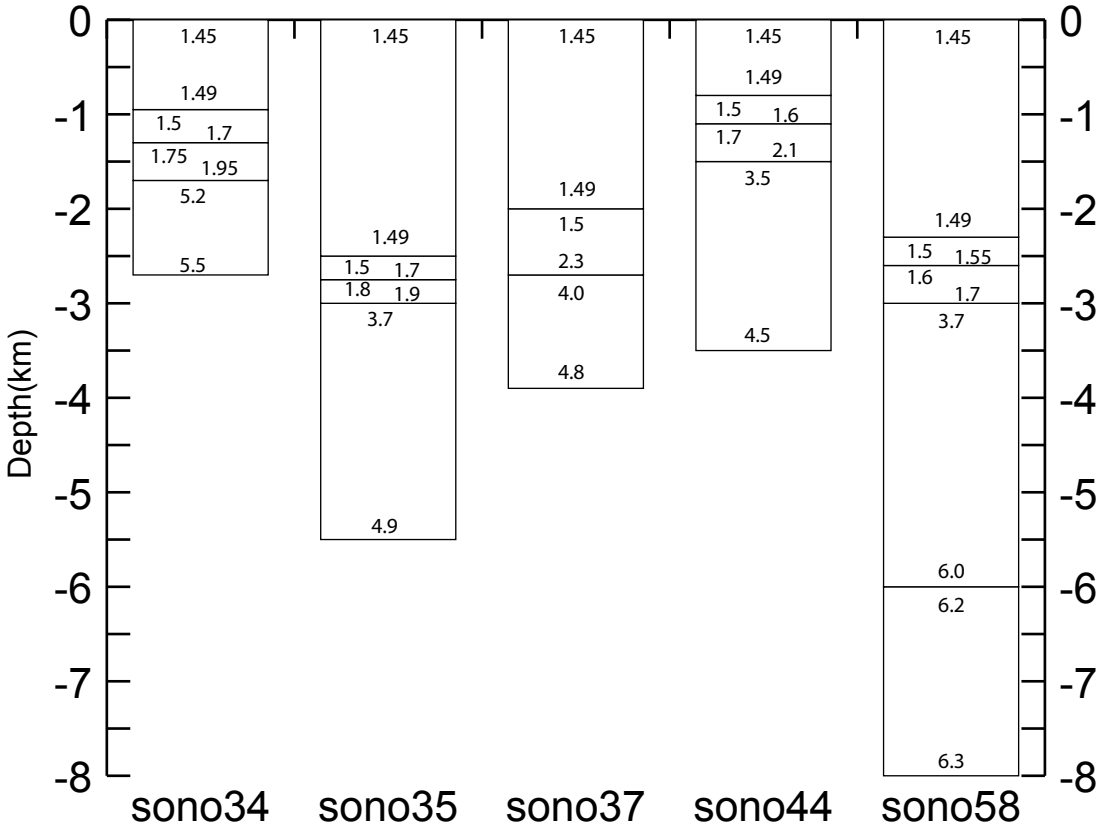

Fig. 13: Compiled Velocity Structure Stack Plots. Velocity structure of the upper crust over the Mendeleev Ridge from 5 sonobuoys (sono). Water: 1.45-1.49 km/s. Sediment Velocities: 1.5-2.3 km/s. All velocities > 3.4 km/s represent basement material. See Fig. 4 for sonobuoy locations.

homogenous nature of basaltic volcanism. If variable basement velocities are observed, there are several possible explanations. Variable velocities may suggest that the Mendeleev is a continental feature, reflecting the normal geologic heterogeneity over large geographic areas, or it might indicate the varying amounts of fracturing, porosity, and weathering observed in the oceanic upper crust (White and McKenzie, 1989). Inconsistent basement is a null result as no unique conclusion can be made.

Sonobuoy 34 (Fig. 8): The best fitting model includes the following velocity gradients: water column (1.45-1.49 km/s); Unit I sediment horizon (1.5-1.7 km/s); Unit II sediment horizon (1.75-1.95 km/s); basement (5.2 - 6.3 km/s at 5 km depth). Model misfit gives RMS = 0.064 seconds.

The partial misfit between observed and calculated seafloor arrivals is likely due to the influence of local bathymetry. This data was collected coming down the flank of the Chukchi Plateau and is a region of high bathymetric variation (Fig. 6a).

Sonobuoy 35 (Fig. 9): Water velocities are the same as for Sonobuoy 34 (1.45-1.49 km/s) and are kept consistent throughout the models. Unit I sediment horizon (1.5-1.7 km/s); Unit II sediment horizon (1.8-1.9 km/s); basement (3.7 - 5.1 km/s at 6 km depth); RMS =0.057 seconds. These basement velocities, lower than sonobuoy 34, may represent a change in basement material or as described above may simply indicate more intense fracturing of the rock. There is a significant misfit for the early basement refractions. A large graben-like sub-basement structure can be seen on MCS line 17 through which these refractions travel (Fig. 6a). It is likely that the observed refractions are influenced by this lower structure. The uppermost basement is responsible for basement reflections as can be seen by the good calculated vs. observed fit. A scenario could not be constructed in the model that could include the reflecting uppermost basement, and yet maintain the refracting character of the sub-basement structure. Despite the refraction misfit, the whole model misfit, RMS = 0.057, is well within the 0.1 second criteria.

Sonobuoy 37 (Fig. 10): The best fitting model includes the following velocity gradients: water column (1.45-1.49 km/s); Total sediment horizon (1.5-2.3 km/s;

basement (4.2-5.8 km/s at 5 km depth.) RMS = 0.030 seconds. Note that this velocity-depth model contains only one sediment horizon.

Sonobuoy 44 (Fig. 11): The best fitting model includes the following velocity gradients: water column (1.45-1.49 km/s); Unit I sediment horizon (1.5-1.6 km/s); Unit II sediment horizon (1.7-2.1 km/s); basement (3.5-5.3 km/s at 5 km depth) RMS = 0.055 seconds.

Sonobuoy 58 (Fig. 12): The best fitting model includes the following velocity gradients: water column (1.45-1.49 km/s); Unit I sediment horizon (1.5-1.55 km/s); Unit II sediment horizon (1.6-1.7 km/s). Offset for basement refractions from sonobuoy 58 extend to ~25 km. In order to compare upper basement velocities to other sonobuoys, shallow arrivals are modeled independently. Upper basement velocities are 3.7 - 6 km/s at 6 km with RMS = 0.075seconds. To reconcile deeper traveling refractions, another velocity layer is required with a smaller velocity gradient (6.2 - 6.4 km/s at 10 km depth). Assigning relief to this lower most boundary reduces misfit for the later arrivals.

Velocity structures from each sonobuoy are compiled in Fig. 13.

Gravity

Experiment and Methodology Overview

Marine gravity data was collected during the trans-arctic crossing using a Bell BGM-3 gravimeter (Bell and Watts, 1986). While underway the gravity data were corrected for Eotvos effects and geographic position. A two-minute Gaussian filter was used to eliminate transients due to ship heave, smoothing the output gravity signal, which was then decimated to one-minute samples. A post cruise gravity tie permitted drift correction. Drift was low, ~0.01 mGal/day during the entire Healy deployment.

Forward modeling of the gravity data is accomplished using GM-Sys software (Won and Bevis, 1987). Initial densities of sediments were derived through empirical relationships according to compressional wave velocities, rock type, and depth (Ludwig et al., 1970; Christensen and Mooney, 1995)). Brocher, (2005) compiled the most widely

used conversions (e.g. Nafe Drake and Gardner), as well as presented original relationships (Fig. 14).

Gravity data are segmented into 2 continuous profiles, each incorporating several seismic lines: Gravity Line A-A' contains seismic lines 17, 18, 20a; Line B-B' contains seismic lines 20b-23. For gravity profile locations, see Fig. 4. Gravity line A-A' begins on the flanks of Chukchi Plateau and ends near the axis of the Mendeleev Ridge whereas gravity line B-B' begins at the axis of the ridge and ends at the margin of the Canada basin. Both profiles are ~225 km in length.

Gravity and co-registered bathymetry data, along with regional unconformity and basement horizons picked off seismic records, were each projected to model profiles, perpendicular to the local ridge axis. Projecting data in this way maximizes variations of mass over the shortest lateral distance so as not to miscalculate anomalies using the technique developed by Talwani and Ewing (1960), which presumes infinite strike length. Gravity data were re-sampled to ½ km intervals in model space.

While the approach to modeling gravity data is to create the simplest model that reproduces the data, including observable structures like acoustic impedance horizons at shallow depths is effective at improving the short wavelength fit, leaving fewer adjustments to be made at greater depths to achieve overall fit between observed and calculated anomalies.

Isostasy provides physical constraints for whole crustal gravity models. To maintain the simplicity and overall accuracy of the model, preference is given to model parameters in which observable information can be applied e.g., sediment horizons, as well as parameters where a priori information can be applied e.g. calculated Moho boundary. Introducing lateral heterogeneity to the models was only applied as a last step, to avoid introducing superfluous complexity to the model.

While the short wavelengths are dominated by bathymetry, the longer wavelength gravity field is controlled by the deeper crustal structure and the geometry of the Moho boundary. A gravity admittance study by Williams and Coakley (2005) showed that the AMR are isostatically compensated according to Airy local isostasy. As a starting model,

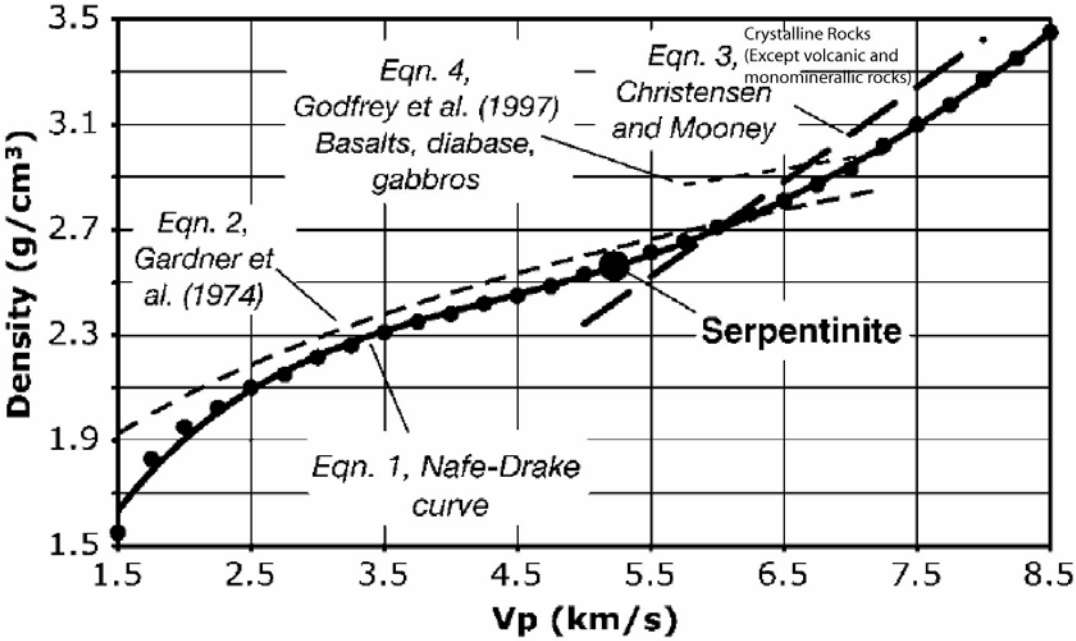

Fig. 14: Empirical Velocity Density Relations for multiple rock types. Taken from Brocher, 2005)

the Moho boundary was calculated assuming Airy compensation of the ridge. Maximum Moho depth was pinned at 32 km, directly beneath the most shallow bathymetry on each ridge profile (Hall, 1970; Ivanova et al., 2006). The shape of the calculated moho boundary depends on the densities used in the calculation, and thus each gravity model includes the Moho boundary specific to the assigned crustal density. After initial density tests, final bulk crustal densities tested are between 2.76 and 2.9 g/cm^3 (Figs. 15 & 16).

As a test, early attempts were made to project to these gravity profiles, the seismically determined Moho depths as observed farther north by Ivanova et al. (2006). It was determined however, that there was no way to accurately project these depths from a distant experiment, and hence this approach would introduce unnecessary bias to the models.

With the seafloor, sediment horizons, and generalized crustal structure in place, fit between observed and calculated anomalies is assessed for each model for crustal densities (2.76 - 2.9 g/cm^3). The best model is chosen according to that which minimizes observed vs. calculated anomaly errors, and best reconciles both short and long wavelength fit. Consideration is also given to potential errors at the edges of the model where the observed anomaly is sensitive to mass outside of the density-depth model bounds. Here, sediment densities may be adjusted to tune the short wavelength field, though in general, preference is given to densities as converted from the refraction modeling. If further discrepancies persist, lateral heterogeneity may be introduced to the crust in order to justify observed and calculated anomalies. Results

No lateral heterogeneity of densities in the crust was required to reproduce observed anomalies with the exception of the transition between the Chukchi Plateau and Mendeleev Ridge. Sediment densities as converted from the refraction experiment were found adequate to reproduce the short wavelength gravity field. A single crustal density, along with the calculated Moho boundary was sufficient to reproduce the long wavelength field. In both profiles A-A' and B-B', sediment densities for sediment horizons I and II were 1.97 g/cm^3 and 2.05 g/cm^3 respectively. The best fittting crustal

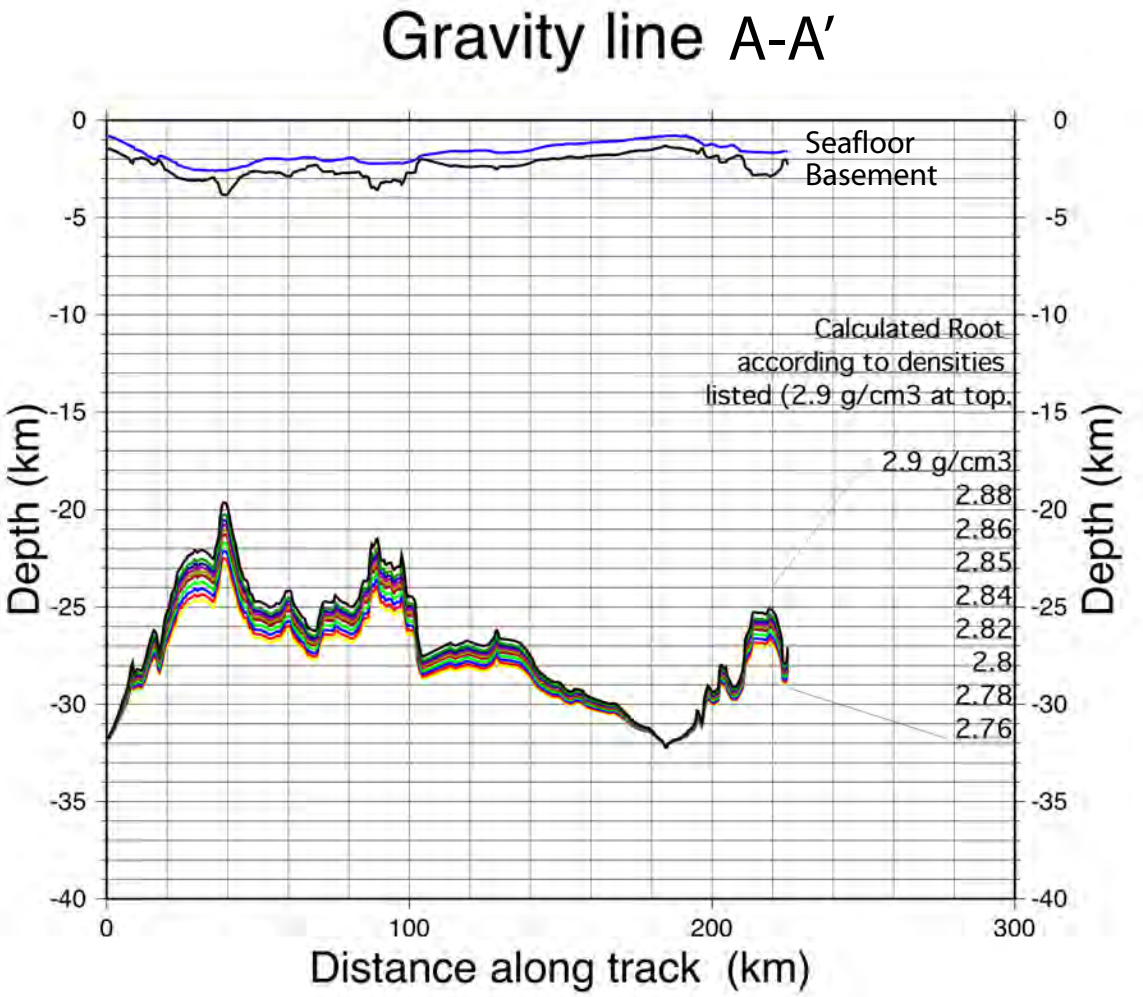

Fig. 15: Gravity Profile A-A'; Plot of Potential Moho Boundaries. Calculated Moho boundaries respective of bulk crustal density. Best-fit gravity model invokes boundary calculated for 2.86 g/cm3.

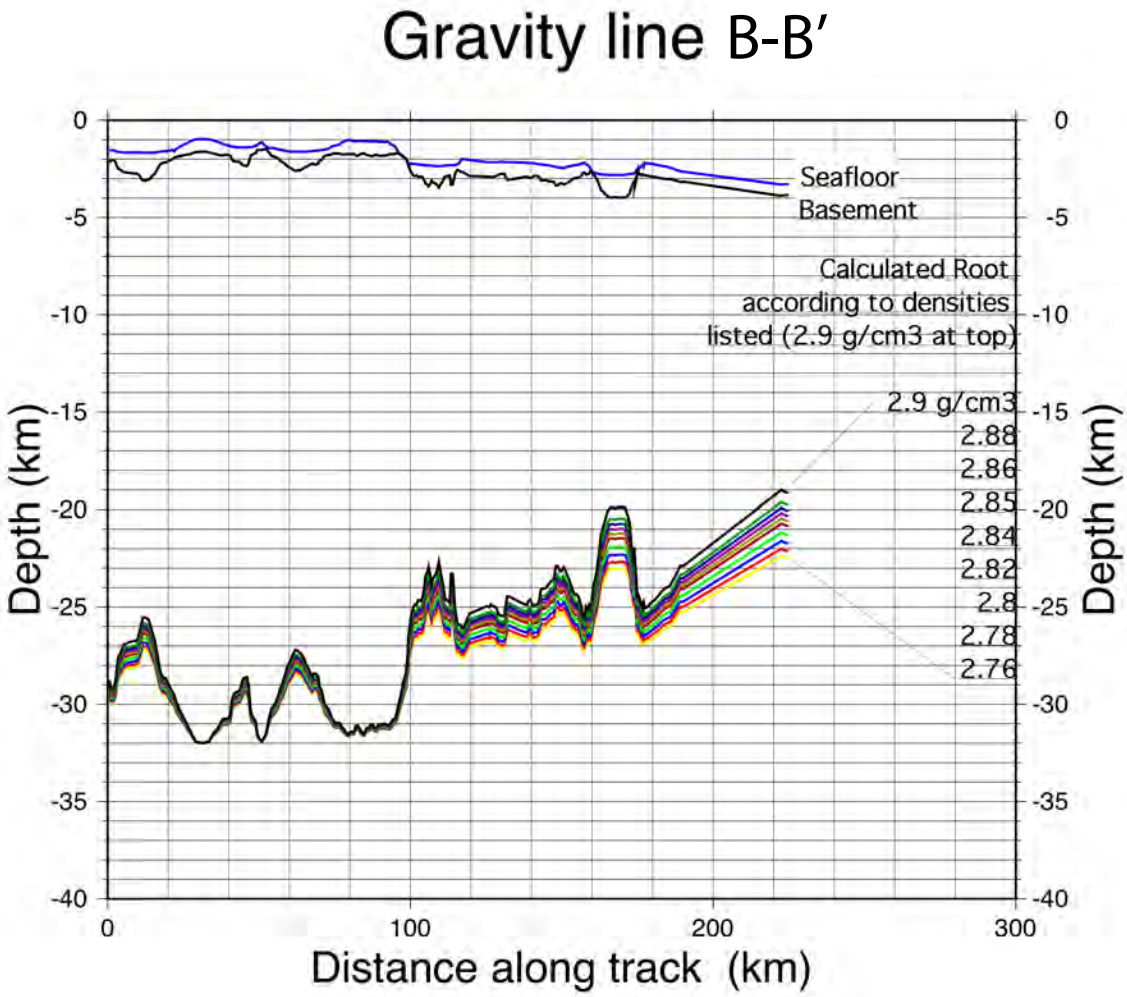

Fig. 16: Gravity Profile B-B'; Plot of Potential Moho Boundaries. Calculated Moho boundaries respective of bulk crustal density. Best-fit gravity model invoked boundary calculated for 2.86 g/cm3.

density was also consistent for both profiles at 2.86 g/cm^3. Mantle density is uniform for both profiles at 3.3 g/cm^3.

Line A-A' (Fig. 17): Observed free-air gravity anomalies range from -32 mGals to 44 mGals. The crustal model has a maximum thickness of 32 km beneath the crest of the Mendeleev Ridge and thins both to the East towards the Makarov Basin, and to the west towards the transition with the Chukchi Plateau. At this transition, the crust thins to 20 km and again thickens up to 32 km, beneath the Chukchi Plateau.

Assuming maximum crustal thicknesses of 32 km at the Chukchi Plateau, there is a distinct and consistent misfit in gravity anomalies between the Chukchi Plateau and the Mendeleev Ridge with a gravity deficit calculated for the Chukchi Plateau. This result indicates that the Chukchi Plateau and Mendeleev Ridge may have likely different compositions, and therefore suggests the presence of a geologic boundary. Previous studies by Hunkins (1966), Hall (1970), Weber and Sweeney (1990), and Grantz et al. (1998) suggest the Chukchi Plateau is a region of thinned continental crust. Hunkins (1966) and Wolf et al. (2002), estimate crustal thickness of the outer Chukchi Shelf at ~32 km depth. It should be noted that the Chukchi Plateau is likely more extended than the shelf, and therefore thinner. Weber (1986) re-calculates crustal structures from the Chukchi Plateau and Canada Basin from gravity profiles first presented by Hall (1970), in order to reconcile newer results from CESAR. Chukchi crust was estimated to be ~22 km thick, with upper basement density of 2.75 g/cm^3 and crust-mantle density contrast of 0.25 g/cm3. While keeping in line with previous studies over the Chukchi Plateau, the most appropriate correction to the crustal model here, involves both thinning the Chukchi crust and reducing the crustal density.

To account for this gravity deficit for the Chukchi Plateau, the Mendeleev Ridge crust is kept at 2.86 g/cm^3, the Chukchi crust is thinned to a maximum of ~29 km and crustal density of 2.85 g/cm^3 (Fig. 17c). This reduces the misfit to a large degree, and the adjustment is not so extreme as to disrupt the long wavelength fit for the whole of the profile. Thinner crust (~29 km) is justified by the previous seismic experiments as noted above. The determined thickness is consistent with the global average of ~31 km for

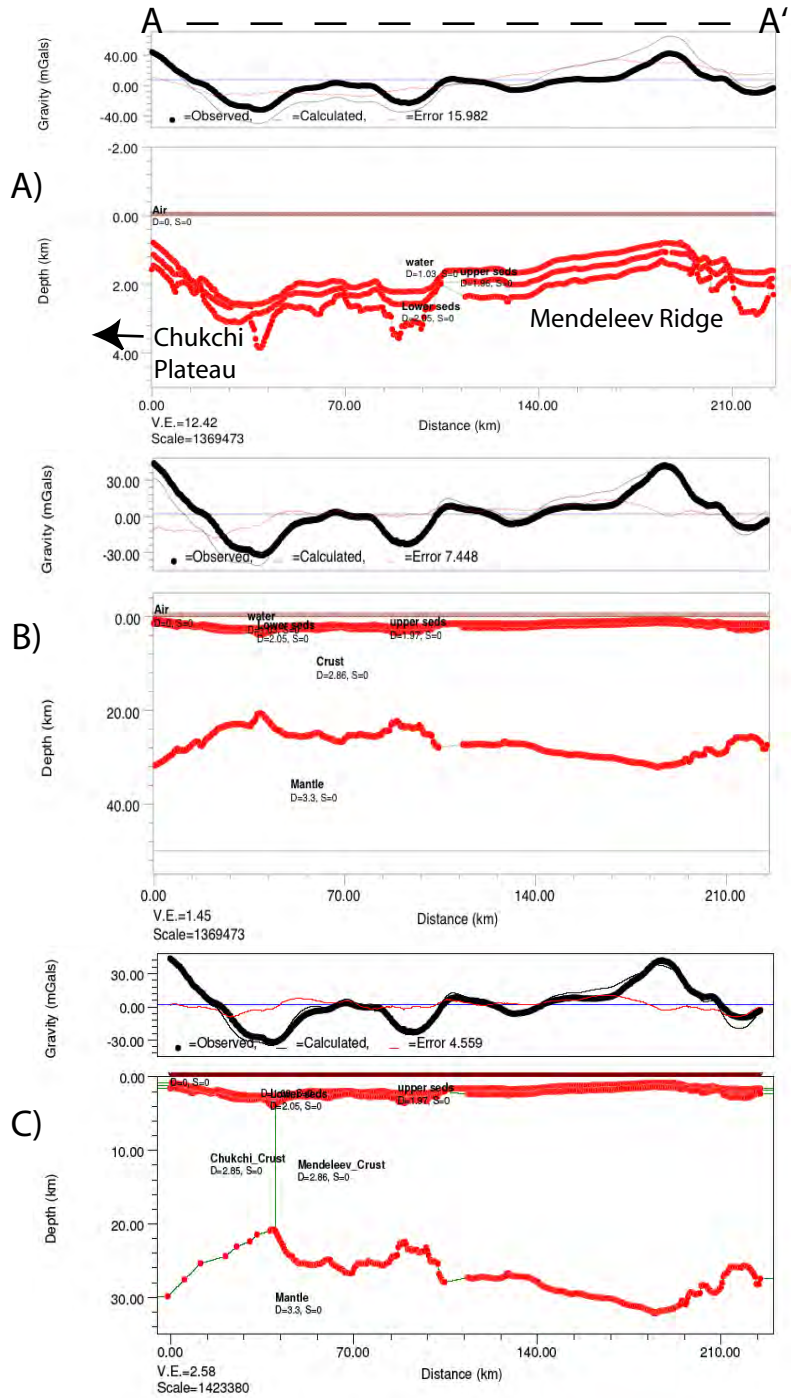

Fig. 17: Gravity Profile A-A'; Gravity Modelling Results. See Fig. 4 for profile location over the MR. Calculated and observed anomalies, along with calculated model error are plotted in the upper panels of A), B), and C), while crustal-density structures are displayed in the lower panels. A) Upper crustal section shows two sediment layers with no basement structure or Moho assigned. Note the calculated gravity surplus over the MR that indicates crustal thickening of the MR is required. B) Full crustal structure with the best-fit density for the MR crust as 2.86 g/cm3. This density assignment leaves a gravity deficit over the flank of the Chukchi Plateau and in C), thinning, and reducing the density of theChukchi Plateau crust reduces model error. A geologic boundary between the Chukchi Plateau and MR is inferred.

extended continental crust (Christensen and Mooney, 1995). One could further thin the Chukchi crust, and reduce the crustal density to maintain isostatic equilibrium. This would require increasing the bulk crustal density for the Mendeleev Ridge.

Ultimately, crustal scale seismic surveying of the Chukchi Plateau and southern Mendeleev Ridge will be necessary to fully understand this boundary.

Another local misfit occurs near to the crest of the Mendeleev Ridge. The high slope of the observed anomaly suggests the presence of a small, higher density body at shallow depths beneath the crest of the ridge. This is not a large misfit however, and is not considered to represent a significant discrepancy in crustal material.

Line B-B' (Fig. 18): Observed free-air gravity anomalies range from -33 mGals to 27 mGals along this profile. Gravity modeling along the more northerly flank of the Mendeleev Ridge reveals much the same result with the ridge axis pinned to 32 km. The ridge thins significantly towards the margin of the Canada Basin where the crust is ~20 km thick. Again sediment densities are 1.97 g/cm^3 and 2.05 g/cm^3 for sediment horizons I and II, and the best fitting crustal density is 2.86 g/cm^3 when only one crustal layer is invoked (Fig. 18b).

Model misfits occur at the edges of the model where adjacent mass is not accounted for in the calculated anomaly. On the Canada Basin side of the profile, this misfit may be due in part to insufficient basement picks from the MCS basement, which results in 30 km gap in the Moho boundary. In the model, this gap was linearly interpolated. There is some indication that at basement lows, the calculated anomaly is excessively low, suggesting that perhaps greater extension and thinning occurred in these localities than that given by the shape of the calculated Moho boundary. Another, very plausible possibility is that the sediments that lie deep in these grabens have greater densities than 2.05 g/cm^3.

In an attempt to correct for these edge misfits, an underplated, high density (3.04 g/cm^3) layer was invoked where the Mendeleev crust was $\geq$ 26 km (Fig. 18c). This lower crust layer was applied to gravity models over the Alpha Ridge, where the upper crustal density is 2.88 g/cm^3 (Weber, 1986). This addition reduces the model error. Ivanova et

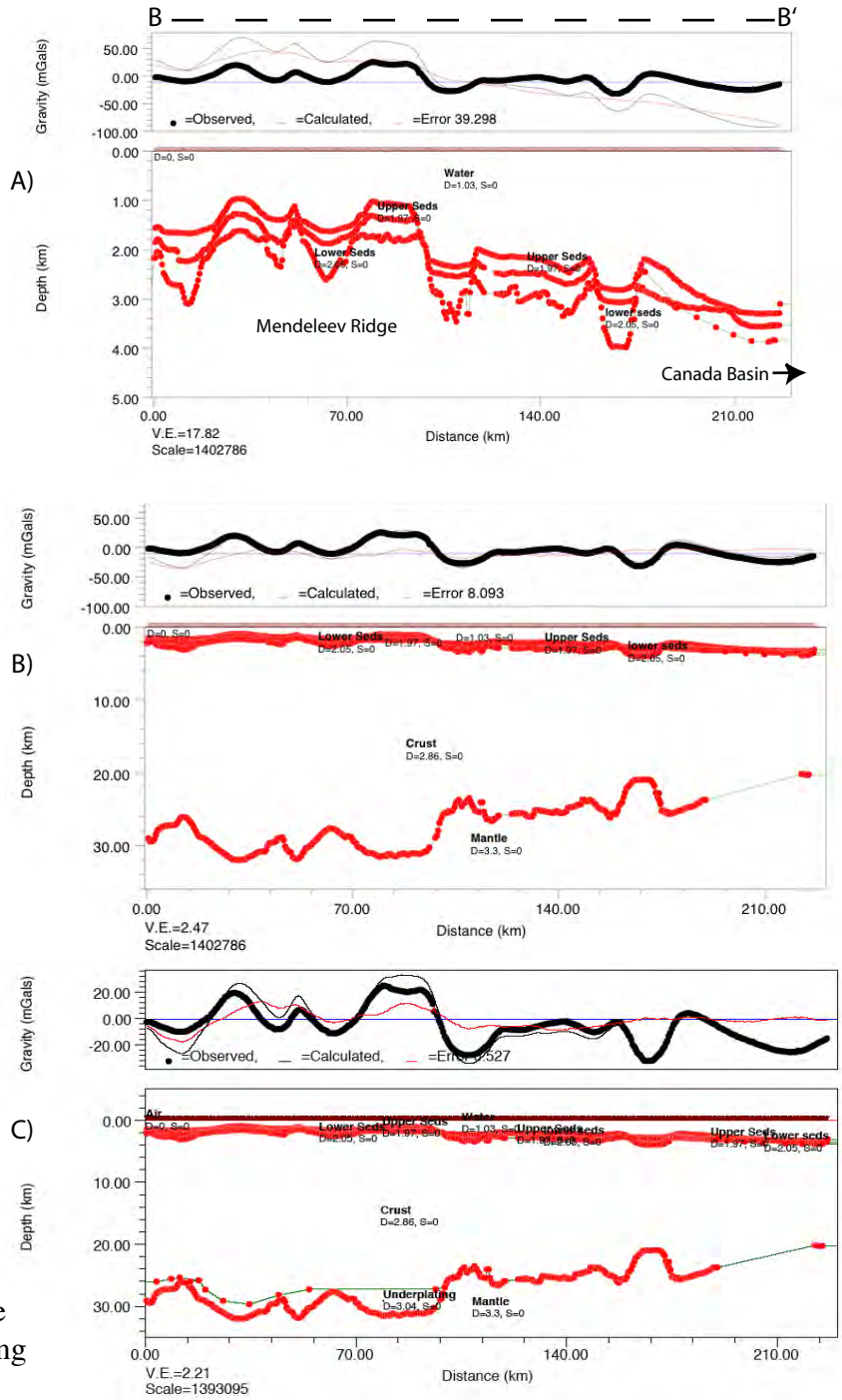

Fig. 18. Gravity Profile B-B'; Gravity Modelling Results. See Fig. 4 for location. A)) Upper crustal section shows two sediment layers with no basement structure or Moho assigned. Note the calculated gravity surplus over the MR that indicates crust thickens toward the crust of the MR. B) Full crustal structure with the best-fit density for the MR crust as 2.86 g/cm3. C) Underplated layer of 3.04 g/cm3 at depths > 26km partially reduces model misfit.

al. (2006) describes a high velocity, 7.4-7.8 km/s, layer at the base of the Mendeleev Ridge that possibly represents underplating. An underplated layer was not invoked for gravity line A-A', as no such layer was necessary to reproduce the observed gravity anomalies.

The most significant result for both profiles is that a single crustal density, 2.86 g/cm^3, consistent through both profiles is sufficient to reproduce the observed free-air gravity anomalies. While in reality, crustal densities would increase gradually with depth, such gradation is not introduced here due to the success of invoking a single crustal density layer. This result suggests the Mendeleev Ridge is composed of a homogenous crustal material and precludes large-scale variation of the crustal structure.

Discussion

Constraints on the Geological Nature of the Mendeleev Ridge Crust

Upper Crust

Within the MCS data, basement reflection character is typically homogenous and interpretations of sub-basement coherent reflections are ambiguous, possibly representative of volcanic flows or lithified, Mesozoic or older sediments. Interpretation is inhibited by depth of penetration and the persistence of multiples. The multiples themselves reveal reflectors in the sub-basement but most of this energy is from peg leg multiples and secondary multiple reflections (Fig. 6b). The reflectors in the multiple are thus not interpreted. The MCS data does not provide significant constraint on the crustal style of the ridge.

Compressional wave velocities for the upper basement are relatively uniform across the Mendeleev Ridge with the possible exception of sonobuoy 34 over the Chukchi Plateau, which samples higher velocity material (Fig. 13). The upper crustal velocities are not lithologically diagnostic due to variations in porosity at shallow crustal depths. Basement velocities reported here may represent high velocity sediments (carbonates), or oceanic layer 2. Oceanic layer 2 is composed of the uppermost extrusive volcanic zone and may include sills, dykes, pillow, basalts, and intercalated sediments.

Lower seismic velocities are recorded in this youngest volcanic layer due to the abundance of fractures, faults, and pore space, but increase rapidly with depth (Ewing and Houtz, 1979; White et al., 1992).

The upper basement velocities are slightly lower than those of the northern Mendeleev Ridge and Alpha Ridge (Fig. 19). This may simply indicate that a different crustal material was sampled, or it may reflect the higher resolution of this survey, which is sensitive to the uppermost basement. Asudeh et al. (1988) describe thickened oceanic layers 2b and 3 on the Makarov Basin and Alpha Ridge, but explain that the relatively low resolution of the experiment prevented resolving oceanic layer 2a. A wide angle, lower resolution, crustal scale seismic experiment presented by Ivanova et al. (2006), found upper basement velocities of 5.0 -5.4 km/s over the northern Mendeleev Ridge. In a seismic experiment similarly scaled to the one presented here, upper-basement velocities of 4.2-4.6 km/s were sampled over the Alpha Ridge by Jokat (2003). Hunkins (1961), presented velocities over the Alpha Ridge of 4.7 km/s for the uppermost 2.8 km of basement.

While absolute values of upper basement velocities are not diagnostic of upper crustal material, velocity-depth gradients are more predictable for particular lithologies. Fig. 20 shows the velocity-depth functions from this study superimposed on the results of White et al. (1992), who compiled velocity-depth functions of normal oceanic crust from the Pacific and Atlantic Oceans, and stacked the respective functions according to crustal age.

Mafic, volcanic rock typically exhibits higher velocity gradients than more felsic continental rock. If the results from the Mendeleev Ridge plot within the envelope of “normal oceanic crust”, the ridge could potentially be composed of oceanic crust, however continental crust is not precluded. Conclusions from this test are tentative as “normal oceanic crust” is compared to the Mendeleev Ridge crust, which is approximately four times as thick, and has undergone significant post-formational extension.

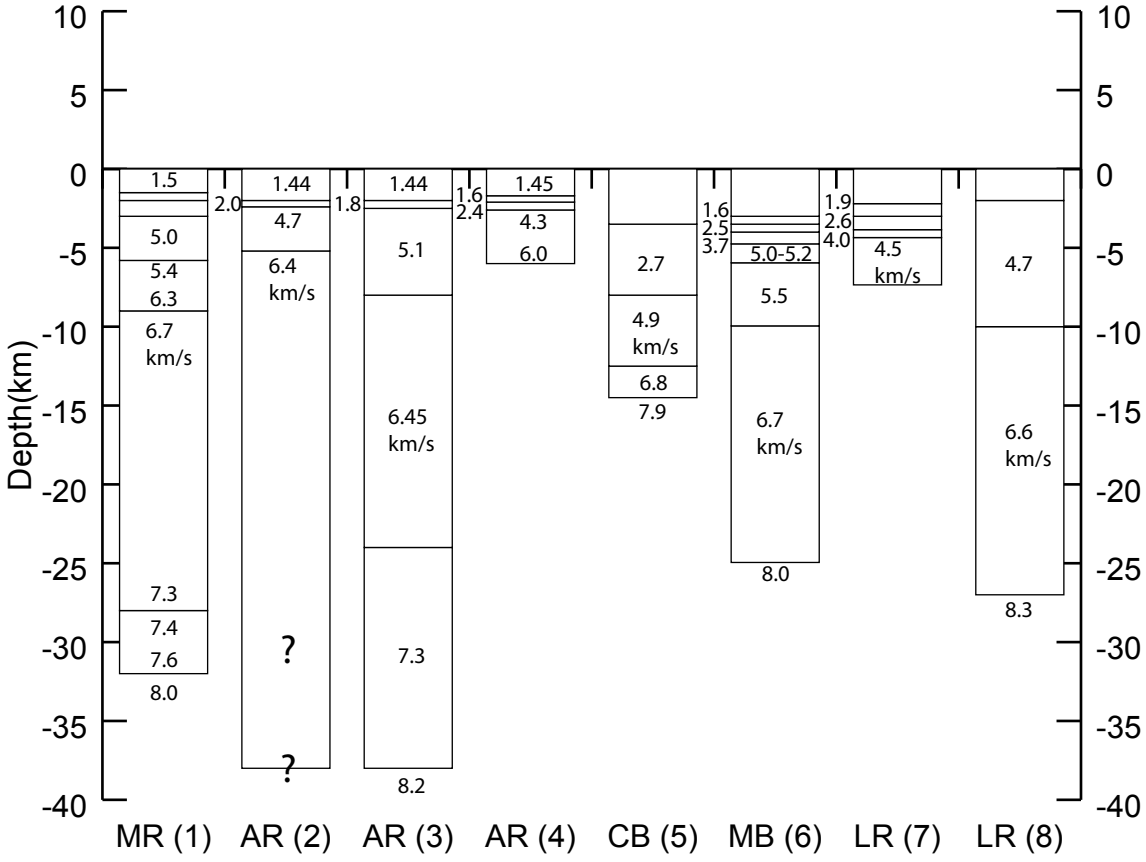

Fig. 19: Regional Seismic Refraction Results from the Amerasian Basin. Crustal velocity structures from ridges and basins of the Amerasian Basin. Mendeleev Ridge (MR), Alpha Ridge (AR), Canada Basin (CB), Makarov Basin (MB), Lomonosov Ridge (LR). (1) Ivanova et al., 2006, (2) Hunkins, 1961, (3) Asudeh et al., 1986, (4) Jokat, 2003, (5), Baggeroer and Falconer, 1982, (6) Sorokin et al., 1999, (7) Jokat, 2005, (8) Forsyth and Mair, 1984.

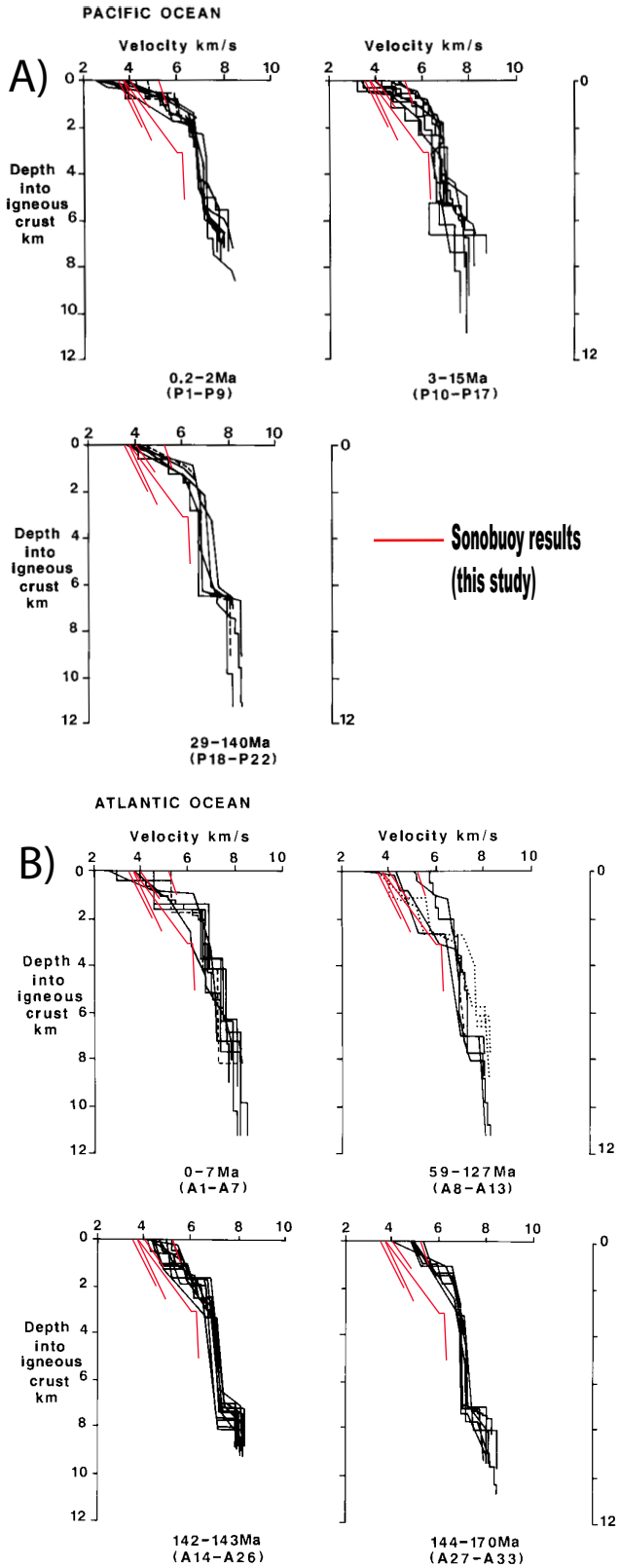

Fig. 20: Velocity-depth Functions Compared with Normal Oceanic Crust. Velocity-depth functions from this study (red) plotted with stacked velocity-depth functions for normal oceanic crust (black) from the A) Pacific and B)Atlantic Oceans. Augmented from White et al. (2002).

Fig. 20 shows that the upper basement velocities from the Mendeleev Ridge are mostly inconsistent with normal oceanic crust. The velocities from the Mendeleev are typically lower than those of oceanic crust of an equivalent depth. The better fit is achieved with Atlantic Ocean results, especially 59-127Ma, which is the most appropriate age for comparison. All sonobuoys, but sonobuoy 44 plot within the bounds set for normal oceanic crust. Sononuboy 35 may be an outlier but due to the uncertainty in the modeling of this sonobuoy (see results) it is less reliable. As a result or this comparison to "normal oceanic crust", it is possible for sonobuoys 34, 37, and 58 to represent oceanic crust, though the overall comparison suggests that the velocities from the Mendeleev Ridge are not compatible with normal oceanic crust.

The basement velocity functions are also compared to those observed in Iceland, (Flovenz and Gunnarsson, 1991), as well as Hatton Bank and the Voring Margin, both rifted volcanic margins within the North Atlantic volcanic province (NAVP)(Fig. 21a). Eldholm and Grue (1994) compile velocity-depth from the two volcanic margins and the oceanic plateau to contrast the velocity-depth functions for the extrusive upper basement. Fig 21b reveals a striking similarity between the velocity structure of oceanic plateaus and volcanic margins, suggesting similar compositions and processes governing magmatic emplacement. The velocity gradients presented in this study are similar with the shallow results from both Iceland, and the volcanic margins. However, considering that velocities presented here only sample the upper crust, and that Iceland and the NAVP are younger in age, implications from these comparisons are only tentative.

Observed variation in the gravity field is not adequately resolved to sense the variation described by the velocity-depth functions. Modeling of the gravity data reveals that a single homogenous crustal layer is effective at reproducing the short wavelengths of the anomaly, though the predominant signature in the short wavelength anomaly field is the seafloor and basement topography, so subtle variations in crustal structure cannot be resolved.

Fig. 21: Velocity-Depth Functions comparedwith Iceland and the NAVP. The vertical axis records depth into basment. A) Velocity-depth functions from this study plotted with results from the MR presented by (Ivanova et al. 2006), Iceland (Flovenz and Gunnarson, 1991), and the Voring Margin (V), More (M), and Hatton Bank (HB) (Eldholm and Grue,1994). Augmented from Eldholm and Grue (1994).

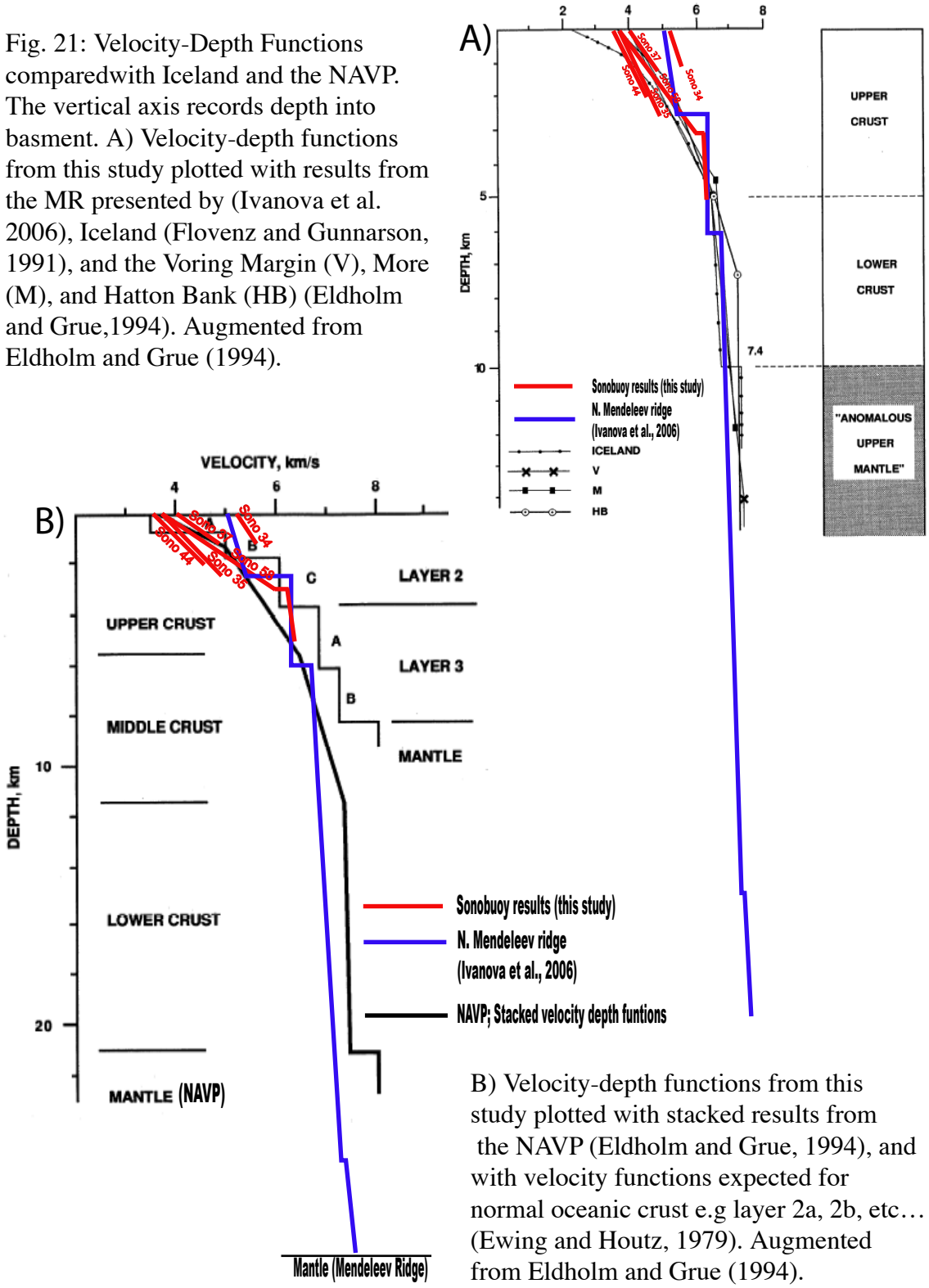

B) Velocity-depth functions from this study plotted with stacked results from the NAVP (Eldholm and Grue, 1994), and with velocity functions expected for normal oceanic crust e.g layer 2a, 2b, etc… (Ewing and Houtz, 1979). Augmented from Eldholm and Grue (1994).

Deeper Crust – Evidence of Homogenous Crust and Contiguity with the Alpha Ridge

Gravity data are consistent with lateral homogeneity of the Mendeleev Ridge crust. Only a single crustal density layer of 2.86 g/cm^3 is required to sufficiently reproduce the gravity field for both ~225 km profiles. These results are compatible with a mafic, largely magmatic crust, and incompatible with the typical lateral heterogeneity of continental crust.

These results are also fully consistent with gravity studies over the Alpha Ridge from the CESAR expedition (Weber, 1986; Sobzak and Hearty, 1990; Weber, 1990; Weber and Sweeny, 1990). Weber (1986) shows that over the Alpha Ridge, a two-tiered crustal model is sufficient to reproduce regional anomalies with bulk crustal densities of 2.88 g/cm^3 to 26 km depth and 3.04 from 26 km to the Moho boundary.

The results presented here are also consistent with the crustal structure for the Northern Mendeleev Ridge (Ivanova et al., 2006). Though the specific densities are not reported, calculated densities, as converted from seismic velocity profiles (Ludwig et al., 1970; Brocher, 2005), reveal a crustal density structure of 2.53 – 3.08 g/cm^3 at 29 km, and an underplated layer of 3.08 - 3.29 g/cm^3.

Seismic refraction results presented by Ivanova et al. (2006) represent the only experiment to sample the crust-mantle boundary over the Mendeleev Ridge, which is estimated at 32 km at the ridge crest. Through interpretation of individual velocity layers, and the velocity structure as a whole, the authors suggest the Mendeleev Ridge is composed of "thinned underplated continental crust or thickened oceanic crust", but prefer a continental origin. In a benchmark paper, Christiansen and Mooney (1995) compile global results for the velocity structure of continental crust. In Fig. 22, rifted continental crust reveals the highest velocity gradients of the various tectonic environments presented. These results for rifted continental crust are considerably less than the velocity gradients observed by Ivanova et al. (2006), potentially arguing against a continental origin for the Mendeleev Ridge.

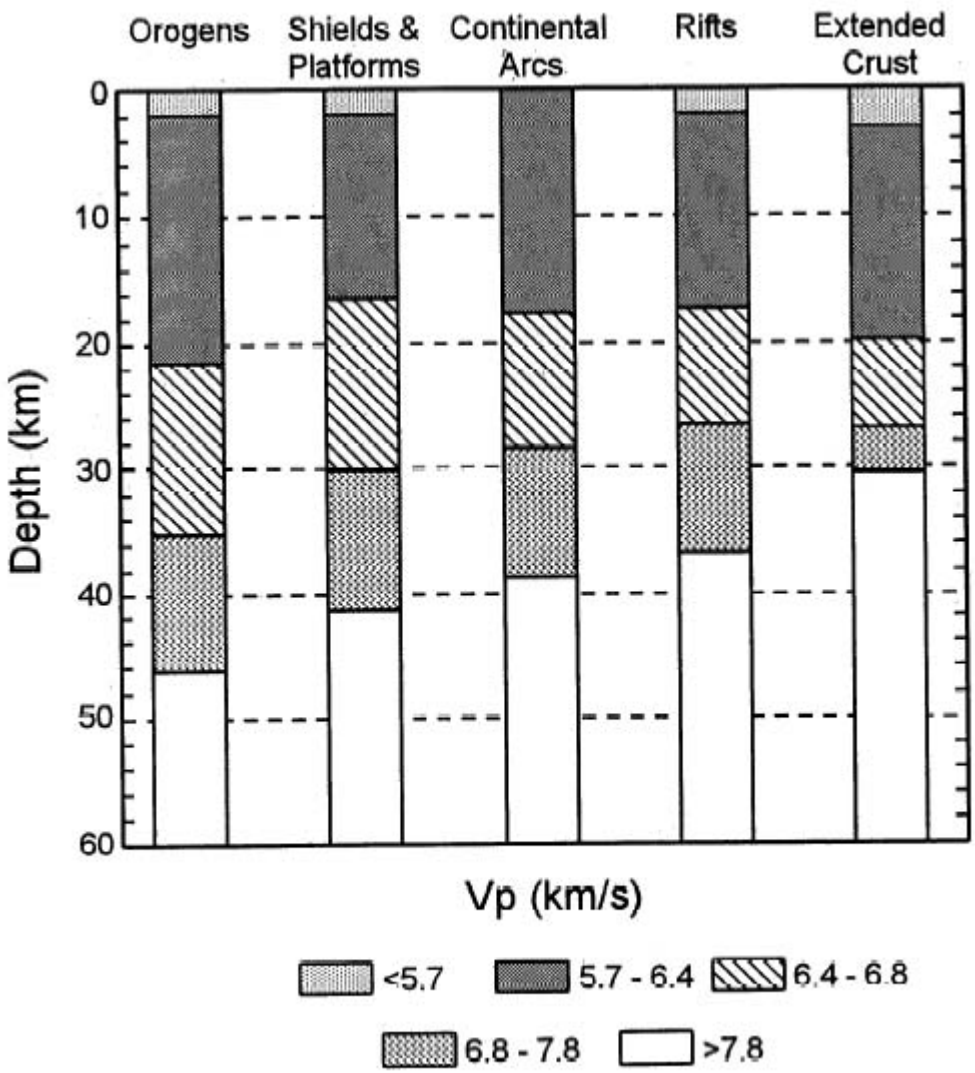

Fig. 22: Average Crustal Velocity Structure for Six Continental Tectonic Provinces. Taken from Christesen and Mooney (1995).

The velocity structure presented by Ivanova et al. (2006) is more consistent with thickened oceanic crust observed at oceanic plateaus (Fig. 21a) (Hussong et al., 1979; Flovenz and Gunnarsson, 1991; White et al., 1992; Coffin and Eldholm, 1994), or volcanic margin crust, as described by Eldholm and Grue (1994) over the NAVP (Hatton Bank, Voring Margin, Jan Mayen Ridge, SE-Greenland, NE-Greenland, More, Lofoten, Vestbakke Volcanic Province).

The crustal structure from the volcanic margins of the NAVP is described as constituting the continental-ocean boundary. The continental-oceanic boundary marks the seaward terminus of the extended continental crust and the overall velocity structure is described as being independent of both oceanic and continental crust. The crustal structure is divided into 3 separate velocity units, the top representing an extrusive basalt layer of 3.7-5 km/s. The lower most velocity unit, 7.2-7.7 km/s, is described as underlying both "oceanic and adjacent intruded, or transitional, continental crust".

Fig. 21b shows the velocity-depth function as interpreted from Ivanova et al. (2006), plotted with the velocity-depth function as averaged for the NAVP, as well as the layered model for normal oceanic crust. The authors do not interpret the velocity structure of the North Atlantic volcanic margins as an expansion of oceanic layers 2 and 3 but as a unique crustal edifice, specific to volcanic margins. While the thickness of the Mendeleev Ridge exceeds that which is plotted for volcanic margin crust, similarity in the crustal velocity structures is evident.

Fig. 23 shows the velocity and density structures of the Mendeleev Ridge compared to the Alpha Ridge. The two ridges share similar velocity and density structures. They are of similar bathymetric morphology, depth, and volume. Regional potential field studies find magnetic and gravity anomalies are well correlated with bathymetry, and consistent with volcanism for the Cretaceous normal period (Sobzak and Hearty, 1990; Laxon and McAdoo, 1994; Vogt et al., 2006). Figs. 2 and 3 show the regional magnetic (Verhoef et al., 1996), and gravity (Kenyon and Forsberg, 2001) anomalies.

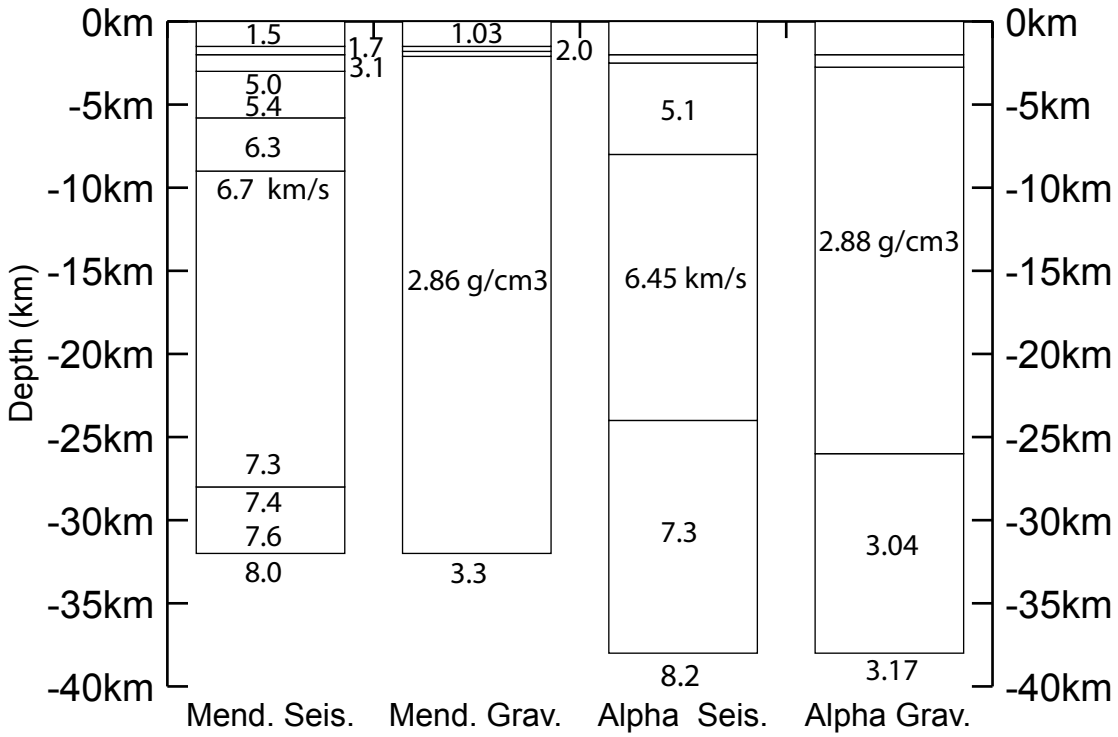

Fig. 23: Velocity and Density Structures of the Mendeleev and Alpha Ridges. From left to right: Compressional velocities from the Mendeleev Ridge (MR) are taken from Ivanova et al. (2006). Densities from the MR result from the gravity modeling in this study. Compressional velocities from the Alpha Ridge (AR) are taken from Forsyth et al. (1986). Density results from the AR are taken from Weber (1986).

Synthesis

Considering the evidence listed above, there appears to no physical criteria to separate the Mendeleev and Alpha ridges. The contiguous AMR is likely formed of either thickened oceanic crust, or highly attenuated continental crust, saturated with mafic rock, presumably shallow basalts with gabbros and ultramafics at depth. Consequently, the geologic origin of the Mendeleev and Alpha Ridges is constrained to either an oceanic plateau, or a rifted volcanic continental margin.

A similar conclusion was reached by Williams and Coakley (2005), where a gravity admittance study supported Airy isostastatic compensation of the AMR. This requires the AMR was emplaced on young, weak lithosphere, consistent with either rifted continental margin or formation at a spreading center.

If in fact the AMR was formed as a rifted volcanic margin, seaward dipping reflectors (SDR's) in the MCS images of the basement might be expected. SDR'S represent sub-aerially extruded basalts and are observed on most volcanic margins due to thermally induced uplift that may either pre-date or accompany extension of the lithosphere (White and McKenzie, 1989). SDR's are common throughout the volcanic continental margins of the NAVP (Eldholm and Grue, 1994; Saunders et al., 1997; Gernigon et al., 2003; Hopper et al., 2003). We do not recognize such reflectors over the Mendeleev Ridge and they have not been observed in the limited MCS data over the Alpha Ridge (Jokat, 2003).

Depositional and Structural Histories

A detailed account for the depositional history of the Mendeleev Ridge is not presented here. This is due to the absence of reliable age control at depths ≥ 10 m. For analysis of the shallow stratigraphy over the Mendeleev Ridge, dominated predominantly by glacial and interglacial cycles, see Thiede et al. (1990) and Polyak et al. (2004).

Seismic reflection images revealed the presence of two primary sediment units, separated by a regional unconformity that is identified across the whole of the project

area. Sediment Units I and II can be further subdivided by locally observed unconformities (layer pinchout and onlap) that represent either hiatuses, or changes in sediment delivery. One exception is on MCS Line 22, where apparent rift-flank uplift has a created an unconformity within sediment Unit II. Younger sediments onlap older sediments that conformably overly the tilted basement (Fig 6d). This observation suggests that extensional deformation of the ridge post-dated original formation of the ridge, but also may have post-dated initial sedimentation over the ridge.

Sediment was deposited before, during, and after deformation of the ridge. If the ridge is an oceanic plateau (Berger et al., 1992), or a volcanic margin (White and McKenzie, 1989), Embry and Dixon, 1990), sediments may be intercalated with volcanic flows. If the ridge is a rifted continental margin, Mesozoic and older sediments may constitute the basement material.

Pelagic sedimentation is the dominant delivery mechanism over the Mendeleev Ridge, certainly for sediment Unit I and most likely for Unit II. Drifting sea ice may also transported terrigenous material to the central Arctic Basin (Thiede et al., 1990). Seismic reflection data reveal Unit I to be conformable to underlying material and to have continuous and widely spaced reflectors (Fig. 6). Unit II has been more disturbed and faulted but the same sediment delivery mechanism is assumed because in areas not impacted by extensional deformation, Unit II is characterized by reflection character similar to Unit I.

Results from seismic refraction modeling are consistent with the predominance of poorly compacted sediments. The absence of a significant seismic-velocity boundary between sediment Units I and II suggests they are similarly compacted, and likely of a shared pelagic origin. Both sediment horizons exhibit low velocities, suggesting limited lithifaction of clastic sediments. The velocities of Unit II are sufficiently low (1.7-2.3 km/s), to indicate that these syn-rift sediments do not contain a significant volume of volcanic sills or dykes. This observation is sustained by the absence of any clear, high reflectivity events in the MCS data that may be interpreted as volcanic flows.

Unconformities observed in both Units I and II are often only locally recognized. They are interpreted to represent minor depositional hiatuses.

Structural History

MCS images reveal that the Mendeleev Ridge is extended, with large graben and half graben structures visible throughout. Bathymetry is in large part controlled by normal faults, which also influences sediment thicknesses. There are similar extensional features observed on the Alpha Ridge, though perhaps to a lesser degree (Jokat, 2003).

Fig. 24 is a structural map of the ridge. Regional bathymetric contours from the International Bathymetric Chart of the Artic Ocean (IBCAO) (Jakobsson et al., 2000) are superimposed onto the regional gravity grid from the Arctic Gravity Project (AGP) (Kenyon and Forsberg, 2001), along with the ship's bathymetry and interpreted structures. To produce the map, structures from seismic reflection images were projected to the ship's bathymetry (Fig. 25). The orientation of faults can typically be observed on the ship's bathymetry e.g. the lineament at the base of a scarp. These structures then are analyzed to test whether they can be extrapolated according to regional bathymetry, gravity, or magnetic data. Fig. 26 shows a graben and scarp on MCS line 22, (Fig. 6d), along with the ship bathymetry.

The primary extensional axis is E-W to NE-SW. Regional gravity data are a good predictor of the large scale structures. Anomaly highs are correlated with horsts, anomaly lows are associated with grabens, and anomaly gradients are normal to the inferred axis of extension.

Given the common extensional texture, it seems reasonable to believe the western side of Chukchi Plateau experienced the same extensional event that deformed the basement and lower sediment Unit II on the Mendeleev Ridge. Gravity results suggest a geologic boundary exists between the Mendeleev Ridge and the Chukchi Plateau. Gravity anomalies over the Chukchi Plateau are not accounted for by the density-depth structure of the Mendeleev Ridge and therefore the Chukchi Plateau is likely a distinct feature (Fig. 18c). Similar to the Mendeleev Ridge though, MCS images and morphology of the Chukchi Plateau suggest large scale ~E-W extension The regional unconformity

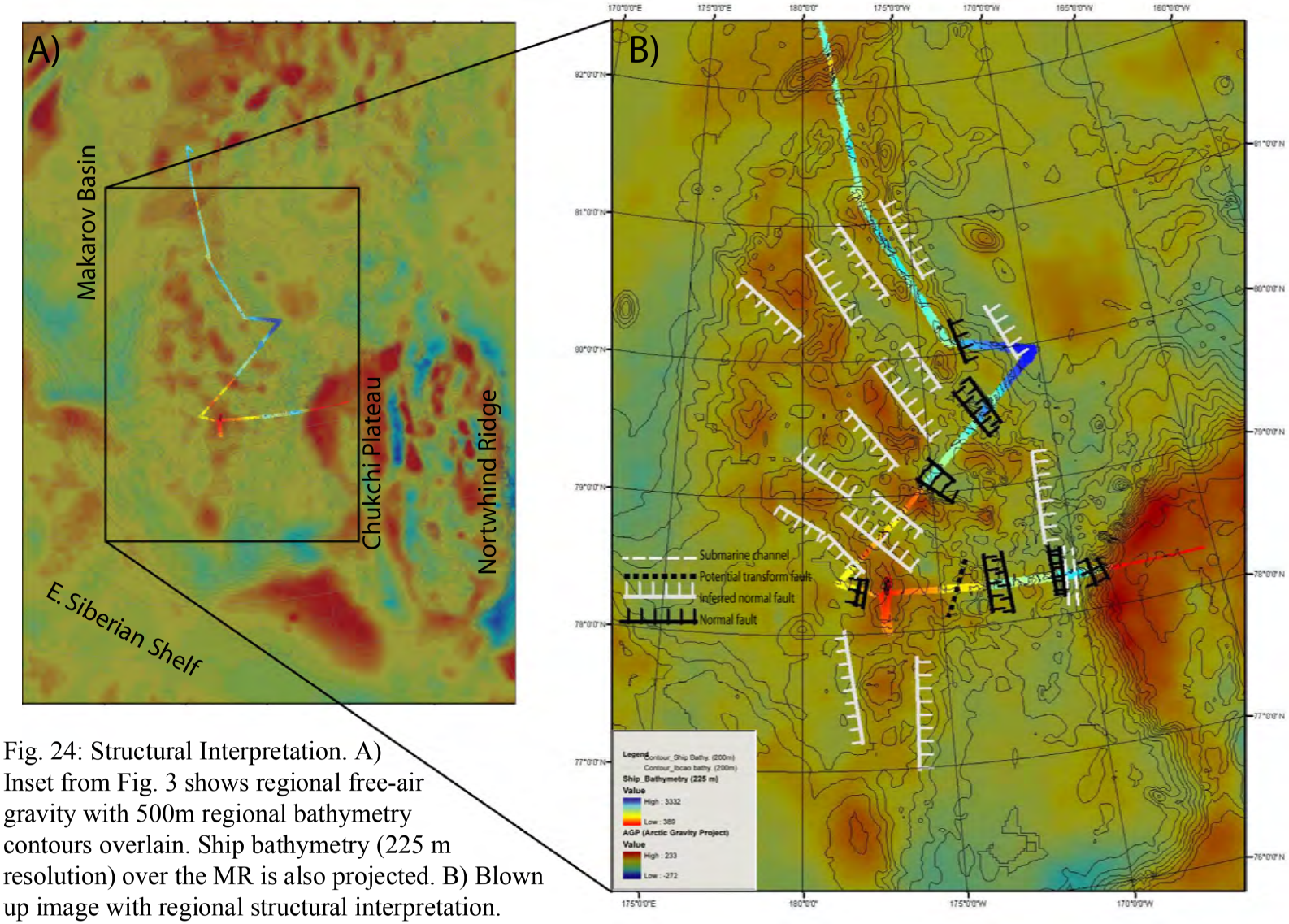

Fig. 24: Structural Interpretation. A) Inset from Fig. 3 shows regional free-air gravity with 500m regional bathymetry contours overlain. Ship bathymetry (225 m resolution) over the MR is also projected. B) Blown up image with regional structural interpretation.

A)

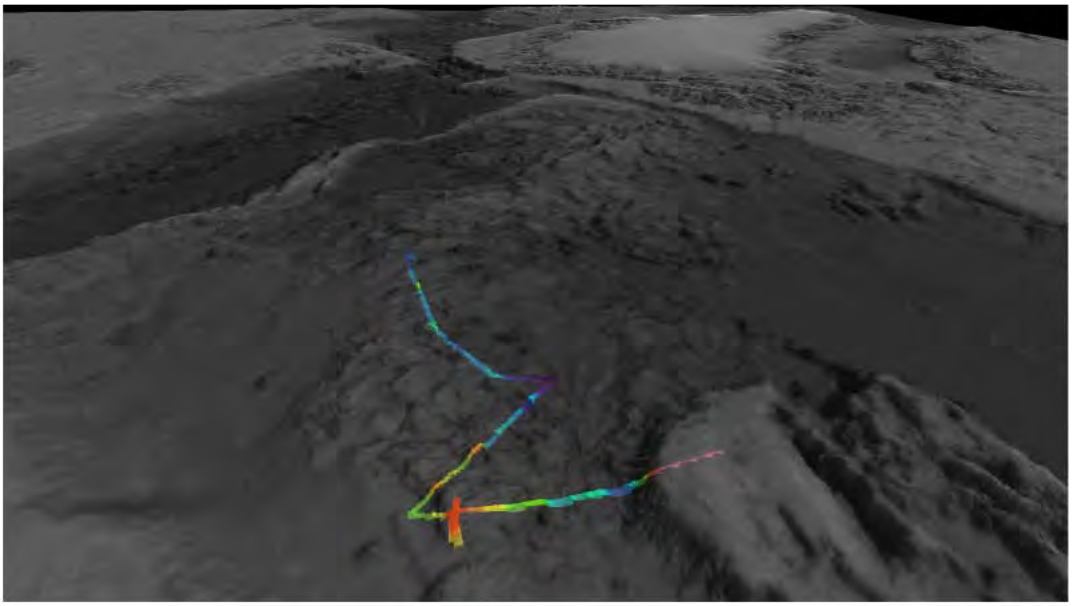

B)

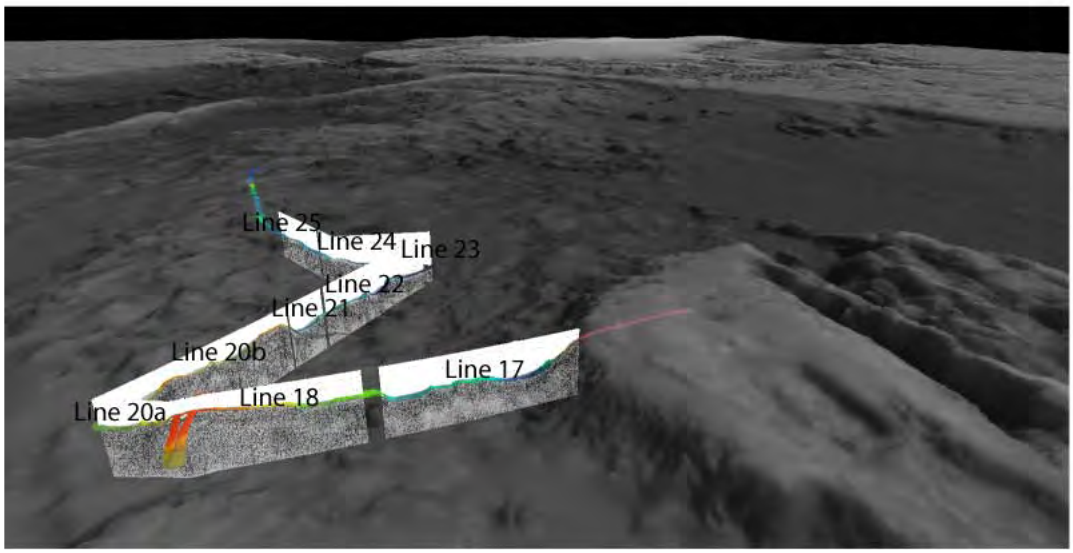

Fig. 25: 3D-Visualization; Regional and Ship Bathymetry with MCS Lines. Both panels look Norh along the ~180°meridian, towards the AMR with the Eurasian Basin in the upper left and Greenland at the top. A) Ship bathymetry (25 m) (rainbow) over the MR plotted over regional bathymetry (grayscale). B) All MCS lines curtained with the bathymetry grids.

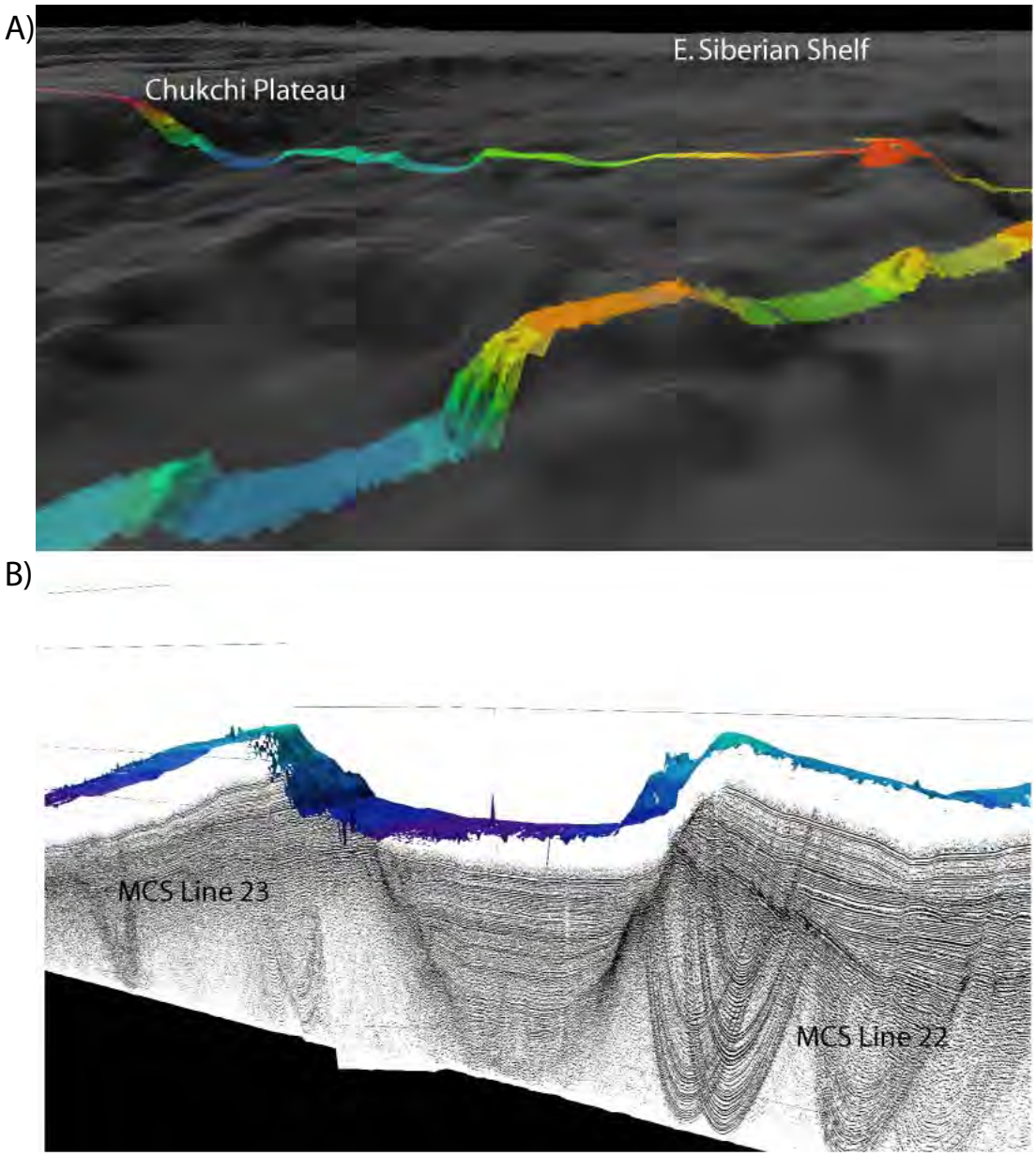

Fig. 26: 3-D-Visualization; View of Large Graben and Associated Scarp. A) Ship bathymetry (25 m resolution) (rainbow) and regional bathymetry (grayscale). In general, the regional bathymetry grid (2500 m resolution) (IBCAO) accurately predicts the gross bathymetry. Here, a scarp is imaged by both bathymetry grids. B) Ship bathymetry and MCS Lines 22 and 23. A large graben is observed in the seismic images and scarps are expressed in the bathymetry data.

observed on the Mendeleev Ridge can be traced onto the Chukchi Plateau until it pinches out at the crest of the plateau where ice erosion may have removed upper sediments (Polyak et al., 2003). This reveals the potential for lower Cenozoic sediments near to the seafloor in this area.

Subsidence

Estimated surface extension ($e = (lf - lo)/lo$) is calculated where lf = observed horizontal length of crust, and lo = original horizontal length of crust. The horizontal offset from all normal faults penetrating through both sediments and basement are summed and scaled in order to calculate lo. Picks were made conservatively and consistently on both lines. For example, only observable offset is recorded, not suspected offset, and no listric or detachment faults are invoked.

This provides a conservative estimate of the degree of stretching undergone by the Mendeleev Ridge. *'e'* can also be used to approximate the crustal stretching factor β, where $\beta = (1 + e)$ and ($\beta = ho/hf$); ho =original crustal thickness, hf =observed crustal thickness. β is a commonly used measure of the crustal stretching and can help to determine total subsidence and state of isostasy. Here it will simply be used to illuminate potential mechanisms of extension and subsidence of the Mendeleev Ridge.

β for MCS lines A-A' and B-B' is calculated at 1.16 and 1.20 respectively. Applying a mechanical model for stretching, McKenzie (1978), ~0.5 km of subsidence is predicted for the β values calculated here, assuming a late Cretaceous (~90 Ma) age for the ridge.

If the AMR is a volcanic rifted margin, these β values likely place a lower boundary on total extension as deeper penetrating faults of multiple generations, and large-scale detachment structures might be expected. At such margins, uplift slightly predates and accompanies breakup before subsidence begins at rates predicted by mechanical stretching (White and McKenzie, 1989). Whether a thermal anomaly (100-200°) over a 1,000-2,000 km diameter region drives lithospheric stretching, or the opposite is true (active vs. passive rifting), an emplacement of melt into the crust may

uplift the crust sub-aerially, potentially leading to the development of SDR's.

If the AMR is an oceanic plateau, this ~0.5 km of subsidence due to extension would be added to subsidence as predicted for normal oceanic crust, where depth is linearly related to time$^{1/2}$ (Parsons and Sclater, 1977). While, subsidence histories of plume affected oceanic lithosphere varies from normal oceanic lithosphere, total plateau subsidence is comparable to that predicted for normal oceanic crust (Ito and Clift, 1998). Magmatic underplating and resulting isostatic uplift is proposed as a possible mechanism for reconciling subsidence as predicted by thermal models for plume-affected lithosphere, with sediment reconstructed subsidence histories. Magmatic underplating also explains the block faulting, and high velocity zones observed around the margins of oceanic plateaus (Hussong et al., 1979).

Along with analyzing gravity and seismic refraction data, Weber (1990), found subsidence histories of the Alpha Ridge and the Iceland-Faroe Ridge to be well correlated. While this is not an exacting experiment over the Alpha Ridge as paleo-depth data is incredibly sparse, it does explain a potential mechanism and analogue for subsidence of the Alpha Ridge. The subsidence history of the Mendeleev Ridge is not constructed here as there is even less paleo-depth information available.

Regional Unconformity and Timing of Most Recent Tectonism

Hall (1970) recognized that some sedimentation post-dated deformation of the Mendeleev Ridge, though he attributed this deformation to fracturing rather than extension. The regional unconformity separating Units I and II has been observed several times over the AMR. Over the Alpha Ridge, Jokat (2003) identifies an unconformity at a similar sub-seafloor depth as reported here (~250 m), and also observed extensional block faulting in the basement. The author suggested the separation of Barents and Siberian shelves at the onset of the opening the Eurasia Basin as a possible mechanism.

The regional unconformity separating sediment Units I and II appears to mark the end of extensional deformation of the Mendeleev Ridge and perhaps the Alpha Ridge. Observed sedimentation rates from the Lomonosv Ridge can be used to make a crude estimate of the age of the unconformity.

Moran et al. (2006) chronicles the recent ACEX drilling of the Lomonsov Ridge. In one location they were able to sample Cretaceous shelf sandstone at ~400 m below the seafloor, that was deposited on the paleo-margin of the Barents shelf. They calculated sedimentation rates for the Neogene and Paleogene at 11.4 m/My and 15.4 m/My respectively. Assuming ~0.3 secs TWT to the unconformity (Fig. 6), 1.6 km/s sediment velocity, and sedimentation rates calculated from the ACEX drilling, the base of sediment Unit I is dated at ~22 Ma. This date postdates any active opening of the Amerasian Basin (~153-127 Ma), the formation of the Alpha and Mendeleev Ridges (120-78 Ma), and the initial opening of the Eurasian Basin (~56 Ma).

This is not an exacting experiment, but it provides useful information using the most complete sedimentation data from the Central Arctic. It may be possible that the Mendeleev and Lomonsov Ridges represent two distinct depositional environments. While pelagic sedimentation is likely dominant over the Mendeleev Ridge, it is host to multiple pronounced bottom currents that may disturb local sediments and redistribute them regionally (Woodgate et al., 2005). It should be noted though, that from the ACEX drilling, a condensed section was discovered, spanning ~44 Ma to 16 Ma (Moran et al., 2006). This similarity in age is enticing, but there is not sufficient evidence at this time to make such a correlation.

The sedimentation rates from the ACEX drilling are higher than previous estimates for bulk sedimentation over the Alpha Ridge. Thiede et al. (1990) describe modern sedimentation rates in the central Arctic of 1-3 m/My, and Witte and Kent (1988), through magnetostratigraphic analysis of T-3 cores from the central Arctic, present rates of 1-3 m/My for the Pleistocene. Thiede et al. (1990) also suggests that rates may have been as much as 50 m/My during the Cretaceous. More recently, Cranston (1997) and Polyak et al. (2004) also describe slow sedimentation in the central Amerasian Basin, observing modern rates of 2-3 m/My. Scott et al. (1989) report average sedimentation rates of 1 m/My for the mid-Pliocene-present.

Higher sedimentation rates would result in a younger estimated age of the unconformity.

Applying Lomonosov Ridge Sedimentation Rates

If the Lomonosov sedimentation rates are appropriate for the Mendeleev Ridge from the Late Cretaceous, and this unconformity is representative of the end of tectonism, the unconformity suggests tectonism persisted in the Amerasian Basin well into the Cenozoic. If we assume a late Cretaceous age of formation and oceanic plateau origin, producing such extension over thickened, cold oceanic crust would be geodynamically very difficult.

The unconformity observed over the Lomonosov Ridge may be related to the regional unconformity that is described here. Geological provinces abutting the Amerasian Basin do not reveal such tectonic activity at this time, and hence to produce such large-scale extension, far field stresses may be required. On the Laptev Shelf, south of the Lomonsov Ridge, Drachev et al. (1998) and Franke and Hinz (2005) identify multiple Cenozoic unconformities that are attributed to Eurasian Basin tectonism, far-field tecontonism, and global eustasy patterns. The Mendeleev Ridge however, was most likely decoupled from extension in the Eurasian Basin, as the maturing Gakkel Ridge spreading system would accommodate these extensional stresses. It is therefore unlikely that this regional unconformity over the MR is associated with tectonism sourcing from the Eurasia Basin if an age of ~22 Ma is assigned.

If we instead hypothesize the AMR is derivative of continental rifting, the lithosphere would be more weak, and would contain pre-existing faults. Under this scenario, extending the AMR to its present state would not be as difficult.

Alternative Hypothesis

Considering the absence of known active tectonism near ~22 Ma, the Lomonosov sedimentation rates may not be reasonable for the AMR, especially during the early history of the Lomonosov Ridge, when it was more proximal to the Barents Shelf and less isolated from sediment sources than the AMR. From this we might assume that applying lower sedimentation rates would be appropriate for the AMR.

An alternative hypothesis for the development of this regional unconformity is the initiation of spreading in the Eurasian Basin. With the Eurasian Basin and north Atlantic

opening at 56 Ma, tectonism over the AMR ending at this time is perhaps more reasonable than introducing an unknown mechanism, extending tectonism into the Neogene. This also provides a means in which to connect the Amerasian and Eurasian Basins into a cohesive tectonic framework, regardless of whether the AMR is an Oceanic Plateau, or rifted continental margin.

If the regional unconformity is ≥ 56 Ma, and the AMR are continental, it may be a breakup unconformity as described by Falvey (1974). Embry and Dixon (1990) describe several possible mechanisms for the creation of a breakup unconformity. Generally they develop along active continental margins, due to the cessation of thinning and rifting of the lithosphere, prior to spreading according to simple rift models (McKenzie, 1978). Breakup unconformities are also observed empirically and are typically coeval with the oldest adjacent oceanic crust.

Without more precise knowledge of sedimentation rates over the AMR, interpretations of this unconformity will remain speculative.

Models for the Origin of the Alpha Mendeleev Ridge (AMR), Implications for the Amerasian Basin, and Potential Global Analogues

Through past studies, the emplacement age of the Alpha and Mendeelev Ridge is constrained to the mid-late Cretaceous (120-78 Ma) due to: the age (~82 Ma) of the basalts recovered from the ridge (Muhe and Jokat, 1999; Jokat, 2003), the oldest sediments (Campanian) sampled from the Alpha Ridge (Thiede et al., 1990), heat flow observations (Langseth et al., 1990), and the magnetic anomaly patterns which suggest formation during the Cretaceous normal period (Weber and Sweeney, 1990). This range of dates post-dates seafloor spreading in the Canada Basin (~148-127.5 Ma), and pre-dates spreading in the Eurasian Basin (~56 Ma–present).

Considering the constraints set by this study of the Mendeleev Ridge, and previous studies of both the Mendeleev and Alpha Ridges, three potential tectonic environments are envisioned that lead to the emplacement of the AMR: 1) A rifted volcanic continental margin, 2) An oceanic plateau formed at a spreading center

~perpendicular to the AMR, 3) An oceanic plateau formed at a spreading center ~parallel to the AMR.

All three hypotheses are consistent with the presence of a LIP during the late Cretaceous. Results from the Canadian Arctic margin, N. Greenland, Svalbard, Franz Joseph Land, and the E. Siberian Sea all reveal Cretaceous basaltic volcanism with two main pulses at ~130 Ma and ~95 Ma, ~95 Ma being more commonly observed.

Recovery of highly altered alkali basalts, from the Alpha Ridge, on two separate expeditions (Van Wagoner et al., 1986; Muhe and Jokat, 1999), suggests an intraplate origin for the rocks or at least small degrees of partial melting. It should be stressed that very little sample material was recovered and the samples exhibit large degrees of low temperature alteration. Still, the chemistry of the rocks is more consistent with the rifted volcanic continental margin hypothesis than the oceanic plateau hypotheses in that greater partial melting at or near a spreading center would yield greater volumes of tholeites, OIB (Ocean Island Basalts), and MORB's (mid-ocean ridge basalts). Despite not being the primary mode of volcanism, alkali basalts are observed on Iceland (Saunders et al., 1997), so an oceanic plateau origin for the AMR is not precluded.

Rifted Volcanic Continental Margin

The AMR may have rifted off of the Barents Shelf with a geometry similar to that of the Lomonosov Ridge (Fig. 27a). This geometry suggests that the Makarov Basin opened with a spreading axis roughly parallel to the orientation of the AMR, and formed either by passive extension or active spreading, following the rifting and magmatic emplacement of the AMR.

Under this scenario, the AMR crust was created by the emplacement of Mg-rich melt into actively thinning continental crust over a broad region of asthenospheric upwelling (White and McKenzie, 1989; Coffin and Eldholm, 1994; Eldholm and Grue, 1994). Physical characteristics observed in other volcanic margins can yield insight into this hypothesis for the AMR. Volcanism preceding initial rifting, dynamic uplift, and the compounding of tensional stresses are all common attributes (White and McKenzie, 1989).

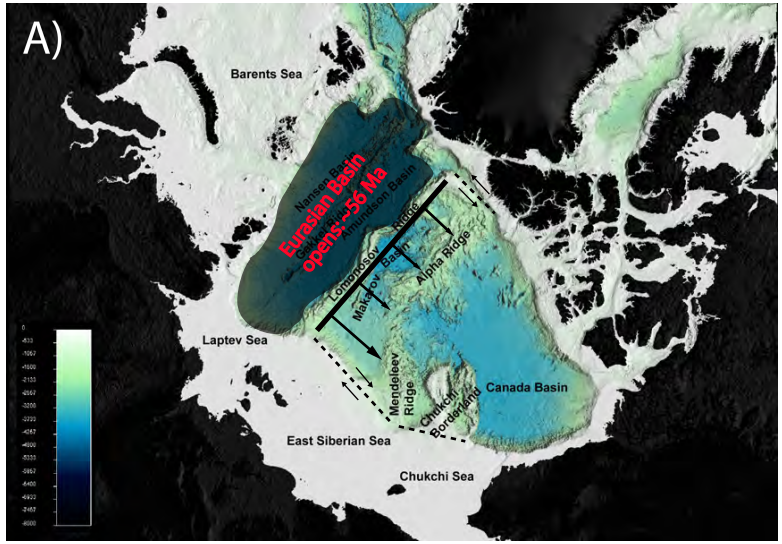

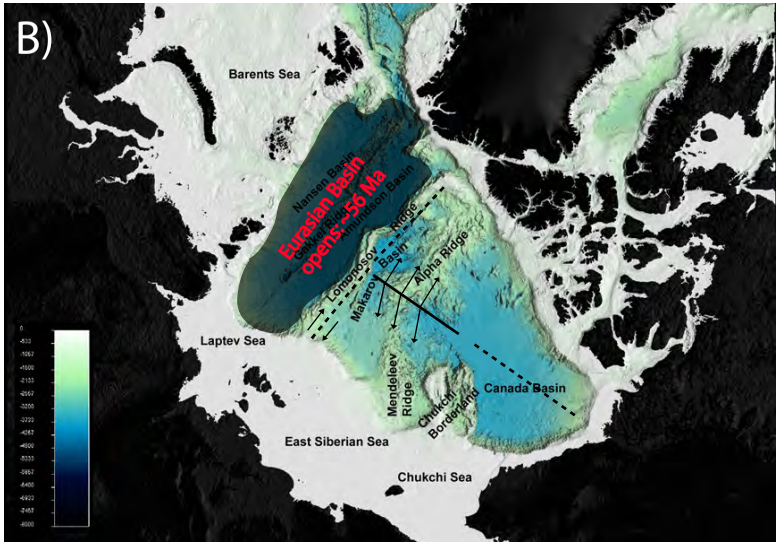

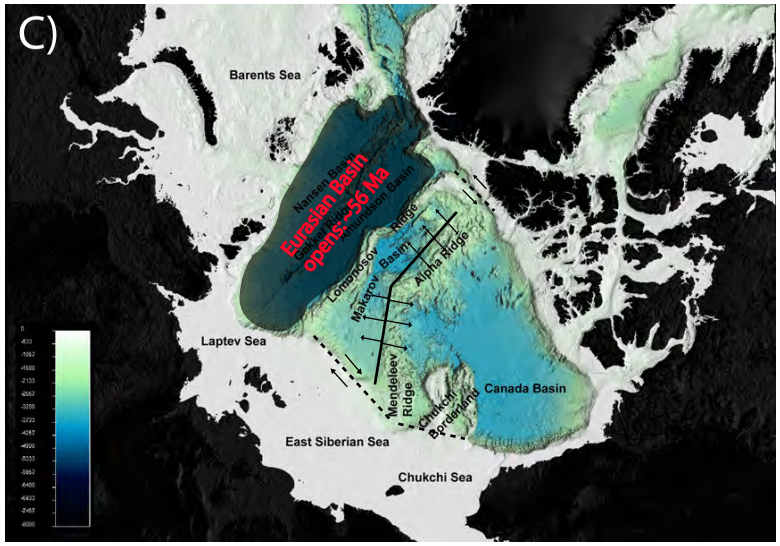

Fig. 27: Simplified Tectonic Models for the Emplacement of the Alpha Mendeleev Ridge.
A) Rifted volcanic continental margin. B) Oceanic Plateau formed at a spreading center ~perpendicular to the Alpha Mendeleev Ridge (AMR). C) Oceanic Plateau formed at a spreadingcenter ~parallel to the AMR.

It has been shown that the Makarov Basin, which has a crustal thickness of ~23 km, was likely influenced by the magmatism that formed the AMR (Ostenso, 1964; Sorokin et al., 1999). Interpretations of the magnetic anomalies of the Makarov Basin are perhaps more difficult than for the Canada Basin, and contradicting results have been presented for the age and spreading orientation of the Ridge (Fig. 2). Taylor et al. (1981) observes lineated anomalies 34-21 (84-49 Ma) coincident with the 87° N parallel, and locally sub-parallel to the Alpha Ridge. Kovacs et al. (1999) present a contradicting model, where axis of spreading is sub-perpendicular to the Lomonosov Ridge, and the age of the extinct spreading axis is ~128 Ma. Constructing an accurate and comprehensive tectonic framework for the Amerasian basin may be limited by our understanding of the Makarov Basin as much as it has been for the AMR.

Without age constraints, no conclusive statements can be made about the mechanism that may have driven rifting, but it could have been caused by the arrival of a plume head, or the onset of regional extensional stresses, or both. Similar to the extension that led to the development of the regional unconformity over, this initial rifting of the AMR may have been driven by extensional stresses propagating north from the Labrador Sea and Baffin Bay. A summation of far field tectonic stresses is also a plausible.

Potential Global Analogues

As discussed earlier, the volcanic rifted margins of the North Atlantic volcanic province (NAVP) may be analogous to the Mendeelev Ridge (Fig. 21) (White and McKenzie, 1989; Eldholm and Grue, 1994; Saunders et al., 1997; Hopper et al., 2003). The Iceland plume helped drive extension and fed massive amounts of mafic material into abutting continental crust at the onset of regional continental rifting. Similar to the AMR, a high velocity layer (7.2-7.7 km/s) resides at the base of the crust, and due to the thorough saturation of mafic material into the crust near the continent-ocean boundary, a homogenous crust is observed. Of note however, is that inboard of the continent-ocean boundary less igneous material is present, and greater lateral complexity would be expected for the crust (Gernigon et al., 2003). This lateral complexity would be

manifested in the gravity anomalies, and may not be consistent with results that demonstrate homogenous crust for the AMR.

Processes from The South China Sea also serve as useful analogues for the Amerasian Basin. Asymmetrical spreading and complex tectonism within the S. China Sea are attributed by Hall (2002), to changing plate directions related to subduction or the rotation of plates while spreading. The Dongha Rise in the S. China Sea is a volcanic margin where margin scale uplift led to the creation of a breakup unconformity, SDR's, and the emplacement of a high velocity lower crust (Lin et al., 2003). The rift-drift stage was sufficiently long to completely rupture the continental crust and isolate the rise. Then, contrary to the Amerasian Basin, seafloor spreading commenced seaward of the Dongha Rise and a foreland basin developed in the relative location occupied by the Makarov Basin in the Amerasian Basin.

Muller et al. (2001) suggest a mechanism for the creation of continental microplates, e.g. Seychelles (Todal and Eldholm, 1998), Jan Mayen, Tasman Plateau, and Gilbert Seamount Complex. These continental slivers are formed when continental margins are re-rifted due to the influence of a mantle plume on young or weakened continental margins. This causes a jump in the spreading location, isolating part of the continental margin (Fig. 28). In each example, volcanism (often tholeitic evolving to alkali basalts of LIP influence) post-dates rifting, and the associated block-faulting in certain cases. While this model cannot apply directly to the Amerasian Basin, because the Canada Basin did not open perpendicular to the Barents Shelf, it provides a mechanism to relate tectonism in the Amerasion to the Eurasia Basin. Applied to the Amerasia Basin, the AMR represents a microcontinent, isolated after arrival of plume influenced rifting and spreading in the Makarov Basin. A final ridge jump follows, as spreading commences at the Gakkel Ridge.

Oceanic Plateau Formed at a Spreading Center ~Perpendicular to the AMR

The AMR is estimated to contain > 10 million km^3 of mafic material (Vogt et al., 2006). If the AMR is an oceanic plateau, it is the second largest on earth next to the Ontong Java Plateau. All plateaus anywhere near this volume formed from mantle

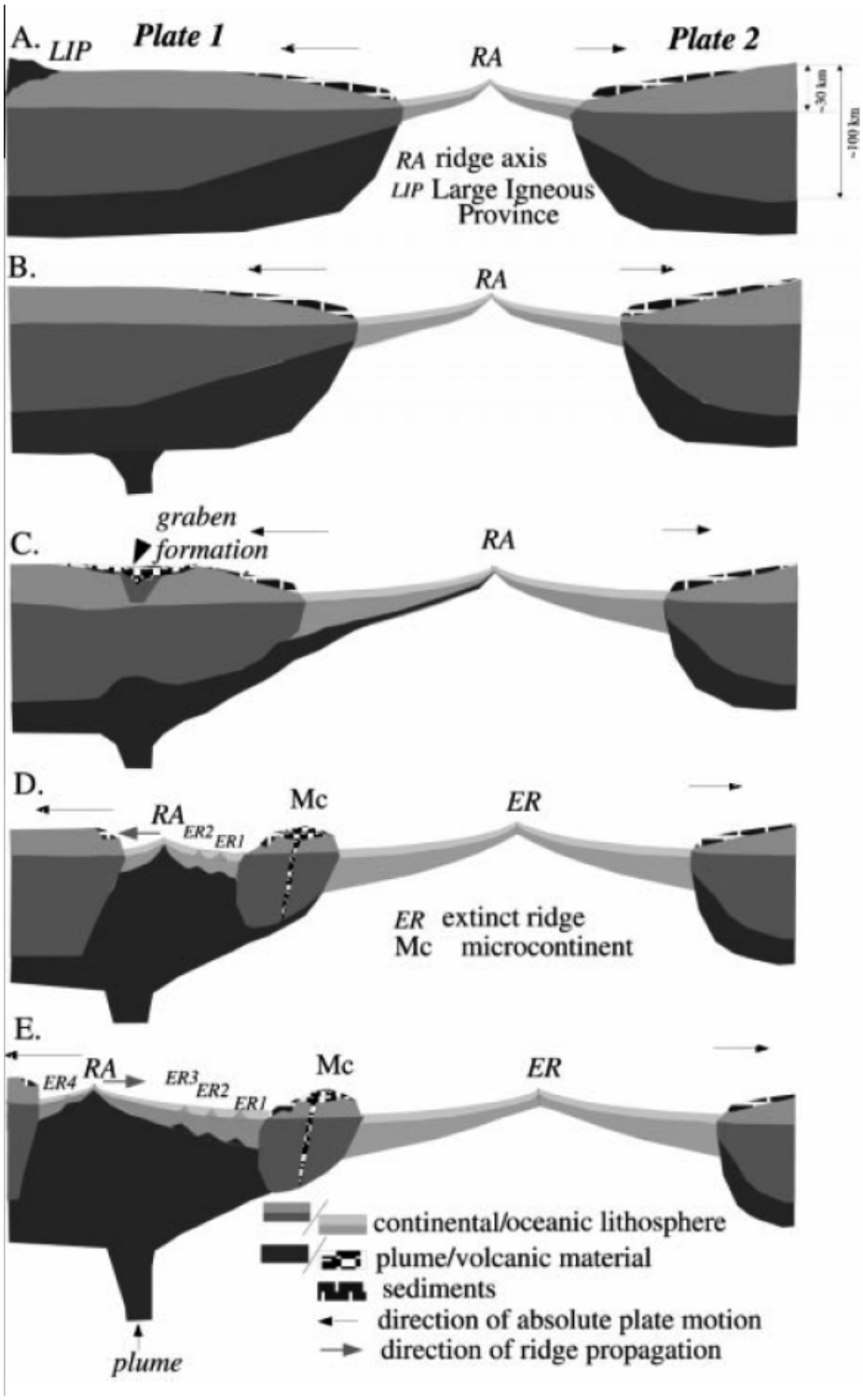

Fig. 28: Model for Continental Microplate Formation. Schematic model for the creation of a continental microplate through interaction with a thermal plume. Taken from Muller et al. (2001).

plumes, with some interaction with an active spreading center (Coffin and Eldholm, 1994).

In this framework, the AMR was created by excess melt at a spreading center coincident to that which formed the Canada Basin (Fig. 27b). The AMR would be perpendicular to, and symmetric about this spreading axis. The oldest crust would be expected near the Canadian and E. Siberian Sea margins. Due to the presumed younger age of the AMR, propagation of this spreading center northward largely post-dated spreading in the Canada Basin. Because of the age uncertainties of the AMR, some overlap in these two spreading events cannot be precluded.

This model requires that the Chukchi Borderland occupied its current position before emplacement of the AMR, presumably rifted off the E. Siberian Sea, after initial opening of the southern Canada Basin (Grantz and May, 1982). It also suggests that the western margin of the Chukchi Plateau along with the eastern margin of the present day Lomonsov Ridge served, to some extent, as transform margins accommodating seafloor spreading and the emplacement of the Mendeleev Ridge. This geometry may be difficult to justify considering how drastically the Chukchi Borderland protrudes into the Amerasian Basin (Fig. 1), and the current structural fabric of the Chukchi Borderland and the Mendeleev Ridge (Fig. 24).

The AMR has long been hypothesized as an oceanic plateau, created at a spreading center under the influence of a mantle plume. Particularly, results from gravity and seismic refraction surveys over the Alpha Ridge during the CESAR expedition led to the mostly unanimous argument that the Alpha Ridge is an oceanic plateau, similar to Iceland (Forsyth et al., 1986; Jackson et al., 1986, Weber et al., 1986; Weber, 1990). Most of this work regards the Alpha Ridge, and only Jackson et al. (1986) extrapolated these results to the Mendeleev Ridge. In fact, Weber (1990) regards the Mendeleev Ridge as continental crust based on the geophysical data available at the time.

Lawver and Muller (1994) and Lawver et al. (2002) also argue the AMR is an oceanic plateau, an expression of the Amerasian Basins rotation over the Iceland hotspot. The author's reconstruction places the Iceland plume at Ellesmere Island at 130 Ma. This

date is incompatible with onshore, presumed equivalent volcanic rocks in that area, where volcanics are dated at ~95 Ma (Tarduno et al., 1998; Villeneuve and Williamson, 2006; Weaver et al., 2006), but ~128Ma rocks are also observed (Villeneuve and Williamson, 2006). This reconstruction is even more incompatible for the AMR (120-78 Ma). Because of the age constraints, it is considered unlikely that the Iceland Plume supplied the magma that formed the ridges.

Through geohistorical analysis of magnetic anomalies in the Canada and Makarov Basins, Gurevich et al. (2005) and Gurevich and Merkouriev (2006), invoke multiple spreading centers for the creation of oceanic basins in the area now occupied by the AMR. The youngest dated magnetic anomaly is 127.5 Ma, and the AMR is proposed as being emplaced later on weakened oceanic crust. This hypothesis is divergent from the general concept being presented here, but falls into the category of emplacement of the AMR onto crust at least recently created by seafloor spreading.

The hypothesis presented here requires some degree of transform motion along the Amerasian side of the Lomonsov Ridge. While the Marvin and Oden spurs on the Amerasian side of the Lomonosov Ridge may provide bathymetric evidence of such motion, no large-scale fault has been observed through other geologic or geophysical studies. An alternative explanation for accommodating the opening of the Amerasian Basin is observed at the Bay of Biscay, which also opened by rotational spreading but exhibits discrete sets of transform faults along its conjugate margins instead of one regional transform fault (Thinon et al., 2003; Mondejar, 1996).

Oceanic Plateau Formed at a Spreading Center ~Parallel to the AMR

While the mode of emplacement at a spreading center ~parallel to the AMR is similar to the previous hypothesis, geometrically, formation of the AMR under this framework may be more similar to the rifted volcanic margin hypothesis (Fig. 27c). Again, the AMR is younger than the Canada Basin. Seafloor spreading would have predominantly ceased in the Canada Basin before being activated, perhaps under the influence of a mantle plume, along the two other arms (Alpha and Mendeleev Ridges).

The Makarov Basin would have been formed as a part of this spreading, opening roughly perpendicular to the former Barents Shelf.

This model is attractive as it provides a more direct way to get the Chukchi Plateau into its current position by rifting off the E. Siberian Sea before emplacement of the Mendeleev Ridge at the spreading center. It also creates a structural fabric that is coincident with the later, inferred E-W to SW-NE extension of the Mendeleev Ridge and Chukchi Plateau.

Considering the respective degrees of normal faulting observed on MCS images of the Alpha and Mendeleev Ridges, this later extension that led to the development of the regional unconformity, may have been more extreme at the Mendeelev Ridge. Also of note, the southern part of the Makarov Basin, known as the Wrangel Abysssal Plain or Podvodnikov Basin, is appreciably wider than the northern Makarov Basin. It is hypothesized that the late stage extension, whether it occurred before ~56 Ma or later in the Cenozoic, may have led to: the Mendeleev Ridge and Chukchi Plateau being rafted farther east, away from the E. Siberian Shelf, and the widening of the Podvodnikov Basin in respect to the northern Makarov Basin. This motion may have been accommodated along the E. Siberian margin to the south and the Arlis Gap, the E-W trending ridge that divides the northern and southern parts of the Makarov Basin, to the north.

The boundary between the Mendeleev Ridge and the E. Siberian Shelf was not crossed during this cruise but regional free-air gravity anomalies reveal the absence of the 'edge effect', typically observed over the continent-ocean boundary at passive margins (Figs. 2 & 3). The edge effect is caused by contrasts of crustal thickness and density. This feature is observed between the Alpha Ridge and the Canadian Arctic Islands.

The absence the 'edge effect' here may suggest magmatic intrusion into the E. Siberian Shelf, or that the E. Siberian Shelf has not remained a passive margin since the initial opening of the Amerasian Basin. Similarities in magnetic anomaly patterns between the Mendeleev Ridge and the Delong Plateau, northeast of the New Siberian Islands, invites speculation that sinistral motion along the E. Siberian Shelf, translated the Mendeleev Ridge away from the more southerly Delong Plateau, from which it was once

connected. The hypothesis that the Delong Plateau and the Mendeleev Ridge may share a common origin was also proposed by Drachev et al. (1999) and Drachev et al. (2006), based on the recovery of Cretaceous Basalts (~119 Ma and ~112 Ma). This proposed motion also explains the present offset between the Mendeleev and Alpha Ridges.

This hypothesis is plausible under all three tectonic models proposed here, however the geometry is somewhat more complex in the "oceanic plateau formed at a spreading center ~perpendicular to the AMR" model.

Potential Global Analogues

Large oceanic plateaus constitute the most voluminous LIP structures on earth (Coffin and Eldholm, 1994). Examples presented here are Iceland, the Ontong Java Plateau, and the Kerguelen Plateau. Each of these features was formed in a unique tectonic environment, but common to their origin is the involvement of some interaction between excess mantle melting and spreading center (Lassiter and DePaulo, 1997). Another characteristic is that that the primary magmatic events are very brief (~5 ma) and may occur at multiple, discrete pulses.

Iceland has been used before as an analogue for the AMR (Forsyth et al., 1986; Weber, 1990; Lawver and Muller, 1994). Iceland is still active and represents a unique opportunity to observe the geological processes that may have led to the formation of the AMR. Volcanism in Iceland is typically ascribed to the presence of the Iceland plume, and its interaction with the N. Atlantic spreading system (Lawver and Muller, 1994; Fitton et al., 1997; Saunders et al., 1997). The AMR is of a similar crustal thickness to Iceland (23-30 km), and exhibits a similar velocity structure as described previously (Fig. 21a) (Flovenz and Gunnarsson, 1991). There is great diversity in the chemistry of basalts found in Iceland, but ~90% of the lavas are tholeitic, with transitional and more alkalic rocks observed off axis where lower degrees of partial melt and deeper sources are inferred (Saunders et al., 1997). SDR's are also observed offshore (Fitton et al., 1997).

The Ontong Java Plateau (OJP) is the largest LIP on earth (1.86×10^6 km^2) and was emplaced almost entirely during two discrete pulses of magmatism in the mid-Cretaceous (Berger et al., 1992; Coffin and Eldholm, 1994; Neal et al., 1997). The ridge

was at least originally formed near a spreading center but large volumes of lava were emplaced off axis (Neal et al., 1997). Like Iceland, the crust is very thick, ~40 km, and through seismic refraction studies is considered a linear expansion of normal oceanic crust, with each layer being ~5 times more thick within the OJP (Hussong et al., 1979). Ocean drilling revealed lower sediments significantly intercalated with basalt flows (Berger et al., 1992). The velocity structure of the upper crust is consistent with results presented here for the Mendeleev Ridge. The full crustal velocity structure is also compatible with that observed over the AMR (Forsyth et al., 1986; Ivanova et al., 2006).

The Kerguelen Plateau (KP) is in the southern Indian Ocean and was formed in the Cretaceous (~110 Ma), through interaction of the Kerguelen Plume with the SE Indian Ridge (Konnecke et al., 1998; Charvis and Operto, 1999; Frey et al., 2002).

Unlike the OJP, which is entirely submarine, the KP saw extensive sub-aerial volcanism as evidenced by the presence of SDR's over the ridge, and the still emergent Kerguelen Archipelago (Konnekcke et al., 1998). The KP consists of thickened crust of 14-24 km. Upper basement velocities of 3.9-4.7 km/s are similar to those observed over the AMR, and are interpreted to contain intercalated sediments (Konnecke et al., 1998; Charvis and Operto, 1999).

One interesting aspect of the KP is the possibility of admixed continental crust amongst the ocean island basalts. While contentious, interpretations based on reflection character, velocity gradients, and the recovery of meta-igneous granulite xenoliths, have led to hypotheses describing the presence of captured slivers of volcanic continental crust (Operto and Charvis, 1995; Frey et al., 2002), or the possibility of continent nucleation in an oceanic setting (Gregoire et al., 1998).

Conclusions

The Alpha Mendeleev Ridge (AMR) is the single largest edifice in the central Arctic Ocean. Until recently, the Alpha Ridge has been more thoroughly studied than the Mendeleev Ridge. Most studies conclude that the Alpha Ridge is an oceanic plateau, formed by plume interaction with a spreading center, similar to Iceland. However, many authors cannot rule out a continental origin.

Due to the paucity of both geological and geophysical data collected at the Mendeleev Ridge, the origin and history of the ridge has long been enigmatic. Hypotheses regarding ridge formation are often inferred from the Alpha Ridge and range from plume affected spreading center to Hawaii-type hotspot track to attenuated continental crust.

During the Mendeleev Ridge leg of the H0503 expedition, bathymetry, MCS, seismic refraction, and gravity data were collected that further enhance our understanding of the ridge and its relationship to neighboring features i.e. the Alpha Ridge and Chukchi Plateau.

MCS images reveal two primary sediment units and a mostly homogenous upper crust. Interpretations of isolated sub-basement coherent reflectors are ambiguous and may represent Mesozoic or older sediments, or volcanic flows. Extension of the ridges is inferred along an E-W to NE-SW axis, that led to pervasive normal faulting of the basement and lower sediments, as well as the development of horst and graben structures.

The two sediment units are separated by an unconformity that appears to mark the end of extensional deformation of the ridge, and likely persists across the whole of the Mendeleev and Alpha ridges. Total sediment thicknesses range from 0 km at basement exposed scarps to ~1.2 km in the deep grabens. Tentative dating of the unconformity, applying sedimentation rates from the Lomonosov Ridge, suggests tectonism in this region may have persisted well into the Cenozoic (~22 Ma). Recognizing that this relatively recent date may be implausible considering the absence of known regional tectonism near that time, and that these sedimentation rates may not be accurate for the Mendeleev Ridge, an alternative hypothesis is that this unconformity represents the conclusion of rifting in the region, prior to the opening of the Eurasia Basin at 56 Ma.

Modeling of the seismic refraction data reveals an upper crustal velocity structure that is mostly inconsistent with normal oceanic crust. The results are compatible with both the crust of volcanic rifted continental margins similar to the North Atlantic Volcanic Province (NAVP), and oceanic plateau crust similar to Iceland and the Kerguelen and Ontong Java Plateaus. However, these comparisons remain tentative as

we sampled only the upper crust in this experiment. Basement velocities reported here may represent high velocity sediments (carbonates), or oceanic layer 2.

Gravity anomalies over 2 ~225 km profiles crossing the Mendeleev Ridge can be reproduced with models containing bathymetry, sediment and basement horizons, and a single density crustal layer of 2.86 g/cm^3. This result is indicative of homogenous, predominantly mafic crust. Model misfits over the Chukchi Plateau suggest that it likely has a different composition than the Mendeleev Ridge, and a separate emplacement history. The similarity of both the velocity and density structures between the Mendeleev and Alpha Ridges, corroborated by potential field and bathymetry observations suggests the ridges are a contiguous feature, sharing a common geologic origin.

A comprehensive model for the tectonic evolution of the Amerasian Basin requires the thorough understanding of the Alpha Mendeelev Ridge. A unique solution to the geologic origin and history of the ridge is not yet apparent and deep-sea drilling of the ridge may be required to solve this question. Three emplacement models for the Alpha Mendeleev Ridge that satisfy constraints set by this and previous studies are: 1) rifted volcanic continental margin, 2) oceanic plateau formed at a spreading center ~perpendicular to the AMR, 3) oceanic plateau formed at a spreading center ~parallel to the AMR.

References

Asudeh, I., A. Green, D. Forsyth, 1988. Canadian expedition to study the Alpha Ridge complex: results of the seismic refraction survey, Geophys. Jour., 92, p. 383-301.

Baggeroer, A.B., R. Falconer, 1982. Array Refraction Profiles and Crustal models of the Canada Basin, J. Geophys. Res., 87 (B7), p. 5461-5476.

Beal, M. A., 1968. Bathymetry and structure of the Arctic Ocean, Ph. D. thesis, Oregon State University, Corvallis, 204p.

Bell, R.E., A. Watts, 1986. Evaluation of the BGM-3 sea gravity meter system on board R/V Conrad, Geophysics, 51, p. 1480-1493.

Berger, W.H., L. Kroenke, L. Mayhaer, J. Backman, T., Jancek, L. Krissek, M. Leckie, M. Lyle, 1992. The record of Ontong Java Plateau: Main results of ODP Leg 130, GSA Bulletin, 104, p. 854-972.

Brocher, T.M., 2005. Empirical Relations between Elastic Wavespeeds and Density in the Earth's Crust, Bulletin of the Seismological Society of America, 95(6), p. 2081-2092.

Carey, S.W., 1958, A tectonic approach to continental drift, in Carey, S.W., ed., Continental drift, A syposium: Hobart, Tasmania, University of Tasmainia, p. 177-355.

Charvis, P., S. Operto, 1999. Structure of the Cretaceous Kerguelen Volcanic Province (southern Indian Ocean) from wide-angle seismic data, Geodynamics, 28, p. 51-71.

Christensen, N.I., W. Mooney, 1995. Seismic velocity structure and composition of the continental crust: A global view, J. Geophys. Res. 100, p. 9761-9788.

Churkin, M., Jr., 1970. Fold belts of Alaska and Siberia and drift between North America and Asia, in Adkison, W.L.,and W. Brosge, eds., Proceedings of the geological seminar on the North Slope of Alaska: American Association of Petroleum Geologists, Pacific Section, G1-G17.

Coakley, B.J., and J.R. Cochran,1998, Gravity evidence of very thin crust at the Gakkel Ridge (Arctic Ocean), Earth and Planetary Sci. Letters, 162, p. 81-95.

Cochran, J.R., G. Kurras, M. Edwards, B. Coakley, 2003. The Gakkel Ridge: Bathymetry, gravity anomalies, and crustal accretion at extremely slow spreading rates, J. Geophys. Res., 108(B2), p. 2116.

Coffin, M.F., O. Eldholm, 1994. Large igneous provinces: crustal structure, dimensions, and external consequences, Rev. Geophys. 32, p. 1–36.

Coles, R.L., W. Hannaford, G. Haines, 1978. Magnetic anomalies and the evolution of the Arcitc, in Sweeney, J.F., ed., Arctic geophysical review: Ottawa, Publication of the Earth Physics Branch, 45, p. 51-66.

Coles, R.L., P. Taylor, 1990. Magnetic anomalies, in Grantz, A., Johnson, L., and Sweeney, J.F., eds., The Arctic Ocean Region: Boulder, Geological Society of America, p. 119-132.

Cranston, R.E., 1997. Organic carbon burial rates across the Arctic Ocean from the 1994 Arctic Ocean Section expedition, Deep-Sea Res., II 44,1705-1724.

Delaurier, J.M., 1978. The Alpha Ridge is not a spreading centre, Publication of the Earth Physics Branch, 45, p. 87-90.

Drachev, S.S., L. Savostin, V. Groschev, I. Bruni, 1998. Structure and geology of the continental shelf of the Laptev Sea, Eastern Russian Arctic, Tectonophysics, 298, p. 357-393.

Drachev, S.S., G. Johnson, D. McAdoo, S. Laxon, H. Kassens, 1999. Main structural elements of eastern Russian Arctic continental margin derived from satellite gravity and multi-channel seismic reflection data, in Kassens, H. et al. eds., Land-Ocean Systems in the Siberian Arctic: Dynamics and History, p. 667-682.

Drachev, S., A. Saunders, 2006. The early Cretaceous Arctic LIP: Its geodynamic setting and implications for Canada Basin opening, in Scott, R.A., D. Thurston, eds., ICAM IV Proceedings, p. 216-223.

Eldholm, O., K. Grue, 1994. North Atlantic volcanic margins: Dimensions and production rates, J. Geophys. Res., 92(B2), p. 2955-2968.

Embry, A.F, J. Dixon, 1990. The breakup unconformity of the Amerasia Basin, Arctic Ocean: Evidence from Arctic Canada, GSA Bulletin, 102, p.1526-1534.

Embry, A.F., K. Osadetz, 1988. Stratigraphy and tectonic significance of Cretaceous volcanism, Queen Charlotte Islands, Arctic Archipelago, Canadian Journal of Earth Sciences, 25, p. 1209-1219

Estrada, S., F. Kunst, 2004. Vocanism in the Canadian High Arctic related to the opening of the Arctic Ocean, Z. dt. geol. Ges., 154/4, p. 579-603.

Ewing, J., R. Houtz, 1979. Acoustic stratigtraphy and structure of the oceanic crust, in Deep Drilling Results in the Atlantic Ocean: Ocean Crust, Maurice Ewing Ser., Talwani, M., et al., eds., AGU, Washington, D.C., 2, p. 1-14.

Falvey, D. A., 1974. The development of continental margins in plate tectonic theory: Australian Petroleum Exploration Association Journal, 14, p. 95-106.

Fitton, J.G., A. Saunders, M. Norry, B. Hardarson, R. Taylor, 1997. Thermal and chemical structure of the Iceland plume, Earth and Planetary Sci. Letters, 153(3), p. 197-208.

Flovenz, O.G., K. Gunnarsson, 1991. Seismic crustal structure in Iceland and surrounding area, Tectonophysics, 189, p. 1-17.

Forsyth D.A., J. Mair, 1984. Crustal structure of the Lomonosov Ridge and the Fram and Makarov Basins near the North Pole: J. Geophys. Res., 89(B1), p. 473-481.

Forsyth, D.A., P. Morel-A-L'Huissier, I. Asudeh, A. Green, H. Jackson, 1986. Alpha ridge and Iceland-products of the sampe plume?, J. Geodyn., 6, p. 197-214.

Franke, D., K Hinz, 2005. The structural style of sedimentary basins on the shelves of the Laptev Sea and western East Siberian Sea, Siberian Arctic, Jour. of Petroleum Geol., 28(3), p. 269-286.

Frey, F.A., D. Weis, Ayu Borisova, G. Xu, 2002, Involvement of Continental Crust in the formation of the Creteaous Kerguelen Plateau: New Perspectives from ODP Leg 120 Sites, J. Petrology, 43(7), p. 1207-1239.

Fujita, K., D. Cook, 1990. The Arctic continental margin of eastern Siberia, in Grantz, A., Johnson, L., and Sweeney, J.F., eds., The Arctic Ocean Region: Boulder, Geological Society of America, p. 289-304.

Gernigon, L., J. Ringenbach, S. Planke, B. Le gall, H. Jonquet-Kolsto, 2003. Extension, crustal structure and magmatism at the outer Voring Basin, Norwegian margin, Jour. Geol. Soc., London, 160, p. 197-208.

Glebovsky, V.Y., Kovacs, L.C., Maschenkov, S.P., Brozena, J.M., 2000. Joint Compilation of Russian and US Navy Aeromagnetic Data in the Central Arctic Seas, Polarforschung, 68, p. 35-40.

Grantz, A.L., S. Eittreim, D. Dinter, 1979. Geology and tectonic development of the continental margin north of Alaska, Tectonophysics, 590, p. 263-291.

Grantz, A.L, S. May, 1982. Rifting history and structural development of the continental margin north of Alaska, in Watkins, J.S., and Drake, C.I., eds, Studies in continental margin geology: American Association of Petroleum Geologists Memoir 34, p. 7-100.

Grantz, A.L., S. May, M. Mullen, L. Gray, J. Lull, D. Clark, C. Stevens, 1990. The Canada Basin, in Grantz, A., Johnson, L., and Sweeney, J.F., eds., The Arctic Ocean Region: Boulder, Geological Society of America, p. 257-288

Grantz, A.L., S. May, P. Hart, 1994. Geology of the Arctic continental margin of Alaska, in Plafker, G., Berg, H.C., eds., The Geology of Alaska: Boulder, Geological Society of America, p. 17-48.

Grantz, A., L. Clark, L. Phillips, P. Srivastava, et al., 1998. Phanerozoic stratigraphy of Northwind Ridge, magnetic anomalies in the Canada basin, and the geometry and timing of rifting in the Amerasia Basin, Arctic Ocean, GSA Bulletin, 110(6), p. 801-820.

Grantz, A.L., 2006. Geophysical and geologic evidence that Amerasia Basin, Arctic Ocean was created by two phases of anti-clockwise rotation, Abs. with Prog. 38(5).

Gregorie, M. J.Y. Cottin, A. Giret, N. Mattielli, D. Weis, 1998 The meta-igneous granulite xenoliths from Kerguelen Archipelago: evidence of a continent nucleation in an oceanic setting, Contributions to mineralogy and petrology, 133(3), p. 259-283.

Gurevich, N.I., S. Merkouriev, A. Abelskaya, 2005. Evolution of the Southern Canada Basin, the Arctic Ocean, on the basis of geohistorical analysis of magnetic anomalies, Geophs. Res. Abstracts, 7, 02710.

Gurevich, N.I., S. Merkouriev, 2006. Evolution of the Makarov Basin on the basis of geohistorical analysis of magnetic anomalies and its relationship with the evolution of the alpha ridge, Geophys. Res. Abstracts, 8, 06075.

Hall, J.K, 1970. Arctic Ocean Geophysical Studies: The Alpha Cordillera and Mendeleyev Ridge: New York, Columbia Univ., Ph.D. dissert., 125p.

Hall, J.K., 1990. Chukchi Borderland, in Grantz, A., Johnson, L., and Sweeney, J.F., eds., The Arctic Ocean Region: Boulder, Geological Society of America, p. 593-616.

Hall, R., 2002. Cenozoic geological and plate tectonic evolution of SE Asia and the SW Pacific: computer-based reconstructions, model and animations, Jour. Asian Earth Sciences 20, p. 353–431.

Heezen, B.C., M. Ewing, 1961. The Mid-Oceanic Ridge and its extension through the Arctic Basin, in Raasch, G.O., ed., Geology of the Arctic, University of Toronto Press, Troronto, 1, p. 622-642.

Henkart, P. 1981. SIOSEIS, Scripps Industrial Associates and National Science Foundation.

Herron, E.M., J. Dewey, W. Pitman, 1974. Plate Tectonics Model for the Evolution of the Arctic, Geology, 2, p. 377-380.

Hopper, J.R., T. Dahl-Jensen, W. Holbrook, H.C. Larson, D. Lizzarralde, J. Korenaga, G. Kent, P. Kelemen, 2003. Structure of the SE Greenland margin from seismic reflection and refraction data: Implications for nascent spreading center subsidence and asymmetric crustal accretion during North Atlantic opening, J. Geophys. Res., 108(B5), 2269.

Hunkins, K.L., 1961. Seismic studies of the Arctic Ocean floor, in Geology of the Arctic, Vol. 1, Raasch, G.O., ed., University of Toronto Press, Toronto, p. 645-665.

Hunkins, K.L., 1966. The Arctic continental shelf north of Alaska, in Continental Margins and Island Arcs, Poole, W.H., ed., Geol. Survey of Canad Paper, 66-15, 197-205.

Hussong, D., L. Wipperman, L. Kroenke,, 1979. The crustal structure of the Ontong Java and Manhiki oceanic plateaus, J. Geophys. Res. 84, p. 6003-6010.

Ito, G., Clift, P., 1998. Subsidence and growth of Pacific Cretaceous plateaus, Earth and Planetary Sci. Letters, 161, p. 85-100.

Ivanova, N.N, Y. Zamansky, A. Langinen, M. Sorokin, 2006. Seismic Profiling across the Mendeleev Ridge at 82 N: Evidence of continental crust, Geopys. J. Int., 165, p. 527-544.

Jackson, H.R., D. Forsyth, G. Johnson, 1986. Oceanic affinities of the Alpha Ridge, Marine Geology, 73, p. 237-261.

Jakobsson, M., N. Cherkis, J. Woodward, B. Coakley. R. Macnab, 2000. A new grid of Arctic bathymetry: A significant resource for scientists and mapmakers. Eos 81(9), p. 89, 93, 96.

Jakobsson, M., A. Grantz, Y. Kristoffersen, R. Macnab, 2003. Physicographic provinces of the Arctic Ocean seafloor, GSA Bulletin, 115(11), p. 1443-1455.

Jokat, W., G. Uenzelmann-Neben, Y. Kristoffersen, T. Rasmussen, 1992. ARCTIC' 91: Lomosov Ridge- a double sided continental margin, Geology, 20, p. 887-890

Jokat, W., 2003. Seismic investigations along the western sector of Alpha Ridge, central Arctic Ocean, Geohysical Journal International, 152, p. 185-201.

Jokat, W., 2005. The sedimentary structure of the Lomonosov Ridge between 88º N and 80ºN, Geophys. J. Int, 163, p. 698-726.

Jones, P.R., 1980. Evidence from Canada and Alaska on plate tectonic evolution of the Arctic Ocean Basin, Nature, 285, p. 215-217.

Kenyon, S., and R. Forsberg, 2001. Arctic Gravity Project – a status, in Gravity*,Geoid, and Geodynamics 2000, International Association of Geodesy Symposia*vol. 123, Sideris, M., ed. p. 391-395.

Klemperer, S. L., E. Miller, A. Grantz, d. Scholl, J. Childs, N. Bogdanov, I. Belykh, H. Gnibidenko, B. Galloway, B. Hicks, F. Cole, J. Toro, 2002. Crustal structure of the Bering and Chukchi shelves; deep seismic reflection profiles across the North American continent between Alaska and Russia, in Miller, E. L., A. Grantz, S. Klemperer, Tectonic Evolution of the Bering Shelf-Chukchi Sea-Arctic Margin and Adjacent Landmasses (GSA Special Paper), Geological Society of America, Geological Society of America, 360, p. 1-24.

Konnecke, L., Coffin, M., Charvis, P., 1998. Early development of the southern Kerguelen Plateau (Indian Ocean) from shallow wide-angle ocean bottom seismometer and multichannel seismic reflection data, J. Geophs. Res. 103(B10), p. 24,085-24,108.

Kovacs L.C., V. Glebovsky, M. Sorokin, S. Mashenkov, J. Brozena, 1999. New.Evidence for Seafloor Spreading in the Makarov Basin, EOS Trans. AGU, 80 (46), Fall meet. abstract, T32B-20.

Kristofferson, Y., 1990. Eurasia Basin. in Grantz, A., Johnson, L., and Sweeney, J.F., eds., The Arctic Ocean Region: Boulder, Geological Society of America, p. 365-378.

Kutschale, H., 1966. Arctic Ocean geophysical studies; The southern half of the Siberian Basin, Geophysics, 21, p. 683-709.

Lane, L.S., 1997. Canada Basin, Arctic Ocean: Evidence against a rotational origin, Tectonics, 16, p. 363-387.

Langseth, M.G., A. Lachenbruch, B. Marshall, 1990. Geothermal observations in the Arctic region, in Grantz, A., Johnson, L., and Sweeney, J.F., eds., The Arctic Ocean Region: Boulder, Geological Society of America, p. 133-152.

Lassiter, J.C., D. DePaulo, 1997. Plume/lithosphere interaction in the generation of continental and oceanic flood basalts: Chemical and Isotopic Constraints, in Mahoney, J., Coffin, M., eds. Large Igneous Provinces, Continental, Oceanic, and Planetary Volcanism, Washington, American Geophysical Union, p. 335-356.

Lawver, L.A., C. Scotese, 1990. A review of tectonic models for the evolution of the Canada Basin, in Grantz, A., Johnson, L., and Sweeney, J.F., eds., The Arctic Ocean Region: Boulder, Geological Society of America, p. 593-618.

Lawver, L.A., R.D. Muller, 1994. Iceland hotspot track, Geology, 22, p. 311-314.

Lawver, L.A, A. Grantz, L.M. Gahagan, 2002. Plate kinematic evolution of the present Arctic region since the Ordovician, Geological Society of America Special Paper, 360, p. 333-358.

Laxon, S., D. McAdoo, 1994. Arctic Ocean gravity field derived from ERS-1 satellite altimetry, Science, 265, p. 621-624.

Lin, A.T., A. Watts, S. Hesselbo, 2003. Cenozoic stratigraphy and subsidence history of the South China Sea margin in the Taiwan region, Basin Research, 15, p. 453-478.

Ludwig, W.J., J. Nafe, L. Drake, 1970. Seismic refraction, in The Sea, Maxwell A.E., ed., Wiley-Interscience,, New York, 4, p. 53–84.

Maher, H.D., 2001. Manifestations of the Createaceous High Arctic Large Igneous Province in Svalbard, Geology, 109, p. 91-104.

McKenzie, D., 1978. Some Remarks on the development of sedimentary basins, Earth and Plantary Science Letters, 40, p. 25-32.

Miller, E.L., J. Toro, G. Gehrels, J. Amato, A. Prokopiev, M. Tuchkova, V. Akinin, T. Dumitru, T. Moore, M. Cecile, 2006. New insights into Arctic paleogeograpy and tectonics from U-Pb detrital zircon geochronology, Tectonics, 25, TC3013.

Mondejar, J.G., 1996. Plate reconstruction of the Bay of Biscay, Geology, 24(7), p. 635-638.

Moran, K., J. Backman, H. Brinkhuis, S. Clemens, T. Cronin, G. Dickens, F. Eynaud, J. Gattacceca, M. Jakobsson, R. Jordan, M. Kaminski, J. King, N. Koc, A. Krylov, N. Martinez, J. Matthiessen, D. McInroy, T. Moore, J. Onodera, M. O'Regan, P. Heiko, B. Rea, D. Rio, T. Sakamoto, D. Smith, R. Stein, K. St. John, I. Suto, N. Suzuki, K. Takahashi, M. Watanabe, M. Yamamoto, J. Farrell, M. Frank, W. Jokat, Y. Kristoffersen, 2006. The Cenozoic palaeoenvironment of the Arctic Ocean, Nature, 441, p. 601-605.

Moore, T.E., W. Wallace, K. Bird, S. Karl, C. Mull, J. Dillon, 1994. Geology of northern Alaska, in Plafker, G., Berg, H.C., eds., The Geology of Alaska: Boulder, Geological Society of America, p. 49-138.

Mudie, P., S. Blasco, 1985. Lithostratigraphy of the CESAR cores, in Jackson, H.R., and others, eds., Initial geological report on CESAR; The Canadian expedition to study the Alpha ridge, Arctic Ocean: Geological Survey of Canada Paper, 84-22, p. 59-100.

Muhe, R. W. Jokat, 1999. Recovery of volcanic rocks from the Alpha Ridge, Arctic Ocean: preliminary Results, EOS, Trans. Am. Geophys. Union, 80, San Francisco, F1000.

Muller, D., C. Gaina, W. Roest, D. Hansen, 2001. A recipe for microcontinent formation, Geology, 29(3), p. 203-206.

Neal, C.R., J. Mahoney, L. Kroenke, R. Duncan, M. Petterson, 1997. The Ontong Java Plateau, in Mahoney, J., Coffin, M., eds. Large Igneous Provinces, Continental, Oceanic, and Planetary Volcanism, Washington, American Geophysical Union, p. 183-216.

Operto, S., P. Charvis, 1995. Kerguelen Plateau: a volcanic passive margin fragment?, Geology 23, p. 137-140.

Ostenso, N.A., 1964. Geophysical investigations of the Arctic Ocean Basins, Geophysical and Polar Research Centre, Research Report Series, University of Wisconsin, Madison, Wi, 62-4, 124p.

Ostenso, N.A., R. Wold, 1973, Aeromagnetic evidence for the origin of Arctic Ocean Basin, in Pitcher, M.G., ed., Arctic geology, American Assoc. of Petroleum Geologists Memoir, 19, p. 506-516.

Parsons, B., J. Sclater, 1977. An analysis of the variation of ocean floor bathymetry and heat flow with age, J. Geophys. Res., 82(5), p. 803-827.

Polyak, L., S. Brachfeld, D. Darby, J. Bischoff, R. Phillips, L. Febo, B. Coakley, M. Edwards, J. Engels, 2003. Multiple glacial erosion on the Chukchi Borderland, Arctic Ocean, as indicated by preliminary data on sediment stratigraphy and sea-floor morphology, XVI INQUA Congress, Paper No. 68-2.

Polyak, L., W. Curry, D. Darby, J. Bischof, T. Cronin, 2004. Contrasting glacial/interglacial regimes in the western Arctic Ocean as exemplified by a sedimentary record from the Mendeleev Ridge, Paleo. Paleo. Paleo., 203, p. 73-93.

Saunders, A.D., J. Fitton, A. Kerr, M. Norry, R. Kent, 1997. The North Atlantic Igneous Province, in Mahoney, J., Coffin, M., eds. Large Igneous Provinces, Continental, Oceanic, and Planetary Volcanism, Washington, American Geophysical Union, p. 45-94.

Scott, D.B., P. Mudie, V. Baki, K. MacKinnon, F. Cole, 1989. Biostratigraphy and Late Cenozoic paleoceanography of the Arctic Ocean: foraminiferal, lithostratigraphic and isotopic evidence, Geological Society of America, Bulletin, 101, p. 260-277.

Shatskiy, N.S., 1935. On the tectonics of the Arctic (in Russian): The geology and mineral resources of the northern USSR Glavsenmorputi, 1st Geological Invitational Conference, Moscow, Translation, 1, p. 149-168.

Sobzak, and D.B Hearty, et al., 1990. Gravity from 64 N to the North Pole, in Grantz, A., et al., eds., The Arctic Ocean Region: Boulder, Geological Society of America, p. 101-115.

Song, J.L., U. ten Brink, 2004. RayGUI 2.0 - A Graphical User Interface for Interactive Forward and Inversion Ray-Tracing, U.S. Geological Survey Open-File Report p. 2004-1426.

Sorokin, M., Zamansky, Y., Langinen, A., Jackson, R., Macnab, R., 1999. Crustal structure of the Makarov Basin, Arctic Ocean determined by seismic refraction, Earth and Planetary Sci. Letters, 168, p. 187-199.

Tailleur, L.L., W. Brosge, 1970, Tectonic history of northern Alaska, in Adkison, W.L., and Brosge, W. P., eds, Proceedings of the geological seminar on the North Slope of Alaska, Amer. Assoc. Of Petroleum Geologists, Pacific Section, E1-E19.

Talwani, M., M. Ewing, 1960. Rapid computation of gravitational attraction of three-dimensional bodies of arbitrary shape, Geophysics, 25, p. 203-225.

Tarduno, J.A, D. Brinkman, P. Renne, R. Cottrell, H. Scher, P. Castillo, 1998. Evidence for extreme climatic warmth from Late Cretaceous Arctic vertebrates. Science, 282, p. 2241-2244.

Taylor, P.T., K. Kovacs, P. Vogt, G. Johnson, 1981. Detailed Aeromagnetic Investigation of the Arctic Basin, 2, J. Geophys. Res., 86(B7), p. 6233-6333.

Thiede, J., D.L Clark, Y. Herman, 1990. Late Mesozoic and Cenozoic paleoceanography of the northern polar oceans, in Grantz, A., Johnson, L., and Sweeney, J.F., eds., The Arctic Ocean Region: Boulder, Geological Society of America, p. 427-458.

Thinon, I., Matias, L., Rehault, J.P., Hirn, A., Fidalgo-Gonzalez, L., Avedik, F., 2003. Deep structure of the Armorican Basin (Bay of Biscay): a review of Norgasis seismic reflection and refraction data, Journal of the Geological society, 160, p. 99-116.

Todal, A., O. Eldholm, 1998, Continental margin off Western India and Deccan Large Igneous Province, Marine Geophysical Researches 20: p. 273-291.

Van Wagoner, N.A., M. Williamson, P. Robinson, I. Gibson, 1986. First samples of acoustic basement recovered from the Alpha Ridge, Arctic Ocean: new constraints for the origin of the ridge, J. Geodyn. 6, p. 177-196.

Verhoef, J., W. Roest, R. Macnab, J. Arkani-Hamed, and Members of the Project team, 1996. Magnetic Anomalies of the Arctic and North Atlantic Oceans and adjacent land areas. Geol. Survey of Canada Open File 3125, Parts A and B.

Villeneuve, M., M.C., Williamson, 2006. ^{40}Ar-^{39}Ar dating of mafic magmatism from the Sverdrup Basin magmatic province, in Scott, R.A., D. Thurston, eds., ICAM IV Proceedings, p. 206-215.

Vogt, P.R., P. Taylor, L. Kovacs, G. Johnson, 1979. Detailed aeromagnetic investigation of the Arctic basin, J. Geophys. Res., 84(B3).

Vogt, P.R., W. Jung, M. Jakobsson, L. Mayer, M. Williamson, 2006. The Alpha Mendeleev Magmatic Province, Arctic Ocean: A new synthesis, EOS, 87 (36).

Weaver K. L., J. Tarduno, D. DePaolo, 2006, Neodymium and strontium isotopic composition of the Strand Fiord Basalts: Cretaceous Volcanism in the Canadian Arctic, Eos Trans. AGU, 87(52), Fall Meet. Suppl. Abstract U21B-0819.

Weber, J.R., 1986. The Alpha Ridge: Gravity, seismic and magnetic evidence for a homogenous, mafic crust, J. Geodyn., 6, p. 117-136.

Weber, J.R., 1990. The Structures of the Alpha Ridge, Arctic Ocean and Iceland-Faeroe Ridge, North Atlantic: Comparisons and implications for the Evolution of the Canada Basin, Marine Geology, 93, p. 43-68.

Weber, J.R., J. Sweeney, 1990. Ridges and Basins in the central Arctic Ocean, in Grantz, A., Johnson, L., and Sweeney, J.F., eds., The Arctic Ocean Region: Boulder, Geological Society of America, p. 305-336.

Wessel, P., and W. H. F. Smith, 1998. New, improved version of Generic Mapping Tools released, EOS Trans. Amer. Geophys. U., 79 (47), p. 579.

White, R. S., and D. McKenzie, 1989. Magmatism at rift zones: The generation of volcanic continental margins and flood basalts, J. Geophys. Res., 94, p. 7685-7729.

White, R, D. McKenzie, R.K. O'Nions, 1992. Oceanic crustal thicknesses. J. Geophys., 97(B13), p. 19,683-19,715.

Williams, C. C., and B. Coakley (2005), Spectral analysis and isostasy of the Alpha-Mendeleev Ridge, Arctic Ocean, Eos Trans. AGU, 85(47), Fall Meet. Suppl., Abstract, T13D-0496.

Witte, W. K., D. Kent, 1988. Revised magnetostratigraphies confirm low sedimentation sates in Arctic Ocean cores, Quaternary Research, 29, 000-000.

Wolf, L. W., R. McCaleb, D. Stone, T. Brocher, K. Fujita, S. Klemperer, 2002, Crustal structure across the Bering Strait, Alaska: Onshore recordings of a marine seismic survey, in Miller, E. L., A. Grantz, S. Klemperer, Tectonic Evolution of the Bering Shelf-Chukchi Sea-Arctic Margin and Adjacent Landmasses (GSA Special Paper), Geological Society of America, 360, p. 25-37.

Won, I. J. and M. Bevis, 1987. Computing the gravitational and magnetic anomalies due to a polygon: Algorithms and Fortran subroutines, Geophysics, 52, p. 232-238.

Woodgate, R. A., K. Aagaard, J. Swift, W. Smethie Jr., K. Falkner, 2005. Atlantic water circulation over the Mendeleev Ridge and Chukchi Borderland from thermohaline intrusions and water mass properties, J. Geophs. Res., 112, C02005

Yilmaz, O., 2001. Seismic Data Analysis, Doherty, S. ed., Soc. of Explor. Geophys., Tulsa, Okla.

Zelt, C.A., Smith, R.B., 1992. Seismic traveltime inversion for 2-D crustal velocity structure, Geophys. J. Int., 108, p. 16-34.

Zelt, C.A., 1999. Modeling strategies and model assessment for wide-angle seismic traveltime data, Geophys. J. Int, 139, p. 183-204.

Appendices

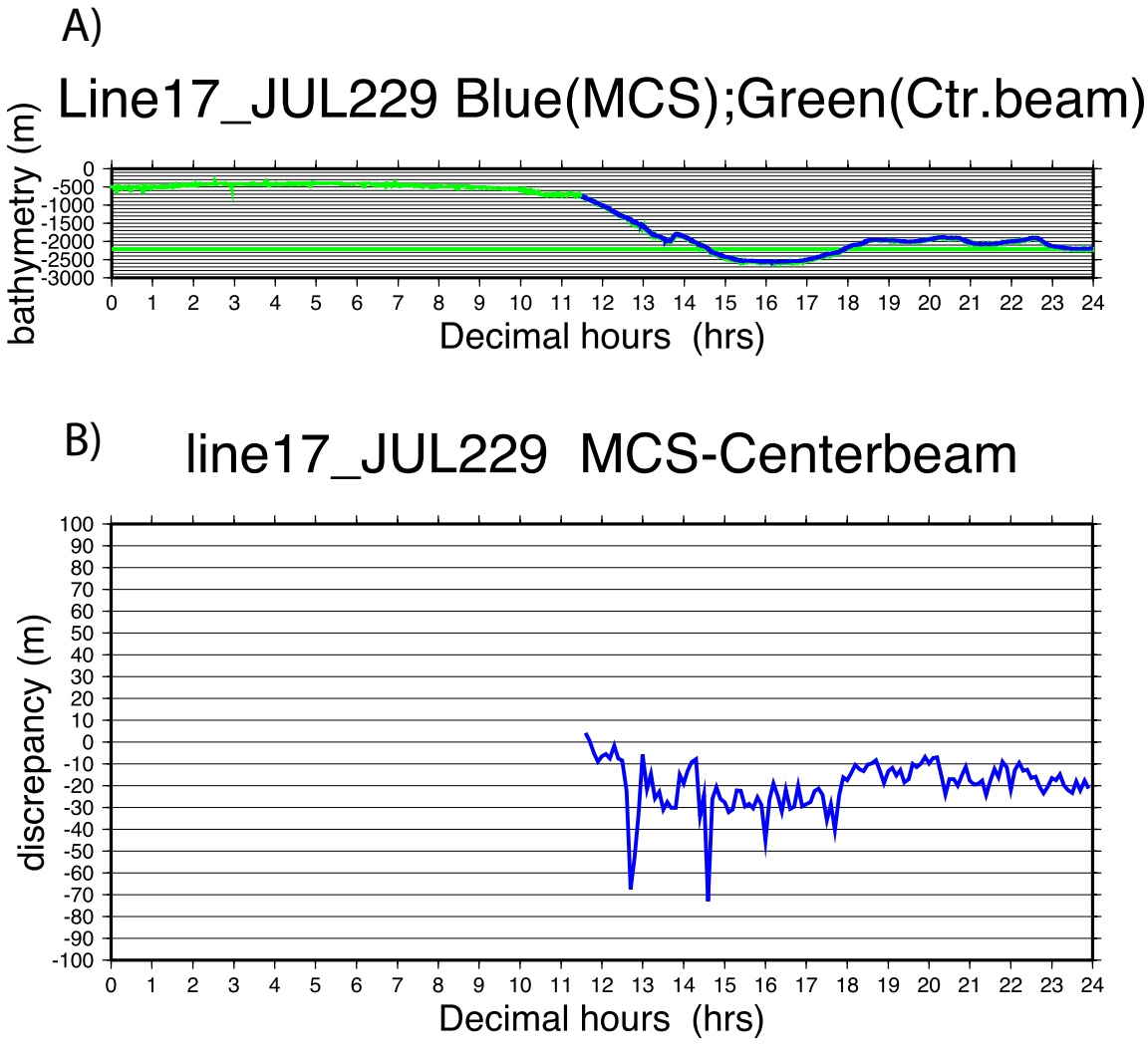

Appendix A: Seafloor Depth Comparisons Between Bathymetry and MCS Data. A comparison between the seafloor as imaged by the center-beam of the multi-beam bathymetry data vs. seafloor calculated from the MCS data. The MCS seafloor is used in both the seismic refraction and gravity models. A) Center-bearm seafloor (green) is plotted for Julian day 229 and MCS seafloor (blue) is plotted where seismic data was collected for the MCS line labeled. Ignore flat green line, artifact. B) Shown is the discrepancy in meters between the two seafloor measurements.

A)

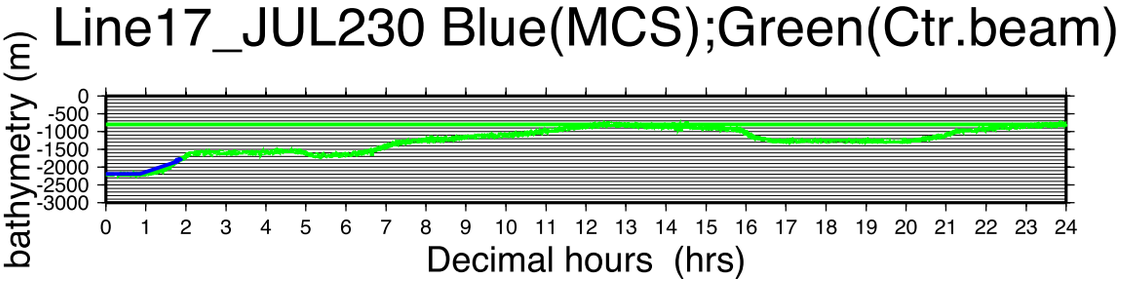

B)

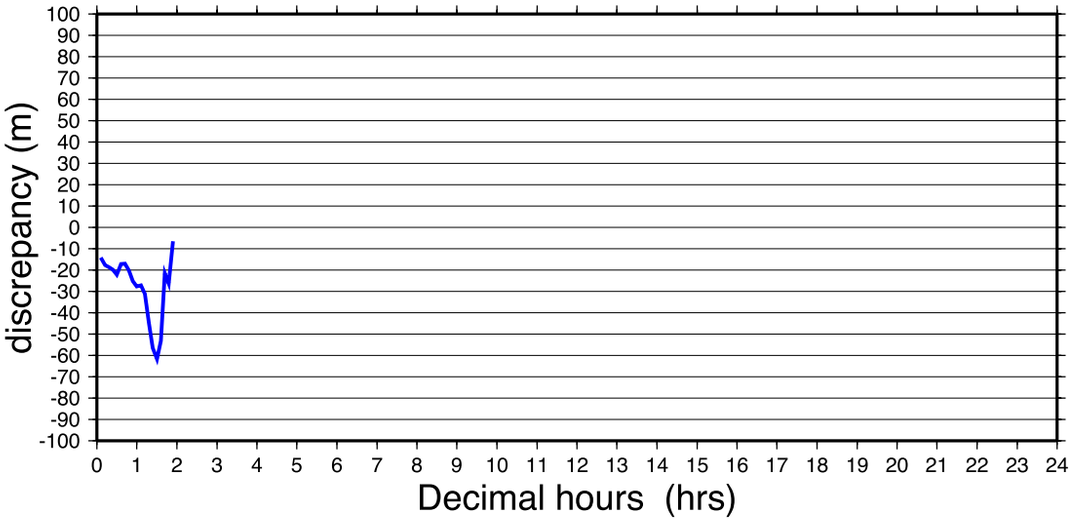

Appendix A. continued.

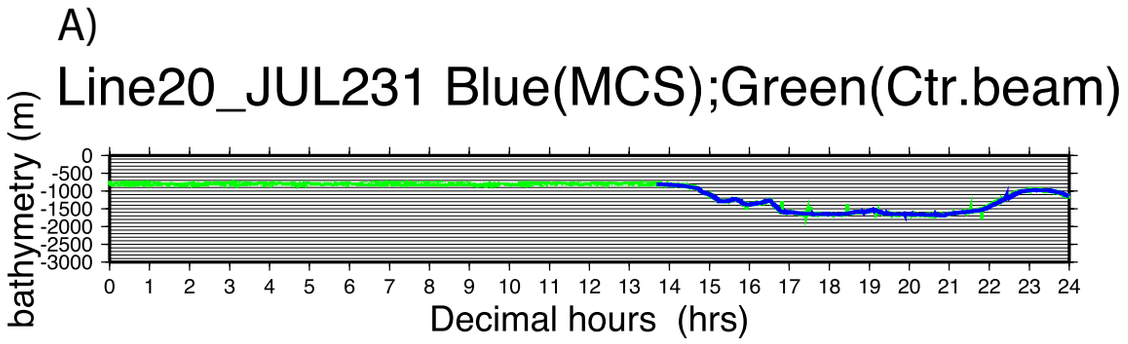

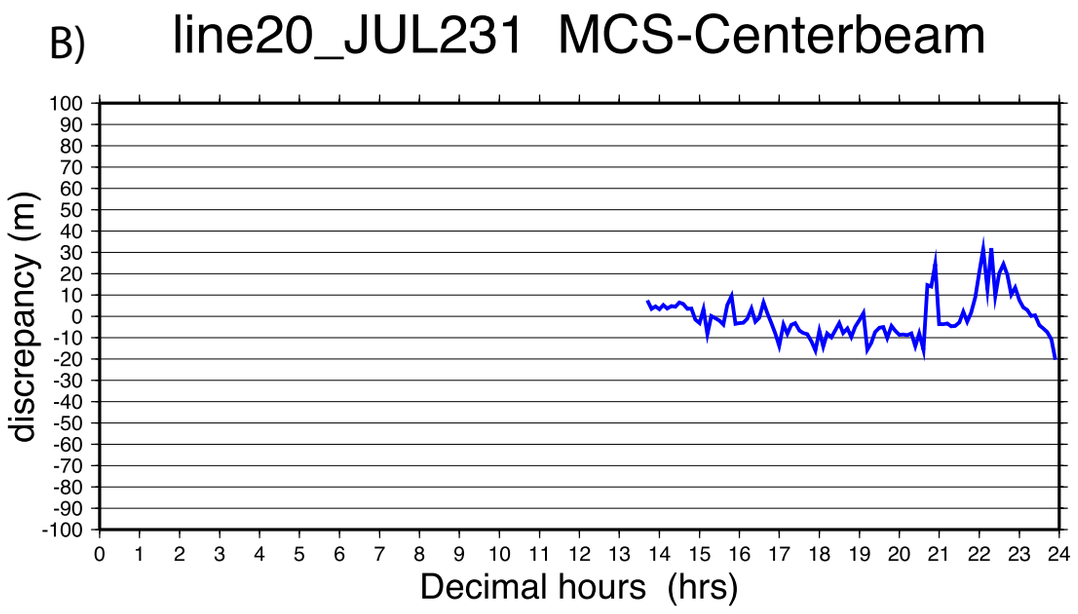

Appendix A. continued.

A)

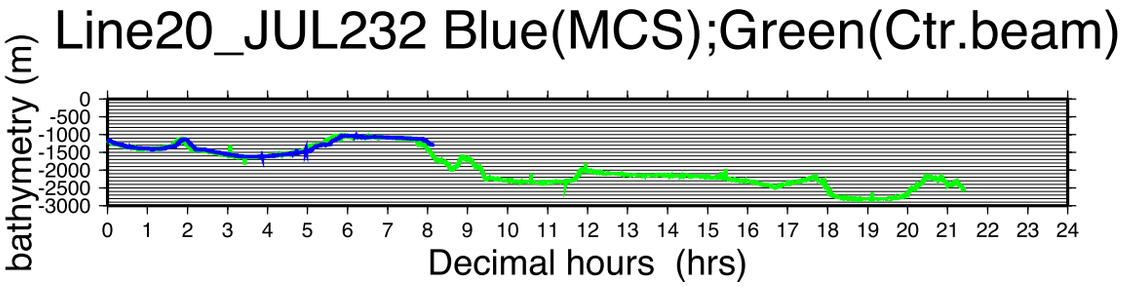

B)

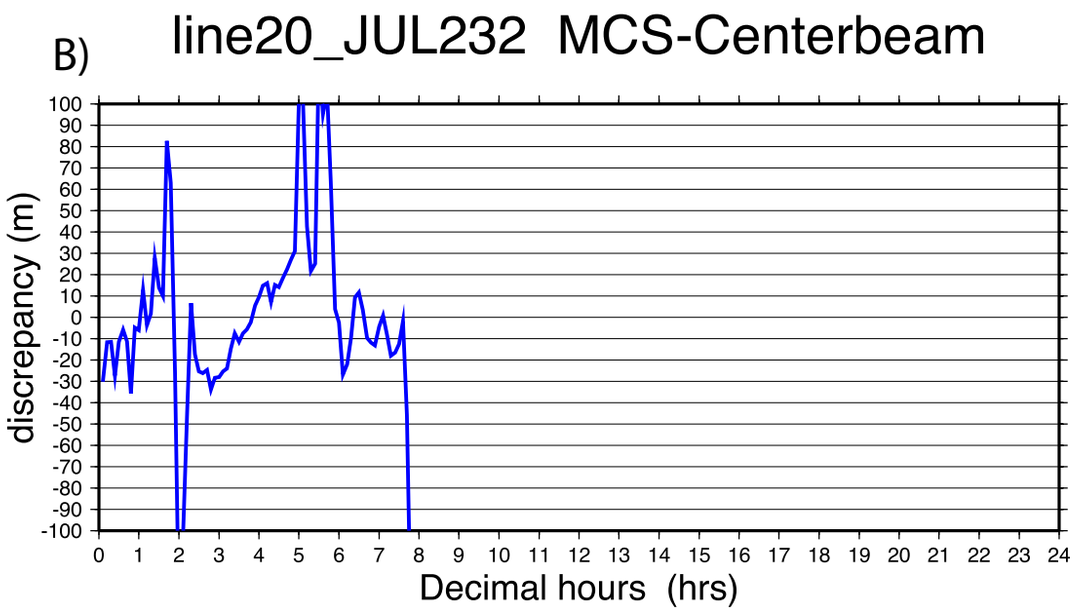

Appendix A. continued.

A)

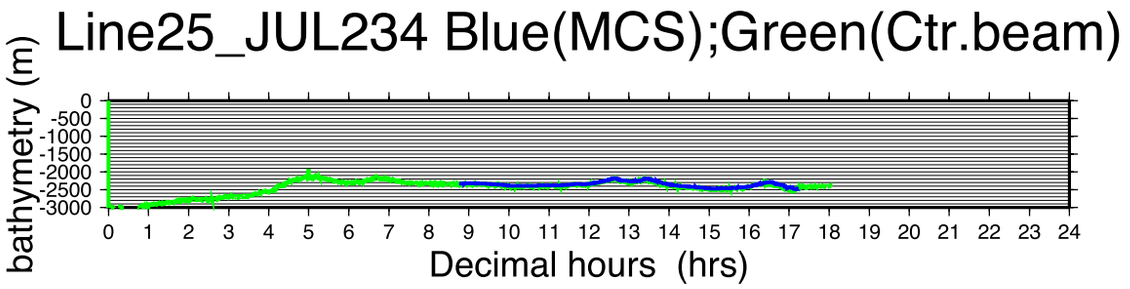

B)

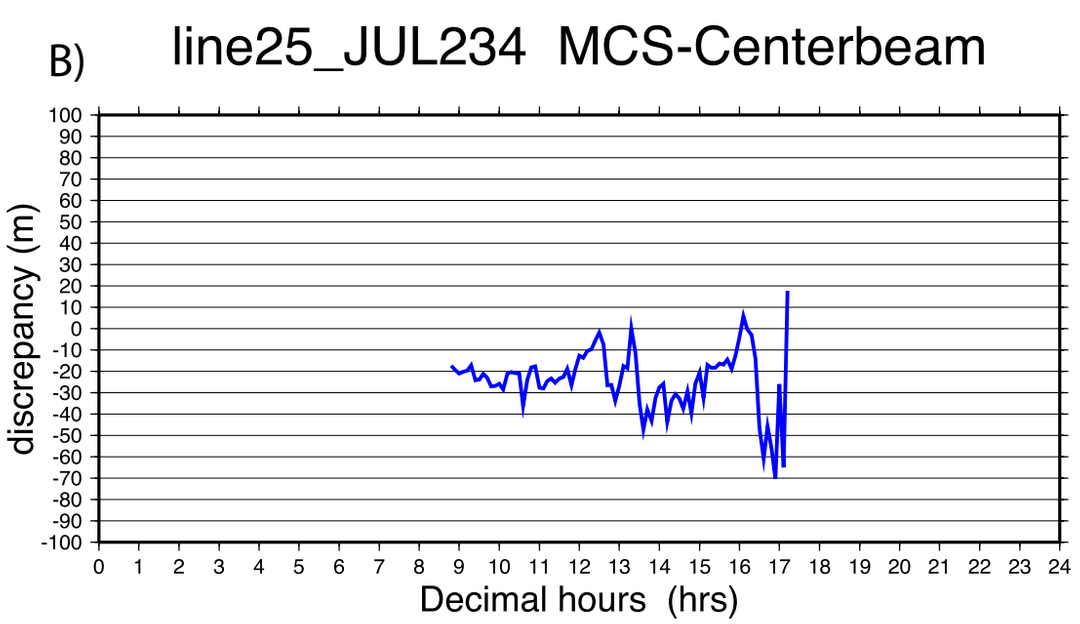

Appendix A. continued.

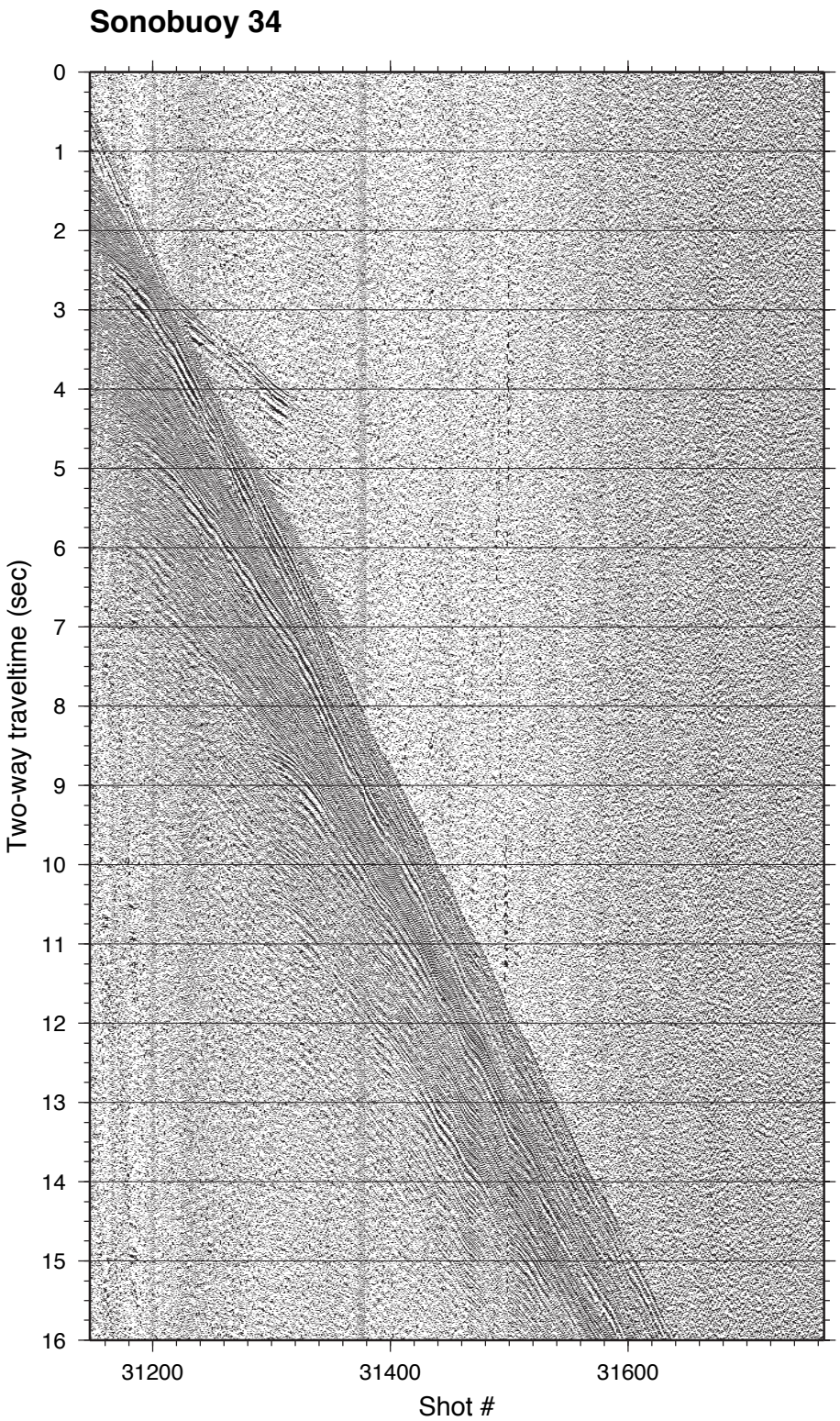

Appendix B: Seismic Refraction Full Record Sections. Record sections for sonobuoys modelled in this study (34,35,37, 44, 58)

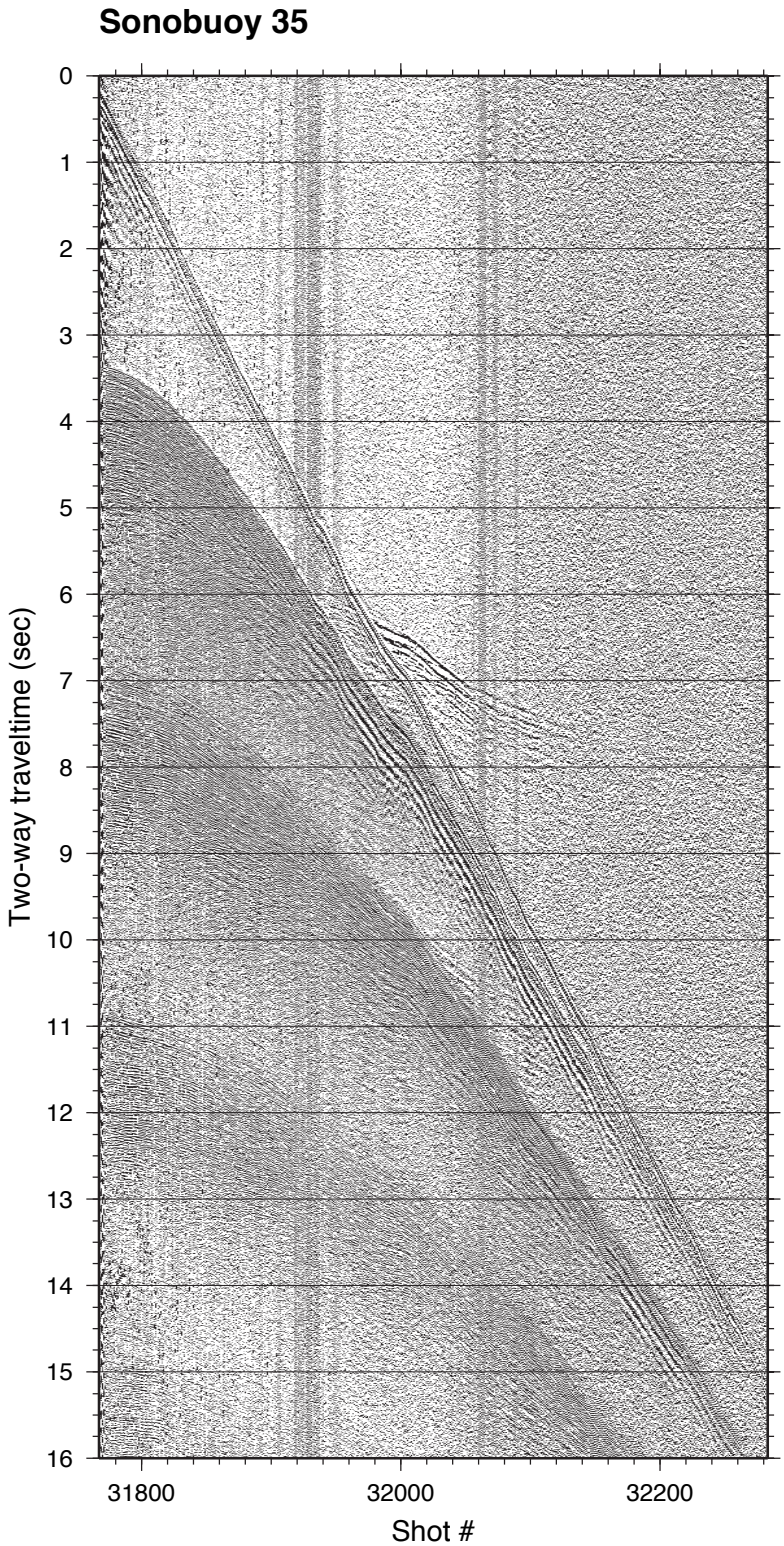

Appendix B. continued.

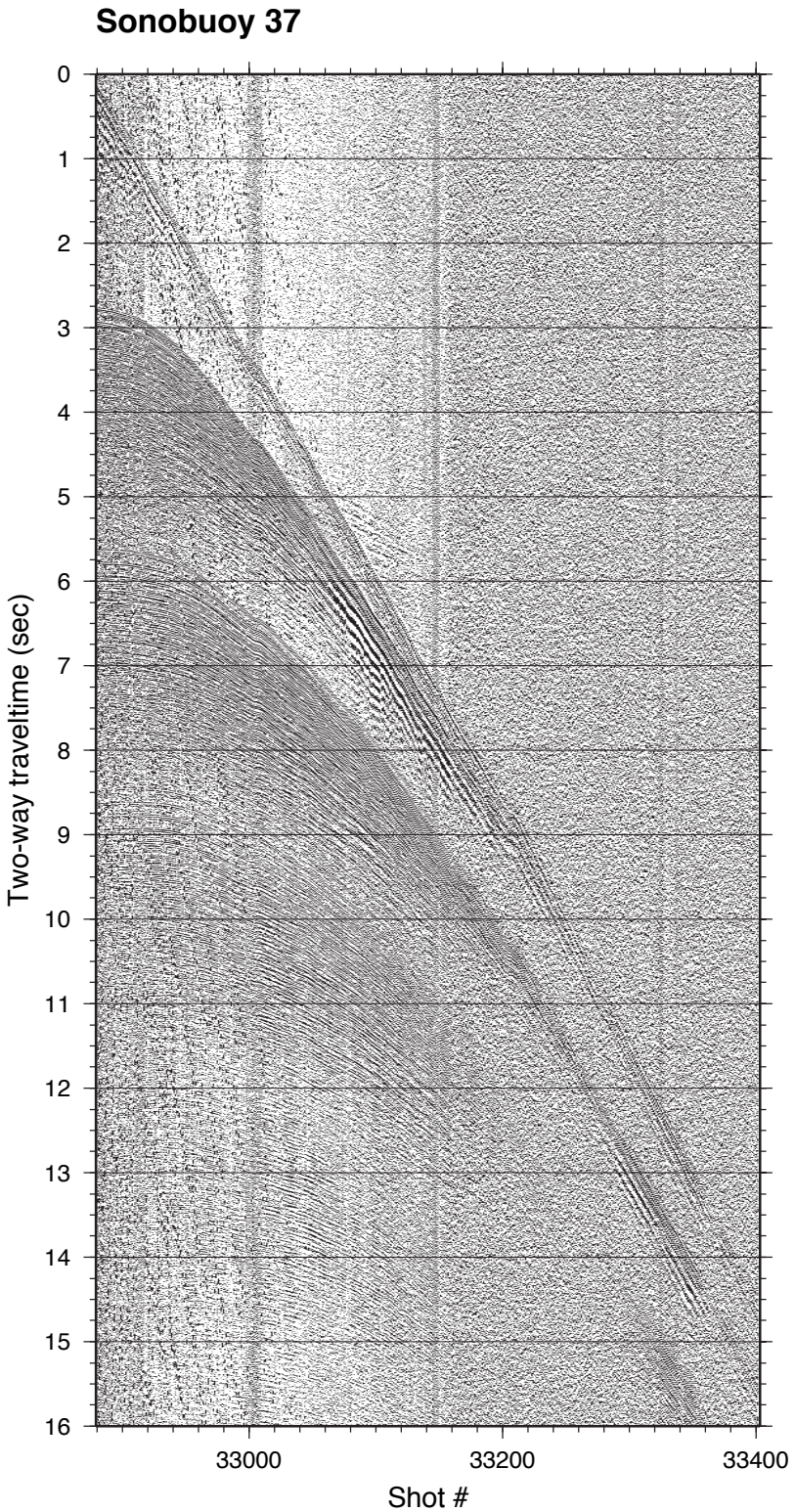

Appendix B. continued.

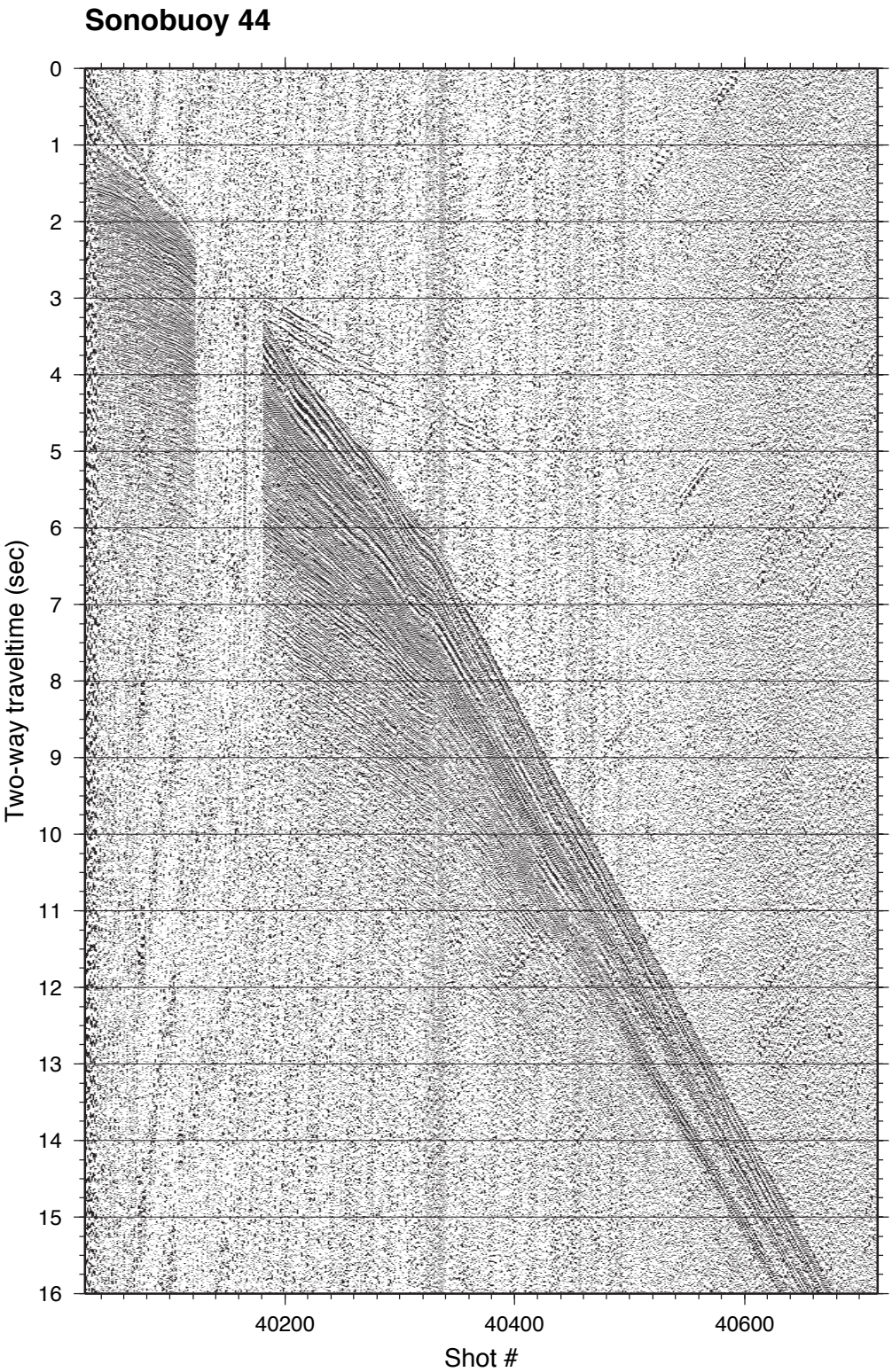

Appendix B. continued.

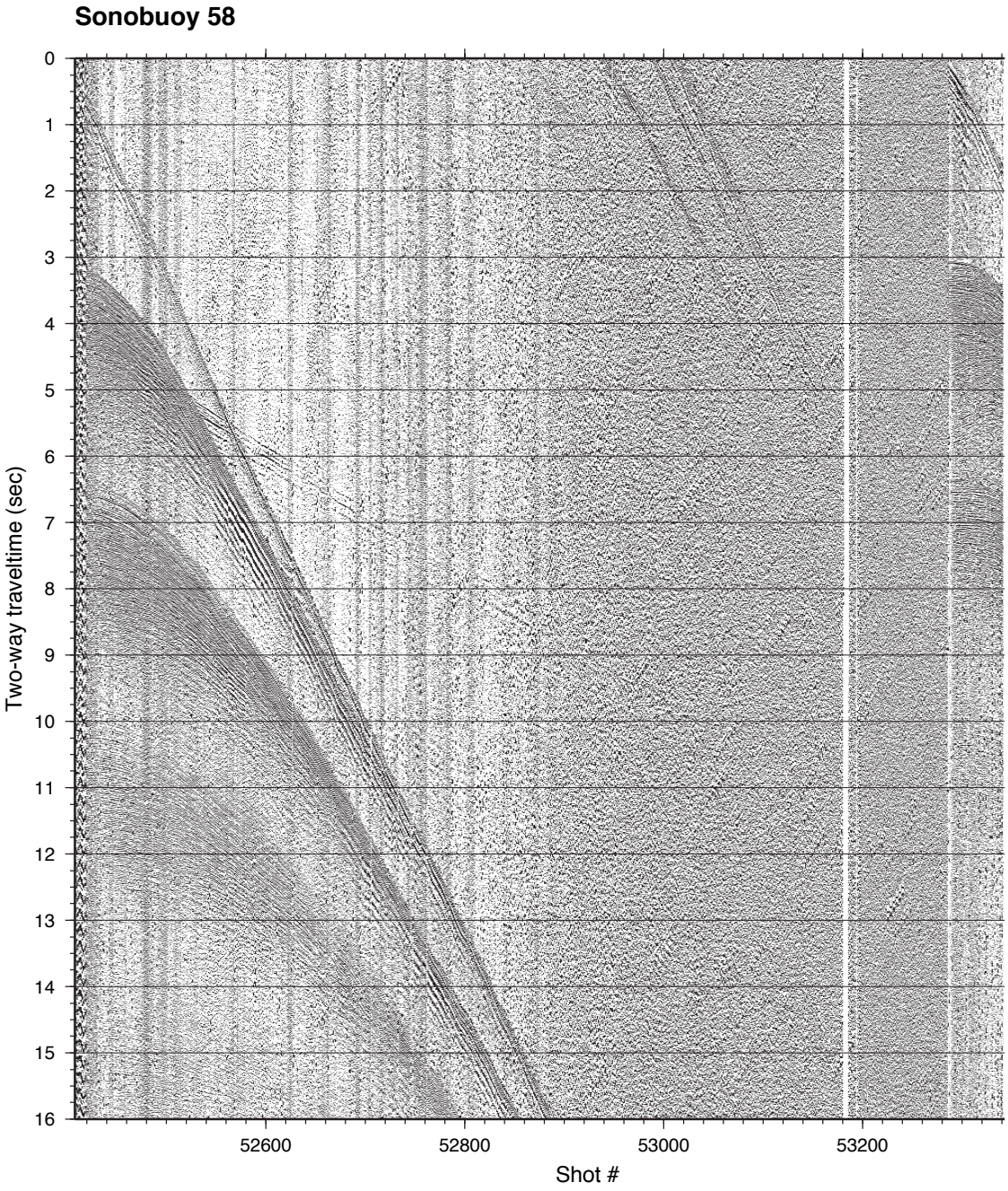

Appendix B. continued.